LAKE AREA CHANGE IN ALASKAN NATIONAL WILDLIFE REFUGES: MAGNITUDE, MECHANISMS, AND HETEROGENEITY

A

DISSERTATION

Presented to the Faculty

of the University of Alaska Fairbanks

In Partial Fulfillment of the Requirements

for the Degree of

DOCTOR OF PHILOSOPHY

By

Jennifer Roach, B.S.

Fairbanks, Alaska

December 2011

LAKE AREA CHANGE IN ALASKAN NATIONAL WILDLIFE REFUGES:

MAGNITUDE, MECHANISMS, AND HETEROGENEITY

By

Jennifer Roach

RECOMMENDED:

Jennifer Harden, PhD

David Verbyla, PhD

Jeremy Jones, PhD

Brad Griffith, PhD
Advisory Committee Chair

Christa Mulder, PhD
Chair, Department of Biology and Wildlife

APPROVED:

Paul Layer, PhD
Dean, College of Natural Science and Mathematics

Lawrence Duffy, PhD
Dean of the Graduate School

Oct 31, 2011

Date

Abstract

The objective of this dissertation was to estimate the magnitude and mechanisms of lake area change in Alaskan National Wildlife Refuges. An efficient and objective approach to classifying lake area from Landsat imagery was developed, tested, and used to estimate lake area trends at multiple spatial and temporal scales for ~23,000 lakes in ten study areas. Seven study areas had long-term declines in lake area and five study areas had recent declines. The mean rate of change across study areas was -1.07% per year for the long-term records and -0.80% per year for the recent records. The presence of net declines in lake area suggests that, while there was substantial among-lake heterogeneity in trends at scales of 3-22 km a dynamic equilibrium in lake area may not be present. Net declines in lake area are consistent with increases in length of the unfrozen season, evapotranspiration, and vegetation expansion.

A field comparison of paired decreasing and non-decreasing lakes identified terrestrialization (i.e., expansion of floating mats into open water with a potential trajectory towards peatland development) as the mechanism for lake area reduction in shallow lakes and thermokarst as the mechanism for non-decreasing lake area in deeper lakes. Consistent with this, study areas with non-decreasing trends tended to be associated with fine-grained soils that tend to be more susceptible to thermokarst due to their higher ice content and a larger percentage of lakes in zones with thermokarst features compared to study areas with decreasing trends. Study areas with decreasing trends tended to have a larger percentage of lakes in herbaceous wetlands and a smaller mean lake size which may be indicative of shallower lakes and enhanced susceptibility to

terrestrialization. Terrestrialization and thermokarst may have been enhanced by recent warming which has both accelerated permafrost thawing and lengthened the unfrozen season.

Future research should characterize the relative habitat qualities of decreasing, increasing, and stable lakes for fish and wildlife populations and the ability of the fine-scale heterogeneity in individual lake trends to provide broad-scale system resiliency. Future work should also clarify the effects of terrestrialization on the global carbon balance and radiative forcing.

Table of Contents

Page

Page

Page

Page

Page

List of Figures

Page

Page

Page

List of Tables

Page

Page

Page

List of Appendices

Page

Acknowledgements

This research would not have been possible without assistance and support from the following Alaskan National Wildlife Refuges: Tetlin, Yukon Flats, Kanuti, Koyukuk, Selawik, Innoko, Togiak, and Becharof. I especially thank Mark Bertram, Bud Johnson, and Brad Scotton, and refuge pilots Mike Hinkes, Nikki Guldager, Joee Huhndorf, and Jim Ellis for field logistics support. I also thank a number of people for taking the time to share their indispensable knowledge of local areas: Karin Bodony, Susan Savage, Lisa Saperstein, Joshua Rose, Steve Kovach, Pat Walsh, Dan Gillikin, and Tina Moran.

This work also would not have been possible without funding from USGS, FWS, the UAF President's Special Projects Fund, and a UAF Thesis Completion Fellowship. I especially thank Erik Taylor for facilitating funding and providing guidance.

I thank Robert Warren and Kevin Wyatt for trudging through bogs and tussocks and enduring swarms of mosquitoes to help me collect data in the field and I thank Steve Ewest, Matthew Balasz, and Garrett Altmann for hours spent processing imagery.

I also thank my committee members, Dr. David Verbyla, Dr. Jeremy Jones, and Dr. Jennifer Harden for their advice, constructive manuscript reviews, and encouragement. I especially thank my advisor, Dr. Brad Griffith, for his guidance and for teaching me the basic principles of scientific research. Merritt Turetsky, Ed Berg, Kenji Yoshikawa, and Bruce Finney also went out of their way to provide advice and expertise.

Finally, I thank my husband, Rob, whose patience and encouragement gave me the strength and perseverance to complete this work.

Chapter 1: General Introduction

Climate warming is pronounced in the Arctic and sub-Arctic (Serreze *et al.* 2000; Hassol 2004; Hinzman *et al.* 2005; Kaufman *et al.* 2009) and has been associated with a net loss in the number and area of lakes during the past ~50 years in permafrost-free regions of south-central Alaska (Klein *et al.* 2005), discontinuous permafrost regions of Siberia (Smith *et al.* 2005) and the Alaskan boreal forest (Riordan *et al.* 2006), and in continuous permafrost in the Yukon Territory (Labrecque *et al.* 2009). Lakes and wetlands are a predominant land-cover type on the sixteen National Wildlife Refuges in Alaska and serve as breeding grounds for waterfowl populations that are an important subsistence resource for local indigenous groups. The maintenance of these habitats and their associated biodiversity is critical to the sustainability of high latitude and global social and ecological systems. High latitude ecosystems contain about one third of global terrestrial carbon (McGuire *et al.* 2009) and the fate of this carbon is closely linked to the hydrological cycle. The loss of lakes due to climate change could fundamentally alter the global carbon balance and have effects on future climate.

In order to project future lake and landscape conditions and their implications for wildlife populations and the global carbon balance, there is a need for accurate estimates of the magnitude and rate of historical lake area change in Alaskan National Wildlife Refuges. A major limitation of previous estimates of broad-scale lake area change has been the use of highly subjective manual delineation techniques to digitize lakes from satellite imagery (Riordan *et* al. 2006; Labrecque *et al.* 2009) which can be very time and

labor intensive. Thus, these studies have included too few images in their time series to use regression models to account for within- and among-year variability when estimating long-term trends. This is especially important in the Alaskan boreal forest where inter- and intra-annual variability in lake area can be substantial and, if not accounted for, could be mistaken for long-term change.

Heterogeneity in lake area trends has been observed both among regions and among neighboring lakes (Smith *et al.* 2005; Riordan *et al.* 2006). An understanding of the spatial processes underlying this heterogeneity at both scales will enable the identification of lakes and refuges that may be most susceptible or resilient to change. This information may help land managers to identify species that may be most affected by lake area change and valuable habitats that should be retained as federally protected lands during land exchanges.

An understanding of these underlying spatial processes may also elucidate potential mechanisms associated with lake area change. A range of climate-related mechanisms for lake area change have been proposed including permafrost degradation (Smith *et al.* 2005) and drainage through taliks (Yoshikawa & Hinzman 2003), increased evapotranspiration (Klein *et al.* 2005; Smol & Douglas 2007), and terrestrialization (i.e., the expansion of floating mat vegetation into open water with a potential trajectory towards peatland development) (Campbell *et al.* 1997; Payette *et al.* 2004). An understanding of these mechanisms is important because different mechanisms may have different implications for wildlife habitats and for the global carbon balance. For example, terrestrialization may provide floating mat nesting habitat (Arnold *et al.* 1993)

and a slower transition to a shrub- and tree-dominated ecosystem compared to other mechanisms which could be beneficial for some waterfowl species. Terrestrialization may also lead to at least a temporary increase in carbon storage due to the accumulation of organic matter in lake basins (Payette *et* al. 2004) compared to other mechanisms that could directly increase respiration rates and CO_2 efflux due to receding shorelines and drier soil conditions (Laine *et al.* 1996).

In this dissertation, three studies were conducted to identify the magnitude, mechanisms, and heterogeneity of lake area change at multiple scales in Alaskan National Wildlife Refuges. In the first study, I conducted field surveys of 15 pairs of lakes. Each pair consisted of one lake that had decreased in area since the ~1950s and one lake that had not to evaluate a suite of hypothesized mechanisms to explain the fine-scale heterogeneity in lake area trends. In the second study, I developed a method for the classification of lakes from Landsat imagery that minimized the bias in estimates of lake number and area when compared to high resolution aerial photography. In the third study, I used these improved methods to estimate historical trends in lake area for more than 23,000 lakes in eight Alaskan National Wildlife Refuges. By using a multi-scale hierarchical approach, I characterized the heterogeneity in lake area trends both among study areas and among individual lakes. I then compared the among-study area heterogeneity in trends with landscape characteristics to identify potential underlying mechanisms for lake area change at the broad study area-scale. The following three chapters were prepared as separate manuscripts and include multiple authors.

References

Arnold TW, Sorenson MD, Rotella JJ (1993) Relative success of overwater and upland mallard nests in southwestern Manitoba. *Journal of Wildlife Management*, **57**, 578-581.

Campbell DR, Duthie HC, Warner BG (1997) Post-glacial development of a kettle-hole peatland in southern Ontario. *Ecoscience*, **4**, 404-418.

Hassol SJ (2004) *ACIA, Impacts of a Warming Arctic: Arctic Climate Impact Assessment.* Cambridge University Press.

Hinzman LD, Bettez ND, Bolton WR, *et al.* (2005) Evidence and implications of recent climate change in northern Alaska and other arctic regions. *Climatic Change*, **72**, 251-298.

Kaufman DS, Schneider DP, McKay NP, *et al.* (2009) Recent Warming Reverses Long-Term Arctic Cooling. *Science*, **325**, 1236-1239.

Klein E, Berg EE, Dial R (2005) Wetland drying and succession across the Kenai Peninsula Lowlands, south-central Alaska. *Canadian Journal of Forest Research*, **35**, 1931-1941.

Labrecque S, Lacelle D, Duguay CR, Lauriol B, Hawkings J (2009). Contemporary (1951–2001) evolution of lakes in the Old Crow Basin, northern Yukon, Canada: Remote sensing, numerical modeling, and stable isotope analysis. *Arctic*, **62**, 226-238.

Laine J, Silvola J, Tolonen K *et al.* (1996) Effect of water-level drawdown on global climatic warming: Northern peatlands. *Ambio*, **25**, 179-184.

McGuire AD, Anderson LG, Christensen TR *et al.* (2009) Sensitivity of the carbon cycle in the Arctic to climate change. *Ecological Monographs*, **79**, 523-555.

Payette S, Delwaide A, Caccianiga M, Beauchemin M (2004) Accelerated thawing of subarctic peatland permafrost over the last 50 years. *Geophysical Research Letters*, **31**, L18208.

Riordan B, Verbyla D, McGuire AD (2006) Shrinking ponds in subarctic Alaska based on 1950-2002 remotely sensed images. *Journal of Geophysical Research*, **111**, G04002.

Serreze MC, Walsh JE, Chapin III FS *et al.* (2000) Observational evidence of recent change in the northern high-latitude environment. *Climatic Change*, **46**, 159-207.

Smith LC, Sheng Y, MacDonald GM, Hinzman LD (2005) Disappearing arctic lakes. *Science*, **308**, 1429.

Smol JP, Douglas MS (2007) Crossing the final ecological threshold in high arctic ponds. *Proceedings of the National Academy of Sciences*, **104**, 12395-12397.

Yoshikawa K, Hinzman LD (2003) Shrinking thermokarst ponds and groundwater dynamics in discontinuous permafrost near Council, Alaska. *Permafrost and Periglacial Processes*, **14**, 151-160.

Chapter 2: Mechanisms influencing changes in lake area in Alaskan boreal forest[1]

Abstract

During the past ~50 years, the number and area of lakes have declined in several regions in boreal forests. However, there has been substantial finer-scale heterogeneity; some lakes decreased in area, some showed no trend, and others increased. The objective of this study was to identify the primary mechanisms underlying heterogeneous trends in closed-basin lake area. Eight lake characteristics ($\delta^{18}O$, electrical conductivity, surface:volume index, bank slope, floating mat width, peat depth, thaw depth at shoreline, and thaw depth at the forest boundary) were compared for 15 lake pairs in Alaskan boreal forest where one lake had decreased in area since ~1950, and the other had not. Mean differences in characteristics between paired lakes were used to identify the most likely of nine mechanistic scenarios that combined three potential mechanisms for decreasing lake area (talik drainage, surface water evaporation, and terrestrialization) with three potential mechanisms for non-decreasing lake area (sub-permafrost groundwater recharge through an open talik, stable permafrost, and thermokarst). A priori expectations of the direction of mean differences between decreasing and non-

[1]Roach J, Griffith B, Verbyla D, & Jones J (2011) Mechanisms influencing changes in lake area in Alaskan boreal forest. *Global Change Biology,* **17**, 2567-2583.

decreasing paired lakes were generated for each scenario. Decreasing lakes had significantly greater electrical conductivity, greater surface:volume indices, shallower bank slopes, wider floating mats, greater peat depths, and shallower thaw depths at the forest boundary. These results indicated that the most likely scenario was terrestrialization as the mechanism for lake area reduction combined with thermokarst as the mechanism for non-decreasing lake area. Terrestrialization and thermokarst may have been enhanced by recent warming which has both accelerated permafrost thawing and lengthened the growing season, thereby increasing plant growth, floating mat encroachment, transpiration rates, and the accumulation of organic matter in lake basins. The transition to peatlands associated with terrestrialization may provide a transient increase in carbon storage enhancing the role of northern ecosystems as major stores of global carbon.

Introduction

Climate warming is pronounced in the Arctic and sub-Arctic (Serreze *et al.* 2000; Hassol 2004; Hinzman *et al.* 2005; Kaufman *et al.* 2009) and has been associated with a net loss in the number (5-54%) and area (4-31%) of closed-basin lakes during the past ~50 years in the discontinuous permafrost regions of the Alaskan boreal forest (Riordan *et al.* 2006), in the permafrost-free regions of south-central Alaska (Klein *et al.* 2005), and both closed- and open-basin lakes in the discontinuous permafrost regions of Siberia (Smith *et al.* 2005). Within Alaskan boreal forest, lakes and wetlands are abundant on National Wildlife Refuges and serve as breeding grounds for millions of waterfowl and

shorebirds that migrate annually from more southerly parts of North America, South America, Asia, and Australia. An understanding of the mechanisms responsible for losses in lake area is essential for robust projections of future landscape conditions and their subsequent implications for wildlife.

Heterogeneous Changes in Lake Area

An important clue to the mechanisms underlying losses in lake area is the presence of fine-scale (Wiens 1989) (< 2km) spatial heterogeneity; some lakes remain stable or increase in area while neighboring lakes decrease substantially in size (Smith *et al.* 2005; Riordan *et al.* 2006) (Fig. 2.1). This fine-scale heterogeneity suggests that net loss in lake area at broader scales (e.g., study area) is not simply the result of a homogeneous phenomenon but rather represents disequilibrium between decreasing and non-decreasing lakes at fine scales. Thus, the mechanisms for overall loss in lake area at both coarse and fine scales may be associated with spatially heterogeneous characteristics that can vary between neighboring lakes. An improved understanding of what causes different trajectories of neighboring lakes could elucidate the mechanisms underlying broad-scale loss in lake area.

Potential Sources of Heterogeneity

The objective of this study was to identify the primary mechanisms underlying the fine-scale heterogeneity in closed-basin lake area changes in National Wildlife Refuges in Alaskan boreal forest. The heterogeneous distribution of lakes with stable, increasing,

and decreasing area within boreal forest may be the result of heterogeneous 1) permafrost stability, 2) hydraulic gradients, and/or 3) lake and catchment topography.

Permafrost (soil, rock, or water that remains at or below 0°C for two or more years (van Everdingen 2005)) is particularly sensitive to the effects of climate warming (Vitt *et al.* 1994; Osterkamp *et al.* 2000; Jorgenson *et al.* 2001; Osterkamp 2005; Jorgenson & Osterkamp 2005). However, the magnitude and rate of its response to increased temperatures (i.e., relative stability) can vary at a fine scale as a result of heterogeneous snow cover, soil moisture, soil organic content, topography, and human or wildlife disturbance (Nelson *et al.* 1999; Anisimov *et al.* 2002). Lakes with more unstable permafrost may be more susceptible to lateral permafrost degradation (i.e., thermokarst formation) which can lead to an increase in lake area (Jorgenson & Osterkamp 2005). They may also be more susceptible to vertical permafrost degradation underneath the lake (i.e., talik growth) which can proceed until the lake is no longer isolated from groundwater systems via a permafrost aquiclude (Swanson 1996; Vörösmarty *et al.* 2001). Once a permafrost aquiclude is removed, lake area may either increase or decrease depending on the relative pressure gradient (i.e., hydraulic gradient) that is present between surface water and formerly sub-permafrost groundwater systems (Britton 1957; Kane & Slaughter 1973; Billings & Peterson 1980; Woo 1986; Jorgenson *et al.* 2001; Yoshikawa & Hinzman 2003). The complex network of aquifers and the heterogeneous distribution of permafrost in the boreal forest may result in opposing hydraulic gradients at neighboring lakes.

Alternatively, neighboring lakes may have different lake and catchment topography which may differentially affect their susceptibility to lake area change. Lakes with larger catchments may receive greater water inputs from precipitation or snowmelt runoff while lakes with a greater surface area relative to water volume may be more susceptible to climate-induced losses in lake area resulting from increased evaporation rates and/or increased rates of terrestrial infilling (Campbell *et al.* 1997, Jorgensen & Shur 2007). One source of fine-scale heterogeneity in lake bathymetry in the boreal forest is the presence of heterogeneous permafrost ice content which affects the size of depressions and thermokarst lakes resulting from permafrost degradation (Hopkins 1949; Burn & Smith 1990; Burn 1992; Hinzman *et al.* 1997; Jorgenson & Osterkamp 2005; Jorgenson & Shur 2007).

Study Design

The fine-scale heterogeneity in lake area change enabled the spatial and temporal pairing of decreasing and non-decreasing lakes to control for broad-scale differences in temperature, precipitation, and substrate heterogeneity in order to isolate the primary mechanisms responsible for lake area change. Several heterogeneity-related mechanisms could explain the differential responses of a population of paired lakes.

The three mechanisms considered to explain lake area reduction were: 1) taliks beneath lakes expanded into sub-permafrost groundwater systems causing lakes to drain in the presence of a negative hydraulic gradient (Britton 1957; Billings & Peterson 1980; Woo 1986; Yoshikawa & Hinzman 2003) (Fig. 2.2a); 2) surface water evaporation

exceeded water inputs leading to receding shorelines, drier conditions, and increased nutrient concentrations and lake productivity (Schindler *et al.* 1990; Klein *et al.* 2005; Smol & Douglas 2007) (Fig. 2.2b); or, 3) floating mat vegetation encroached towards the center of the lake obscuring surface water in remotely sensed imagery and causing increased rates of transpiration and basin infilling with organic matter (i.e., terrrestrialization) (Gates 1942; Dansereau & Segadas-Vianna 1951; Drury 1956; Tallis 1983; Kratz & DeWitt 1986; Hu & Davis 1995; Campbell *et al.* 1997) (Fig. 2.2c).

The three mechanisms considered to explain lake area stability or increase were: 1) permafrost remained stable and acted as an aquiclude (Swanson 1996; Vörösmarty *et al.* 2001) minimizing surface and sub-permafrost groundwater interactions (Fig. 2.2d); 2) taliks underneath lakes expanded to sub-permafrost groundwater systems and the presence of a positive hydraulic gradient led to artesian conditions recharging the lake (Kane & Slaughter 1973; Jorgenson *et al.* 2001) (Fig. 2.2e); or 3) ice-rich permafrost degraded laterally (i.e., thermokarst) facilitating lake expansion (Jorgenson & Osterkamp 2005) (Fig. 2.2f).

For eight variables (Table 2.1), a priori expectations for the direction of mean differences between paired decreasing and non-decreasing lakes for all nine possible combinations (i.e., scenarios) of the proposed decreasing vs. non-decreasing mechanisms were generated (Fig. 2.2). Observed results from statistical tests of the null hypotheses of no difference between paired decreasing and non-decreasing lakes were then compared to these predictions to identify which mechanisms were most likely to be primarily responsible for the fine-scale heterogeneity in lake area change.

Materials and Methods

Study Design

Differences in characteristics between paired closed-basin lakes, where one lake had lost area since the 1950s and the other lake had not, were evaluated. Closed-basin lakes were defined as those with no detectable connection to any river or stream system. Assessment was restricted to closed-basin lakes because the potential effects of climatic variables such as evaporation, evapotranspiration, and permafrost stability on water levels are often masked by stream flow into and out of open-basin lakes (Anderson *et al.* 2007). Mechanisms of long-term area change in open-basin lakes would likely include changes in the pattern and magnitude of river and stream flow which were not addressed in this study.

Paired lakes were located 0.2 to 1.8 km apart and all data were collected for both pair members on the same day or on two consecutive days. This paired design enabled the direct detection of fine-scale mechanisms of lake area change that may have been masked or biased by study area or within-season differences. The paired design controlled for extraneous sources of broad-scale spatial (e.g., among study area variance in substrate characteristics) and temporal (e.g., within summer variability in precipitation and thawing) heterogeneity. For example, the design enabled the direct comparison oxygen isotopic composition between paired lakes by controlling for broad-scale variability in precipitation and enabled the direct comparisons of thaw depth between paired lakes by controlling for within-season thaw progression.

Study Areas

Lake pairs were located in four study areas that ranged in size from 630 – 2,020 km^2 (Fig. 2.3) in Alaskan boreal forest. These areas were selected because previous work had estimated rates of change for closed-basin lakes in these areas since the 1950s (-4 to -31%) and provided an initial dataset for selection of potential lake pairs (Riordan *et al.* 2006).

The boreal forest is characterized by a dynamic mosaic of spruce forests, shrub areas dominated by willows, bogs and fens dominated by mosses and sedges, and lakes. Principal lake types in Alaska include thermokarst lakes, fluvial lakes such as oxbows, glacial lakes such as kettles and tarns, and moraine-dammed lakes (Arp & Jones 2009). Lakes included in this study are likely of the former two types because the study areas were located in lowland areas that were unglaciated in the Pleistocene (Manley & Kaufman 2002). The areas were underlain by either continuous or discontinuous permafrost (Brown *et al.* 2001; Jorgenson *et al.* 2008). The permafrost layer in these areas affects surface and sub-surface hydrology by acting as an aquiclude which leads to an abundance of relatively shallow lakes and wetlands that would otherwise be unusual for the dry climate found in interior Alaska.

Lake Area Change Analysis and Lake Pair Selection

A population of paired decreasing and non-decreasing lakes that were float plane accessible and < 1.8 km apart was identified using data presented by Riordan *et al.* (2006). Float plane accessibility and distance between lakes was assessed using aerial

reconnaissance and Geographic Information System (GIS) analysis. Lake pairs were then ranked based on the difference in magnitude of change between decreasing and non-decreasing lakes and sampled in this order until either six paired lakes per study area were sampled or all remaining lake pairs had been discarded due to changing float plane accessibility during the season. In order to improve our ability to account for inter- and intra-annual variability in trend detection, initial estimates of lake area change were verified with a regression analysis that included at least six image dates for each lake from the 1950s to 2002, with at least two images from early season (May-June) and two images from late season (July-August). Lake boundaries were manually digitized from historical black and white aerial photography from the 1950s, color infrared aerial photography from 1978-1984, and satellite imagery from the Landsat Enhanced Thematic Mapper Plus sensor (ETM+) and the Landsat Thematic Mapper sensor (TM) from 1991 to 2002. All images were georectified to the UTM map projection, NAD27, using a linear affine transformation model and nearest neighbor re-sampling. Each model was based on well-defined image-based control points using the statewide coverage of 1:63,360 topographic maps and had a root mean squared error (RMSE) of less than 1 pixel, corresponding to 2 to 9 meters for the aerial photographs and 15 to 30 m for the Landsat TM/ETM+ images. Each image was rectified using at least 25 control points and a density of at least 0.5 points per km^2. A linear regression (SAS Institute, Inc. 2003) was performed for each lake to identify whether there was a significant trend in lake area (m^2) from 1950 to 2002. Date of image acquisition expressed as days beginning on 1 Jan 1900 was used as the independent variable in order to simultaneously account for day,

month, and year in the regression model. Lakes with a significant ($P < 0.05$) negative effect of day on lake area were classified as decreasing lakes. Lakes with a significant ($P < 0.05$) positive effect or a non-significant ($P > 0.05$) effect of day on lake area were classified as non-decreasing lakes (Table 2.2). Lakes with positive or no effect of day on lake area were combined into one category because the primary interest was in identifying mechanisms for area reduction. Based on this analysis, 15 lake pairs that consisted of one decreasing lake and one non-decreasing lake were retained (Table 2.2). These 15 pairs included five pairs in the Yukon Flats West study area, three pairs in the Yukon Flats East study area, four pairs in the Kaiyuh Flats study area, and three pairs in the Tetlin study area (Fig. 2.3, Table 2.2).

Scenario Expectations

The nine possible combinations of the three hypothetical mechanisms for decreasing lakes and the three hypothetical mechanisms for non-decreasing lakes were referred to as Scenarios A-I (Table 2.1). Assuming that the non-decreasing lakes could be used as control sites for decreasing lakes, a "+" indicates that the variable was expected to be greater, a "-" indicates that the variable was expected to be lower, and a "0" indicates that the variable was not expected to be different at decreasing lakes compared to paired non-decreasing lakes. Expected differences were classified as unknown when the direction of the difference was unclear. Variables and the direction of the difference expected between decreasing and non-decreasing lakes for each scenario are as follows:

Variable 1: ^{18}O Enrichment. Oxygen isotope ratios can be used to clarify the relative role of evaporation compared to water inputs in a lake's hydrological budget (Anderson *et al.* 2007; Clegg & Hu 2010; Turner *et al.* 2010). For a closed-basin lake, water inputs can be from groundwater, surface runoff derived from snowmelt or precipitation, or precipitation falling directly on a lake surface. Evaporation leads to enrichment of lake ^{18}O, because the lighter isotope (^{16}O) has weaker bonds causing it to fractionate during evaporation. In contrast, precipitation and especially groundwater and snowmelt tend to be depleted in ^{18}O (Craig 1961; Payne 1970; Gat 1996; Turner *et al.* 2010). Therefore, the degree of isotopic enrichment of a lake may indicate the relative difference between evaporation and water inputs in a lake's water balance. If a reduction in lake area was due to surface water evaporation that exceeded water inputs, the lake would be expected to be relatively enriched in ^{18}O compared to a lake with stable or increasing water levels.

In contrast with surface water evaporation, isotopes do not fractionate when roots take up water (Gonfiantini *et al.* 1965; Dawson & Ehleringer 1991; Gat 1996; Gibson & Edwards 2002). Instead, evaporative enrichment during transpiration occurs within the leaf water (Gonfiantini *et al.* 1965; Cooper *et al.* 1991; Gat 1996) and is reflected in the isotopic composition of plant cellulose (Epstein *et al.* 1977; DeNiro & Epstein 1979). Thus, a reduction in lake water balance due to transpiration would not affect lake water oxygen isotopic composition.

Sub-permafrost groundwater is relatively depleted in the heavier isotopes due to isolation from evaporative effects (Gat 1996). Thus groundwater recharge to a lake

through an open talik in the presence of a positive hydraulic gradient (i.e., artesian conditions) would result in a large influx of water that was relatively depleted in ^{18}O compared to a lake not receiving a comparable influx of sub-permafrost groundwater. Thus, greater relative enrichment of oxygen isotopes at decreasing lakes compared to paired non-decreasing lakes (+) was expected if either surface water evaporation was the primary decreasing mechanism (i.e., isotopic enrichment at the decreasing lake) or if groundwater recharge was the non-decreasing mechanism (i.e., depletion of heavier isotopes at the non-decreasing lake) (Table 2.1: Scenarios A, D, E, F, & G). No net difference in oxygen isotope enrichment was expected if terrestrialization/evapotranspiration was the decreasing mechanism and if stable permafrost or thermokarst was the non-decreasing mechanism (Table 2.1: Scenarios H & I) because neither of these mechanisms are likely to have a substantial effect on lake oxygen isotopic composition. The expectation for talik drainage as a decreasing mechanism in combination with stable permafrost or thermokarst as a non-decreasing mechanism was classified as unknown (Table 2.1: Scenarios B & C) because talik drainage could have either no effect or a slight depleting effect on ^{18}O depending on whether drainage was actively occurring or if an equilibrium had been reached involving steady state exchange with sub-permafrost groundwater. For Scenario A, it was assumed that even if talik drainage had reached equilibrium, groundwater recharge to non-decreasing lakes through an open talik would still lead to relatively more depleted ^{18}O at non-decreasing lakes compared to paired decreasing lakes.

Variable 2: Electrical Conductivity. Similar to oxygen isotopic composition, electrical conductivity can be used to identify the relative inputs and outputs affecting lake water balance. Lakes receiving formerly sub-permafrost groundwater tend to have a higher electrical conductivity than precipitation fed lakes because sub-permafrost groundwater is typically enriched in cations due to a longer residence time in contact with earth materials (Rouse *et al.* 1997; Yoshikawa & Hinzman 2003). In contrast with oxygen isotopes which give different signals for evaporation and transpiration, electrical conductivity may be increased by both evaporation and transpiration, thus reflecting the net evapotranspiration rate of a lake. Evaporation of water from the surface of a lake directly increases electrical conductivity by concentrating dissolved ions in the lake water (Smol & Douglas 2007). Aquatic macrophytes can indirectly increase electrical conductivity over the course of several years by removing water from a lake through transpiration and leaching nutrients into the water column upon death and decomposition of plant tissues in fall and winter (Boyd & Hess 1970; Gaudet 1977; Carpenter 1980; Johnston 1991; Kroger *et al.* 2007). For example, *Typha latifolia* and *Phragmites australis*, common species found at study lakes, lost 90-93% of their potassium, sodium, nitrogen, and phosphorus to the water column after 20 days of submerged tissue senescence (Boyd & Hess 1970; Nichols and Keeney 1972; Gaudet 1977).

Because surface water evaporation, terrestrialization/evapotranspiration, and groundwater recharge all lead to greater electrical conductivity, scenarios that combined the former two decreasing mechanisms with the latter non-decreasing mechanism were classified as unknown since it was not possible to assess the relative effects of these

mechanisms on electrical conductivity (Table 2.1: Scenarios D & G). For scenarios that compared surface water evaporation and terrestrialization/evapotranspiration as decreasing mechanisms with stable permafrost and thermokarst as non-decreasing mechanisms (Table 2.1: Scenarios E, F, H, & I), a greater electrical conductivity was expected at decreasing lakes compared to paired non-decreasing lakes (+). Scenarios that compared talik drainage as a decreasing mechanism with stable permafrost and thermokarst as non-decreasing mechanisms (Table 2.1: Scenarios B & C) were classified as unknown because talik drainage may have either no effect or cause a slight increase in conductivity depending on whether the lake has reached equilibrium with sub-permafrost groundwater. However, for Scenario A (Table 2.1), it was expected that even if talik drainage had reached equilibrium with sub-permafrost groundwater at the decreasing lake, groundwater recharge due to artesian conditions at the non-decreasing lake would have had a positive overall effect on electrical conductivity resulting in a relatively lower conductivity at decreasing lakes compared to paired non-decreasing lakes (-).

Variable 3: Surface:Volume Index. Surface to volume index was used to estimate current lake bathymetry. Shallow lakes with a greater surface to volume index may have greater direct evaporation rates and/or greater rates of floating mat encroachment, basin infilling, and therefore greater evapotranspiration rates. Thus, a greater surface to volume index (+) was expected at decreasing lakes compared to paired non-decreasing lakes if surface water evaporation or terrestrialization /evapotranspiration was the primary decreasing mechanism (Table 2.1: Scenarios D - I). In contrast, open taliks are more likely to form at deeper lakes with smaller surface to volume indices due

to the increased thermal conductivity of the lake water as the volume of water increases (Brewer 1958; Mackay 1992; Burn 2002; Yoshikawa & Hinzman 2003). Thus, a smaller surface to volume index (-) was expected at decreasing lakes compared to paired non-decreasing lakes if talik drainage was the primary decreasing mechanism and groundwater recharge via an open talik was not the primary non-decreasing mechanism (Table 2.1: Scenarios B & C). For Scenario A (Table 2.1), no difference was expected in surface to volume ratio (0) because both the talik drainage and groundwater recharge hypotheses involve the formation of open taliks underneath lakes that are sufficiently deep.

Variable 4: Bank Slope. The slope of the banks between shoreline (terrestrial edge of the floating mat if present) and the forest boundary was used to estimate former lake bathymetry. Using the same logic as stated above for surface:volume index, shallower bank slopes (-) were expected at decreasing lakes compared to paired non-decreasing lakes if surface water evaporation or terrestrialization/evapotranspiration was the primary decreasing mechanism (Table 2.1: Scenarios D - I). Similarly, steeper bank slopes (+) were expected at decreasing lakes compared to paired non-decreasing lakes if talik drainage was the primary decreasing mechanism and stable permafrost or thermokarst was the non-decreasing mechanism (Table 2.1: Scenarios B & C) and no difference (0) was expected if talik drainage was the decreasing mechanism and groundwater recharge via an open talik was the non-decreasing mechanism (Table 2.1: Scenario A).

Variable 5: Floating Mat Width. The width of floating mat vegetation on a lake surface may be indicative of the rate of floating mat encroachment and terrestrialization (Dansereau & Segadas-Vianna 1951; Drury 1956; Kratz & DeWitt 1986). Thus, decreasing lakes were expected to have wider floating mats compared to paired non-decreasing lakes (+) if terrestrialization/evapotranspiration (i.e., floating mat encroachment) was the primary decreasing mechanism (Table 2.1: Scenarios G – I). No difference (0) in floating mat width was expected for Scenarios A – F (Table 2.1) because floating mat encroachment is only relevant to the terrestrialization/evapotranspiration mechanism.

Variable 6: Peat Depth. The depth of peat at the shoreline of decreasing lakes may be indicative of the rate of organic matter accumulation resulting from the establishment and encroachment of floating mats and the subsequent basin infilling associated with terrestrialization (Dansereau & Segadas-Vianna 1951; Drury 1956; Kratz & DeWitt 1986). Thus, decreasing lakes were expected to have greater shoreline peat depth compared to paired non-decreasing lakes (+) if terrestrialization/evapotranspiration (i.e., floating mat encroachment) was the primary decreasing mechanism (Table 2.1: Scenarios G – I). No difference (0) in peat depth was expected for Scenarios A – F (Table 2.1) because, in contrast with the peat-forming process of terrestrialization, evaporation and talik drainage are not expected to have as large of an effect on the accumulation of organic matter at the shoreline.

Variable 7: Thaw Depth at Shoreline. Thaw depth (depth to frozen ground, cm) is influenced by many factors including surface temperature, thermal properties of

the surface cover and substrate, soil moisture, and the duration and thickness of snow cover (Brown *et al.* 2000). These factors also influence the stability of permafrost and, therefore, a relatively shallow thaw depth is often used as an easily obtainable indicator of relative permafrost stability (Brown *et al.* 2000). Thus, thaw depth at the shoreline of a lake may be indicative of relative permafrost stability underneath the lake (i.e., vertical permafrost degradation and talik enlargement). In contrast, greater thaw depth at the forest boundary may be indicative of lateral permafrost degradation that is often associated with thermokarst formation and lake growth. Because the effects of vertical and lateral permafrost degradation may be difficult to isolate from one another, expectations for thaw depth at shoreline were classified as unknown when there was a difference expected for thaw depth at the forest boundary (Table 2.1: Scenarios C, F, & I). For Scenario B (Table 2.1), it was expected that the presence of an open talik at decreasing lakes compared to stable permafrost at the paired non-decreasing lakes would be associated with a greater thaw depth at the shoreline (+) at decreasing lakes compared to paired non-decreasing lakes. Similarly, a shallower relative thaw depth at the shoreline of decreasing lakes compared to paired non-decreasing lakes (-) was expected when groundwater recharge (i.e., open talik with a positive hydraulic gradient) was the primary non-decreasing mechanism and talik drainage (i.e., open talik with a negative hydraulic gradient) was not the primary decreasing mechanism (Table 2.1: Scenarios D & G). No difference in thaw depth at shoreline (0) was expected if open taliks were present at both decreasing and non-decreasing lakes (Table 2.1: Scenario A) or if neither

decreasing nor non-decreasing mechanisms involved permafrost degradation (Table 2.1: Scenarios E & H).

Variable 8: Thaw Depth at Forest Boundary. Greater thaw depth at the forest boundary may be indicative of lateral permafrost degradation that is often associated with thermokarst formation and lake growth. The expectation for thaw depth at the forest boundary was classified as unknown whenever there was a difference expected for thaw depth at shoreline because the effects of vertical and lateral permafrost degradation may be difficult to isolate (Table 2.1: Scenarios B, C, D, & G). With the exception of Scenario C, in which the expectation was classified as unknown due an opposing signal for thaw depth at shoreline, a shallower relative thaw depth (more stable permafrost) at the forest boundary of decreasing lakes (-) was expected when thermokarst (i.e., unstable permafrost) was the non-decreasing mechanism (Table 2.1: Scenarios F & I). No difference in thaw depth at the forest boundary (0) was expected if both decreasing and non-decreasing mechanisms were associated with similar levels of permafrost stability (Table 2.1: Scenario A) or did not involve permafrost degradation (Table 2.1: Scenarios E & H).

Supplemental Variable 9: Tree Age. A ninth variable, tree age, was also estimated on the banks of paired lakes. While these data were not critical to the discrimination among competing scenarios, they were used to elucidate the nature of vegetation changes associated with lake area reduction. Younger trees on the banks of decreasing lakes compared to paired non-decreasing lakes may indicate that former lake beds were becoming drier (terrestrial species were invading the former lake bed)

(Vasander *et al.* 1993; Jukaine & Laiho 1995; Klein *et al.* 2005) rather than remaining wet as would be expected if terrestrialization and the resulting peatlands expanded into surrounding forests (i.e., paludification) (Klinger 1996). To investigate this further, a linear regression of relative tree age against transect position was performed for decreasing lakes to identify whether the age of trees at decreasing lakes was directly related to distance from shoreline (i.e., past receding water levels).

Transect Sampling

Sampling was conducted from June 29th to August 28th in 2006 and 2007. All measurements were made along two randomly oriented transects that were perpendicular to one another, passed through the center of each lake and ended at the adjacent forest boundary. Terrestrial measurements were made at the shoreline, at the forest boundary, and at the midpoint between shoreline and the forest boundary. Shoreline was defined as the point where open water or floating mat vegetation transitioned to dry ground (i.e., water table below the ground surface). The forest boundary was defined as the point along the transect where tree cover became dominant (i.e., ratio of tree to shrub and herbaceous vegetation areal cover was greater than one). At non-decreasing lake transects, the forest boundary was often located at or near the shoreline. In these cases (n = 4), the locations were classified as forest boundary with shoreline data being absent in order to avoid erroneous results that could arise from comparing ecosystem types with different moisture content. For example, if these locations had been classified as shoreline they would have been expected to have shallower thaw depths compared to

shoreline locations of decreasing lakes as a result of the lower soil moisture content of a more forested ecosystem type.

Water samples were collected at nominal depths of 30 cm at the center of each lake because thorough mixing was assumed for this sample of shallow lakes. Water samples were analyzed for oxygen isotopic composition by the Alaska Stable Isotope Facility at the University of Alaska Fairbanks. Stable isotope data was obtained using continuous-flow isotope ratio mass spectrometry (CFIRMS). Instrumentation was a Thermo DeltaV Isotope ratio mass spectrometer interfaced with a Thermo thermal conversation elemental analyzer (TC/EA). Stable isotope ratios were reported in δ notation as parts per thousand (‰) deviation from the international standards of Vienna standard mean ocean water (V-SMOW). Electrical conductivity (μS/cm) was measured on-site at the center of each lake with an Oakton^{TM} electrical conductivity meter. Water depth measurements (m) were made at nominal intervals of 5 m along each transect from the edge of floating mat vegetation through the center of the lake. All lakes were shallow enough to allow direct measurement of water depth with a marked string attached to a weight. As an index of surface area, the distance (m) was estimated along each transect from shoreline to shoreline including floating mat vegetation on the surface of the lake. It is important to note that this field-based estimation may not be equivalent to estimates of surface area derived from remotely sensed imagery which may exclude floating mat vegetation. As an index of lake volume, the trapezoidal method (Cox 2007) was used to estimate the cross-sectional area (m^2) of water underneath each transect, extrapolating to

estimate water depth underneath the floating mat. A bathymetric profile was then obtained for each transect by dividing the surface area index by the volume index.

The steepness of lake banks was estimated by measuring the slope (degrees) of the ground surface along each transect at the shoreline, the forest boundary, and at the midpoint between the shoreline and the forest boundary. Slope was measured with a clinometer placed on a 1 meter straight steel probe parallel to the ground surface.

The width (m) of the floating mat vegetation was estimated along each transect starting at the shoreline and ending at open water. Floating mat vegetation was defined as any expanse of herbaceous or shrub vegetation rooted in a thick mat of organic material floating on the water surface and did not include emergent vegetation species rooted at the lake bottom.

Thaw depth (depth to frozen ground, cm) was measured at the shoreline and at the forest boundary with a 3 m steel probe pushed into the ground until frozen ground was reached. When frozen ground was not reached, a minimum thaw depth value of 300 cm was assigned. Peat depth (cm) was measured at the shoreline by digging until mineral soil was reached or to a depth of 40 cm. When mineral soil was not present at 40 cm, a minimum peat depth of 40 cm was assigned. When frozen organic soil was reached before mineral soil, a peat depth equivalent to depth to the frozen layer was assigned.

Dendrochronology was used to estimate the age of trees and shrubs along each transect. Ages were estimated for the tree or shrub species located closest to 6 evenly spaced intervals along each transect from shoreline to the forest boundary. Transect position was denoted with an ordinal integer scale ranging from 1 for the shoreline

position to 6 for the forest boundary position. Stems were collected from small trees and shrubs and a Suunto^{TM} increment borer was used to obtain cores at the root collar of larger trees. Stems and cores were sanded and rings were counted using a magnifying lens.

For some variables, sample sizes were less than the original 15 lake pairs due either to equipment failure ($\delta^{18}O$ and tree age) or to the absence of shoreline data (peat depth at shoreline and thaw depth at shoreline). To avoid pseudoreplication, surface to volume indices, bank slopes, width of floating mats, thaw depths, peat depths, and relative tree ages from the transects at each lake were averaged to obtain a single composite value for each sampled lake.

Statistical Analysis of Differences in Lake Characteristics

The Shapiro-Wilk test with an alpha level of 0.05 was used to test the null hypothesis that the paired differences for each variable came from a normally distributed population. Five variables (electrical conductivity, bank slope, floating mat width, thaw depth at shoreline, and thaw depth at forest boundary) required natural log transformation of the raw data in order to normalize the distributions of paired differences.

Linear regression was used to estimate the relationship between average relative tree age and transect position at decreasing lakes (SAS Institute, Inc. 2003). Tree ages were converted to relative age by dividing by the oldest tree age along each transect to enable combination of data from all lakes into a single analysis. The untransformed relative ages were left skewed and ranged from .05 to 1. These data were normalized

with an arcsine (radians) square root transformation which is the standard transformation for skewed proportion data that range from 0 to 1(Ahrens *et al.* 1990).

Two-tailed paired t-tests (SAS Institute, Inc. 2003) were conducted to test the null hypotheses that the mean differences in lake characteristics between paired decreasing and non-decreasing lakes were zero. When a null hypothesis was rejected, the result (+ or -) was assigned based on the direction of the mean difference between paired decreasing and non-decreasing lakes.

A single paired t-test with an alpha level of 0.05 was used to compare tree age (Supplemental Variable 9) between decreasing and non-decreasing lakes. Multiple paired t-tests for the remaining eight variables (Table 2.1) were used to discriminate among competing mechanistic scenarios because a multivariate logistic regression approach resulted in complete separation.

For the eight discriminatory variables (Table 2.1), Holm's Sequentially Selective Bonferroni Method (Holm 1979) was used to reduce the Type I error rate when making multiple comparisons (i.e., the probability of rejecting any one of the eight independent variable null hypotheses when true). Experiment-wise alpha level was set at 0.1 a priori to reduce the Type II error rate when making multiple comparisons (i.e., probability of accepting any one of the eight null hypotheses when false) (Manderscheid 1965). Thus, to declare experiment-wise significance at alpha = 0.1, individual variable P-values had to be much lower than 0.05.

Conditional probabilities were calculated for each of the nine possible scenarios of contrasting paired-lake mechanisms (Table 2.1: Scenarios A-I). Conditional

probabilities update the probability of a certain event (e.g. a scenario) based on new information (e.g. observed results). The formula used to calculate conditional probabilities was: $P_C = P_{scen}/P_{res}$ where P_C = conditional probability, P_{scen} = random probability of scenario, P_{res} = random probability of the number of results that match variable expectations for the specified scenario (Casella & Berger 2002). Unknown expectations were excluded from the calculations of conditional probabilities. Under the assumption that the outcomes for the eight variables in Table 2.1 are independent events, P_{scen} is the random probability that any combination of x of the 3 possible results (+, -, 0) would occur ($1/3^x$, where x = the number of known expectations). P_{res} is the random probability of observing y number of results that match the expectations ($1/3^y$). Higher probabilities indicate a higher likelihood for the scenarios. Although the assumption of independence is most likely false, leading to inflated probabilities, the calculation of these conditional probabilities did enable the rank ordering and comparison of competing scenarios. The scenario that had the best match between predicted and observed results (i.e., the greatest probability given the results) was then identified.

Results

The area of decreasing and non-decreasing lakes from the earliest imagery ranged from 0.38 - 44.64 hectares ($\bar{x}$ = 9.35 ha, SE = 3.77 ha, n = 15) and 0.46 - 15.66 hectares ($\bar{x}$ = 3.40 ha, SE = 1.19 ha, n = 15), respectively and from the most current imagery ranged 0.12 - 19.24 hectares ($\bar{x}$ = 3.72 ha, SE = 1.50 ha, n = 15) and 0.24 - 16.83 hectares ($\bar{x}$ = 3.62 ha, SE = 1.26 ha, n = 15), respectively. Two of the 15 non-decreasing

lakes increased significantly ($P < 0.05$) in size since the 1950s, increasing by 13% and 46% of their total lake area from the earliest to the latest imagery date. The remaining 13 non-decreasing lakes had non-significant ($P > 0.05$) trends in lake area. Twelve of these 13 non-decreasing lakes had coefficients of variation that were less than 0.20 (Table 2.2) suggesting that non-significant trends in lake area were the result of relative stability as opposed to large bi-directional changes in lake area. On average, the surface area of sampled decreasing lakes declined 61% (SE = 3.89%, n = 15) from the earliest to the latest imagery date, which corresponded to an average loss of 5.63 hectares (SE = 2.42 ha, n = 15) of surface area per lake. The maximum depth of decreasing and non-decreasing lakes ranged 0.42 - 1.64 m ($\bar{x}$ = 0.98 m, SE = 0.09 m, n = 15) and 0.70 - 3.20 m ($\bar{x}$ = 1.97 m, SE = 0.19 m, n = 15), respectively.

Trees were significantly ($P = 0.0003$, Fig. 2.4a) younger on the banks of decreasing lakes compared to non-decreasing lakes. In addition, the relative age of trees significantly ($P < 0.0001$; $R^2 = 0.55$, Fig. 2.5) increased with distance from shoreline at decreasing lakes indicating that the banks of decreasing lakes were succeeding toward drier forest vegetation types.

Decreasing lakes had significantly greater electrical conductivity ($P = 0.0331$, Fig. 2.4b), greater surface:volume indices ($P = 0.0001$, Fig. 2.4c), shallower bank slopes ($P < 0.0001$, Fig. 2.4d), wider floating mats ($P < 0.0001$, Fig. 2.4e), greater shoreline peat depths ($P = 0.0026$, Fig. 2.4f), and shallower thaw depths at the forest boundary ($P = 0.0151$, Fig. 2.4g). Each of these individual P-values was significant using the Holm's Sequentially Selective Bonferroni Method with an experiment-wise alpha level of 0.1.

The conditional probability of obtaining these results (Fig. 2.4, Table 2.3) was highest (Table 2.4) for the scenario that postulated terrestrialization/evapotranspiration (Fig. 2.2c) as the primary driver of lake area reduction combined with thermokarst formation (Fig. 2.2f) as the primary mechanism for non-decreasing lake area (Table 2.1: Scenario I).

The observation of significantly greater surface to volume indices (Fig. 2.4c) and significantly shallower bank slopes (Fig. 2.4d) at decreasing lakes was inconsistent with talik drainage as a decreasing mechanism (Table 2.1: Scenarios B & C) because open taliks are more likely to form in deeper lakes. In addition, there was no difference ($P = 0.3774$, Fig. 2.4h) in thaw depth at the shoreline between paired lakes and this observation did not lend support to the presence of greater talik enlargement at decreasing lakes compared to paired non-decreasing lakes (Table 2.1: Scenario B).

All scenarios with surface water evaporation as the primary decreasing mechanism (Table 2.1: Scenarios D-F) had expectations of greater ^{18}O enrichment at decreasing lakes compared to paired non-decreasing lakes and no such difference ($P = 0.4903$, Fig. 2.4i) in ^{18}O enrichment was observed. The lack of a difference in ^{18}O enrichment was primarily due to high variability in the direction of the difference between paired lakes indicating substantial heterogeneity in the relative role of evaporation and water inputs on water balances for this sample of lakes. Thus, the results did not support the presence of consistently greater surface water evaporation rates that exceeded water inputs at decreasing lakes (Table 2.1: Scenarios D, E, & F). This result was, however, consistent with greater rates of transpiration at decreasing lakes that would

result from wider floating mats of vegetation (Table 2.1: Scenarios H & I) and have no effect on relative isotopic enrichment (Gonfiantini *et al.* 1965; Dawson & Ehleringer 1991; Gat 1996; Gibson & Edwards 2002). In further support of terrestrialization/evapotranspiration as the mechanism for lake area reduction (Table 2.1: Scenarios H & I), greater electrical conductivity (Fig. 2.4b), floating mat width (Fig. 2.4e), and shoreline peat depth (Fig. 2.4f) were observed at decreasing lakes compared to paired non-decreasing lakes.

Thaw depth at the forest boundary was critical for discriminating between Scenarios H & I (Table 2.1) and isolating thermokarst as the primary non-decreasing mechanism. The presence of greater thaw depths at the forest boundary of non-decreasing lakes (Fig. 2.4g) was consistent with the expectation for Scenario I of more unstable permafrost at the forest boundary of non-decreasing lakes and did not support the expectation for Scenario H of more stable permafrost at the forest boundary of non-decreasing lakes. The lack of a difference in $\delta^{18}O$ signatures did not lend support to groundwater recharge as the primary non-decreasing mechanism (Table 2.1: Scenarios A, D, & G) because groundwater recharge would have led to relatively depleted ^{18}O at non-decreasing lakes compared to paired decreasing lakes (Payne 1970; Gat 1996; Turner *et al.* 2010). Likewise, the electrical conductivity results did not lend support to sub-permafrost groundwater recharge at non-decreasing lakes (Table 2.1: Scenario A). In addition, the lack of a difference in thaw depth at shoreline did not lend support to greater talik enlargement and, therefore, sub-permafrost groundwater recharge at non-decreasing lakes (Table 2.1: Scenarios D & G). Thus, the results provided the strongest support for

Scenario I, that terrestrialization/evapotranspiration was the primary mechanism for lake area reduction combined with thermokarst as the primary mechanism for non-decreasing area for this sample of lakes.

Discussion

This work is the first to use a widely distributed sample of lakes in the boreal forest to simultaneously evaluate a suite of hypotheses that might explain why one member of a pair of adjacent closed-basin lakes was decreasing in area while the other was not. The fine-scale mechanisms identified here are critical to understanding the implications of observed broad-scale reductions in lake number and area both in these study areas and in other study areas in discontinuous permafrost (Smith *et al.* 2005; Riordan *et al.* 2006) during the past ~50 years.

Non-decreasing lakes were deeper (mean difference in maximum depth = 1 m) with steeper banks and lower surface to volume indices than decreasing lakes (Fig. 2.4). Deeper lakes formed from thermokarst in relatively ice-rich permafrost may be more persistent features on the landscape while shallow lakes may be more susceptible to floating mat development, encroachment, and basin infilling (Jorgensen & Shur 2007). Because the size and depth of thermokarst lakes is largely controlled by relative permafrost ice content (the higher the ice content, the greater the degree of subsidence) (Hopkins 1949; Burn 1992; Jorgenson & Shur 2007), regions of relatively ice-poor permafrost may be dominated by shallow lakes that are more susceptible to losses in lake area resulting from terrestrialization (Payette *et al.* 2004). The large degree of subsidence

that occurs when deep lakes are formed may more effectively separate the former terrestrial system from the surface of the new thermokarst lake. In contrast, shallow subsidence in comparatively ice-poor permafrost may leave an overhanging organic mat in close contact with the new aquatic system that serves as a substrate for colonization by floating aquatic vegetation (Racine *et al.* 1998). In addition, shallow lakes tend to have warmer water temperatures than deep lakes which may facilitate terrestrialization. Broad-scale maps of permafrost ice content have been developed based on the correlation of ice content with the thickness of surficial deposits and proximity to bedrock and could be useful in future studies to identify regional susceptibility to lake area reduction (Heginbottom & Radburn 1992; Brown *et al.* 2001).

The lack of a difference in $\delta^{18}O$ between paired lakes did not lend support to evaporation exceeding water inputs at decreasing lakes. While decreasing lakes may have had greater evaporation rates compared to non-decreasing lakes due to a greater surface to volume ratio, these increased evaporation rates may have been offset by greater runoff from relatively larger catchments at decreasing lakes thus leading to no net effect on lake water balance, and consequently $\delta^{18}O$, as a result of evaporation. Consistent with this concept, average transect length from shoreline to forest boundary (i.e., catchment area) was greater at decreasing lakes compared to non-decreasing lakes at 13 of the 15 lake pairs. Proportionately greater surface runoff at decreasing lakes may also deliver more dissolved ions to these aquatic systems further enhancing productivity and floating mat encroachment at these sites. The non-significant difference in $\delta^{18}O$ observed for our *population* of paired lakes was characterized by a large degree of variability in the

direction and magnitude of $\delta^{18}O$ differences among individual lake pairs. Thus, it remains a possibility that evaporation may have exceeded water inputs at some decreasing lakes although not for the sampled population as a whole. There was no indication of regional differences in the direction and magnitude of $\delta^{18}O$ differences between paired lakes. Although $\delta^{18}O$ is a useful inferential tool for understanding the relative role of evaporation compared to water inputs in a lake's hydrological budget, it is limited in its ability to identify the absolute magnitudes and sources of water inputs and outputs (e.g., snowmelt, lateral flow, and subsurface flow). More thorough investigations of the various components of the water budgets at lakes in future studies may provide an additional context for the interpretation of oxygen isotope results.

The observations of decreasing lake area were most likely the result of the encroachment of floating mat vegetation on the surface of the lake while decreases in both lake area and volume may result from increased transpiration rates that result from increased aquatic vegetation. Observations of $\delta^{18}O$ and electrical conductivity were consistent with increased transpiration rates that have no effect on lake $\delta^{18}O$ (Gonfiantini *et al.* 1965; Dawson & Ehleringer 1991; Gat 1996; Gibson & Edwards 2002) but may cause an increase in lake ion concentrations. Similarly, Simpson *et al.* 1987 concluded that a water deficit accompanied by increased ion concentrations and no change in $\delta^{18}O$ was primarily due to transpiration. Evapotranspiration from floating sedge fens and sphagnum bogs can be an important component of a lake water balance and can exceed evaporation from a pan or open water surface (Sturges 1968; Clymo 1973; Rutherford & Byers 1973; Nichols & Brown 1980; Koerselman & Beltman 1988). Thus, an initial loss

in surface area due to encroaching floating mat vegetation provides a mechanism for, and thus potentially precedes, losses in water volume resulting from transpiration. In contrast with evaporation and talik drainage which would lead to receding shorelines and a loss in water volume proportional to remotely detected losses in surface area, terrestrialization initially obscures surface water potentially leading to overestimates of remotely inferred water volume loss.

Terrestrialization was originally described as an autogenic successional process by which an open water aquatic system transitions to a terrestrial system via a specific sequence of wetland communities (Clements 1916; Tallis 1983). Later work has emphasized the dynamic nature of this process and has demonstrated that terrestrialization can involve a wide variety of successional trajectories which can be greatly influenced by external allogenic processes related to climate (Walker 1970; Tallis 1983). For example, an ombrotrophic raised bog phase is most likely to occur in wet climates where rainfall is sufficient to support *Sphagnum* growth and the accumulation of peat in isolation from minerotrophic waters. In contrast, terrestrialization in drier climates tends to proceed towards a mesophytic forested community (Tallis 1983). The observation of younger trees and shrubs at infilling lakes may be indicative of a trajectory towards a forested ecosystem as would be expected in regions of interior Alaska with low precipitation.

Terrestrialization usually involves a minerotrophic floating fen phase at some point during its trajectory. This phase is characterized by aquatic systems with high productivity (Tallis 1983; Hu & Davis 1995) and rapid rates of mat encroachment onto

open water. Previous studies have documented rates of floating mat encroachment of 42 m over 24 years (Gates 1942) and complete overgrowth of a 92 m by 18 m open water area by a floating mat over 3 years (Jewell & Brown 1929). Our observations of encroaching floating mats over shallow lakes with relatively high electrical conductivities in the Yukon Flats and Tetlin study areas over the past ~50 years may be indicative of this minerotrophic fen phase of peatland development. In contrast, even though decreasing lakes in the Kaiyuh Flats had higher electrical conductivities compared to non-decreasing lakes, the average electrical conductivity of all sampled lakes in the Kaiyuh Flats ($\bar{x}$ = 42 µS/cm, SE = 3.3 µS/cm) was lower than the average electrical conductivity of lakes in the other study areas ($\bar{x}$ = 269 µS/cm, SE = 37.6 µS/cm) suggesting that this region may be relatively more ombrotrophic.

While terrestrialization likely involves some autogenic internal processes (Kratz & DeWitt 1986; Korhola 1992; Hu & Davis 1995), several studies have identified climate warming as an important external force in initiating and accelerating terrestrialization during warm, dry periods of the Holocene (Nicholson & Vitt 1994; Hu & Davis 1995; Korhola 1995; Campbell *et al.* 1997). Observations of floating mat encroachment at multiple independent sites located in four areas that had weak (R^2 from 0.068 to 0.17) but significant positive linear trends in mean annual temperature ($P < 0.05$) and annual total PET ($P < 0.1$) since the 1950s (Riordan *et al.* 2006) suggests that a drier, warmer climate may have initiated or accelerated terrestrialization at these sites. Contemporary climate warming may facilitate floating mat development by lengthening the growing season (Smith *et al.* 2004; Euskirchen *et al.* 2006), thereby increasing water temperatures,

carbon uptake, vegetation growth (Keeling *et al.* 1996; Myneni *et al.* 1997) and evapotranspiration rates (Oechel *et al.* 2000) which can increase aquatic system productivity.

In contrast with evaporation and talik drainage, which would involve receding shorelines and an immediate shift to drier conditions, terrestrialization involves the gradual infilling of a lake basin with organic matter which would convert a lake to a temporary carbon sink providing an initial negative feedback to climate warming (Whiting & Chanton 2001; Payette *et al.* 2004). The observation of greater peat depths at the shorelines of decreasing lakes is indicative of this increased carbon storage. An additional negative feedback may result if the development of broad-leaved macrophytes on the surface of the lake leads to increased albedo. Alternatively, the development of sedge vegetation may serve as a positive feedback by facilitating methane release (King *et al.* 1998).

While terrestrialization may lead to a transient increase in carbon storage at the water's edge, a transition to drier conditions on lake banks may lead to higher decomposition rates, increased fire frequency (Pitkanen *et al.* 1999) and greater CO_2 efflux (Gorman 1991; Gignac & Vitt 1994; Keyser *et al.* 2000; McGuire *et al.* 2000; Chapin *et al.* 2000). The observation of new tree recruitment on decreasing lake banks suggests that as terrestrialization proceeds, transpiration rates may eventually exceed the water retaining capacity of the newly formed peat leading to drier conditions that can support new tree growth and higher decomposition rates. The net effect of drier conditions on carbon storage will depend on the balance between enhanced CO_2 efflux,

increased carbon storage in new tree biomass, and decreased methane efflux associated with a declining water table (Roulet *et al.* 1992; Laine *et al.* 1996; Minkkinen *et al.* 2002; Hargreaves *et al.* 2003). An improved understanding of the net effect of terrestrialization on carbon storage, albedo, and global radiative forcing should be the focus of future research.

While the results lend strong support to terrestrialization as the primary mechanism in lake area reduction, it remains a possibility that evaporation or talik drainage mechanisms may be occurring in conjunction with or may have facilitated terrestrialization prior to field sampling. Although the results did not support the involvement of talik drainage in lake area reduction, logistical constraints prevented the use of ground penetrating radar and piezometers to directly detect the presence of taliks and the direction of the hydraulic gradient. In addition, more reliable and fine-scaled descriptions of surficial geology, parent material and lake origin (e.g., silty floodplain vs. eolian sand sheets) may be able to further elucidate susceptibility to permafrost thaw and the roles of surface and subsurface flow at lake sites.

Among the various lake area reduction hypotheses considered, terrestrialization may have the most positive implications for ecosystem services. The involvement of terrestrialization suggests that 1) losses of water volume may occur at a slower rate than that inferred from remotely sensed losses in lake area, 2) the losses in water volume that do occur may lead to initial increases in carbon storage in former lake basins, and 3) the loss of open water area to floating mat vegetation may lead to an initial increase in high quality waterfowl nesting habitat (Krapu *et al.* 1979; Bouffard *et al.* 1988; Arnold *et al.*

1993; Solberg & Higgins 1993) compared to evaporation or talik drainage. The net effect of heterogeneous lake area change in the boreal forest will depend on specific regional balances of lake area growth and reduction.

Acknowledgements

We thank Robert Warren and Kevin Wyatt for help with field work and Bruce Finney for assistance with isotope analyses. U.S. Fish and Wildlife Service (FWS) staff at Yukon Flats, Tetlin, and Koyukuk/Nowitna National Wildlife Refuges helped with logistics and float plane access to field sites. Funding was provided by FWS, U.S. Geological Survey Climate Effects Network, the University of Alaska Fairbanks (UAF) Special President's Fund, and a UAF Graduate School Thesis Completion Fellowship. We thank Eric J. Taylor, Jennifer Harden, A. Dave McGuire, and Joshua Rose for their assistance and reviews of earlier drafts. Any use of trade names is for descriptive purposes only and does not imply endorsement by the U.S. Government.

References

Ahrens WH, Cox DJ, Budhwar G (1990) Use of the arcsine and square root transformations for subjectively determined percentage data. *Weed Science*, **38**, 452-458.

Anderson LA, Abbott MB, Finney BP, Burns SJ (2007) Late Holocene moisture balance variability in the southwest Yukon Territory, Canada. *Quaternary Science Reviews*, **26**, 130-141.

Anisimov OA, Shiklomanov NI, Nelson FE (2002) Variability of seasonal thaw depth in permafrost regions: a stochastic modeling approach. *Ecological Modelling*, **153**, 217-227.

Arnold TW, Sorenson MD, Rotella JJ (1993) Relative success of overwater and upland mallard nests in southwestern Manitoba. *Journal of Wildlife Management*, **57**, 578-581.

Arp CD, Jones BM (2009) Geography of Alaska lake districts: identification, description, and analysis of lake-rich regions of a diverse and dynamic state: U.S. Geological Survey Scientific Investigations Report 2008-5215, 40 pp.

Billings WD, Peterson KM (1980) Vegetational change and ice-wedge polygons through the thaw-lake cycle in arctic Alaska. *Arctic and Alpine Research*, **12**, 413-432.

Bouffard SH, Sharp DE, Evans CC (1988) Overwater nesting by ducks: a review and management implications. In: *Eighth Great Plains wildlife damage control workshop proceeding. USDA Forest Service General Technical Report* eds (Uresk DW, Schenbeck GL, Sefkin R), pp 153-158.

Britton ME (1957) Vegetation of the arctic tundra. In: *Arctic Biology* ed (Hansen HP), pp 26-72, Oregon State University Press, Corvallis.

Boyd CE, Hess LW (1970) Factors influencing shoot production and mineral nutrient levels in *Typha latifolia*. *Ecology*, **51**, 296-300.

Brewer MC (1958) Some results of geothermal investigations of permafrost in Northern Alaska. *Transactions, American Geophysical Union*, **39**, 19-26.

Brown J, Ferrians Jr. O, Heginbottom JA, Melnikov ES (2001) Circum-Arctic map of permafrost and ground-ice conditions. Boulder, CO, National Snow and Ice Data Center/World Center for Glaciology. Digital Media.

Brown J, Hinkel KM, Nelson FE (2000) The Circumpolar Active Layer Monitoring (CALM) Program: research designs and initial results. *Polar Geography*, **24**, 165-258.

Burn CR (1992) Canadian landform examples – 24. Thermokarst lakes. *The Canadian Geographer*, **36**, 81-85.

Burn CR (2002) Tundra lakes and permafrost, Richards Island, western Arctic coast, Canada. *Canadian Journal of Earth Sciences*, **39**, 1281-1298.

Burn CR, Smith MW (1990) Developmant of thermokarst lakes during the Holocene at sites near Mayo, Yukon Territory. *Permafrost and Periglacial Processes*, **1**, 161-176.

Campbell DR, Duthie HC, Warner BG (1997) Post-glacial development of a kettle-hole peatland in southern Ontario. *Ecoscience*, **4**, 404-418.

Carpenter SR (1980) Enrichment of Lake Wingra, Wisconsin, by submerged macrophyte decay. *Ecology*, **61**, 1145-1155.

Casella G, Berger RL (2002) *Statistical Inference* eds (Crockett C), pp 660, Duxbury, Pacific Grove, CA.

Chapin III FS, McGuire AD, Randerson J, *et al.* (2000) Arctic and boreal ecosystems of western North America as components of the climate system, *Global Change Biology*, **6**, 211-223.

Clegg BF, Hu FS (2010) An oxygen-isotope record of Holocene climate change in the south-central Brooks Range, Alaska, *Quaternary Science Reviews*, in press.

Clements FE (1916) *Plant Succession*, pp 512, Carnegie Institution of Washington, Washington, DC.

Clymo RS (1973) The growth of sphagnum: some effects of environment. *Journal of Ecology*, **61**, 849-869.

Cooper LW, DeNiro MJ, Keeley JE (1991) The relationship between stable oxygen and hydrogen isotope ratios of water in astomatal plants, In *Stable Isotope Geochemistry: A Tribute to Sam Epstein*. pp 247-255 eds (Taylor HP, O'Neill JR, Kaplan IR) Geochemical Society, San Antonio.

Cox MG (2007) The area under a curve specified by measured values. *Metrologia*, **44**, 365-378.

Craig H (1961) Standards for reporting concentrations of deuterium and oxygen-18 in natural waters. *Science*, **133**, 1833-1834.

Dansereau P, Segadas-Vianna F (1951) Ecological study of the peat bogs of eastern North America. *Canadian Journal of Botany*, **30**, 490-520.

Dawson TE, Ehleringer JR (1991) Streamside trees that do not use stream water. *Nature*, **350**, 335-337.

DeNiro MJ, Epstein S (1979) Relationship between the oxygen isotope ratios of terrestrial plant cellulose, carbon dioxide, and water. *Science*, **204**, 51-53.

Drury WH (1956) *Bog Flats and Physiographic Processes in the Upper Kuskokwim River Region, Alaska* eds (Rollins RC, Foster RC), pp 130, The Gray Herbarium of Harvard University, Cambridge.

Epstein S, Thompson P, Yapp CJ (1977) Oxygen and hydrogen isotopic ratios in plant cellulose. *Science*, **198**, 1209-1215.

Euskirchen ES, McGuire AD, Kicklighter DW *et al.* (2006) Recent shifts in the dynamics governing growing season length and productivity in terrestrial high-latitude ecosystems. *Global Change Biology*, **12**, 731-750.

Gat JR (1996) Oxygen and hydrogen isotopes in the hydrologic cycle. *Annual Review of Earth and Planetary Sciences*, **24**, 225-262.

Gates FC (1942) The bogs of northern lower Michigan. *Ecological Monographs*, **12**, 213-254.

Gaudet JJ (1977) Uptake, accumulation and loss of nutrients by papyrus in tropical swamps. *Ecology*, **58**, 415-422.

Gibson JJ, Edwards TWD (2002) Regional water balance trends and evaporation-transpiration partitioning from a stable isotope survey of lakes in northern Canada. *Global Biogeochemical Cycles*, **16**, 1-18.

Gignac LD, Vitt DH (1994) Responses of northern peatlands to climate change: effects on bryophytes. *The Journal of the Hattori Botanical Laboratory*, **75**, 119-132.

Gonfiantini R, Gratziu S, Tangiorgi E (1965) Oxygen isotopic composition of water in leaves. In: *Isotopes and radiation in soil-plant nutrition studies*, pp 405-410, Vienna, International Atomic Energy Association.

Gorman E (1991) Northern peatlands: role in the carbon cycle and probable responses to climate warming. *Ecological Applications* **1**, 182-195.

Hargreaves KJ, Milne R, Cannell MGR (2003) Carbon balance of afforested peatland in Scotland. *Forestry*, **76**, 299-317.

Hassol SJ (2004) *ACIA, Impacts of a Warming Arctic: Arctic Climate Impact Assessment.* Cambridge University Press.

Heginbottom JA, Radburn LK (1992) Permafrost and ground ice conditions of northwestern Canada; Geological Survey of Canada, Map 1691A, scale 1:1,000,000. Digitized by S. Smith, Geological Survey of Canada. Boulder, CO: National Snow and Ice Data Center/World Data Center for Glaciology. Digital Media.

Hinzman LD, Bettez ND, Bolton WR, *et al.* (2005) Evidence and implications of recent climate change in northern Alaska and other arctic regions. *Climatic Change*, **72**, 251-298.

Hinzman LD, Goering DJ, Li S, Kinney TC (1997) Numeric simulation of thermokarst formation during disturbance. In: *Disturbance and Recovery in Arctic Lands: An Ecological Perspective* ed (Crawford RM), pp 621, Kluwer Academic Publishers, Dordrecht.

Holm S (1979) A simple sequentially rejective multiple test procedure. *Scandinavian Journal of Statistics*, **6**, 65-70.

Hopkins DM (1949) Thaw lakes and thaw sinks in the Imuruk Lake area, Seward Peninsula, Alaska. *The Journal of Geology*, **57**, 119-131.

Hu FS, Davis RB (1995) Postglacial development of a Maine bog and paleoenvironmental implications. *Canadian Journal of Botany*, **73**, 638-649.

Jewell ME, Brown HW (1929) Studies on northern Michigan bog lakes. *Ecology*, **10**, 427-475.

Johnston CA (1991) Sediment and nutrient retention by freshwater wetlands: effects on surface water quality. *Critical Reviews in Environmental Control*, **21**, 491-565.

Jorgenson MT, Yoshikawa K, Kanveskiy M, Shur YL, Romanovsky V, Marchenko S, Grosse G, Brown J, Jones B (2008) Permafrost characteristics of Alaska. In: *Proceedings of the Ninth International Conference on Permafrost*, 29 June – 3 July 2008, Fairbanks , Alaska eds (Kane DL, Hinkel KM), pp. 121-122, Institute of Northern Engineering, University of Alaska Fairbanks.

Jorgenson MT, Osterkamp TE (2005) Response of boreal ecosystems to varying modes of permafrost degradation. *Canadian Journal of Forest Research*, **35**, 2100-2111.

Jorgenson MT, Racine CH, Walter JC, Osterkamp TE (2001) Permafrost degradation and ecological changes associated with a warming climate in central Alaska. *Climate Change*, **48**, 551-579.

Jorgenson MT, Shur Y (2007) Evolution of lakes and basins in northern Alaska and discussion of the thaw lake cycle. *Journal of Geophysical Research,* **112**, F02S17.

Jukaine HV, Laiho R (1995) Long-term effects of water level drawdown on the vegetation of drained pine mires in southern Finland. *Journal of Applied Ecology*, **32**, 785-802.

Kane DL, Slaughter CW (1973) Recharge of a central Alaska lake by subpermafrost groundwater. In: *Permafrost. Proceedings of the 2nd International Conference, Yakutsk* eds (Pewe TL, MacKay JR), pp 458-462, North American Contribution, National Academy of Sciences, Washington, DC.

Kaufman DS, Schneider DP, McKay NP, *et al.* (2009) Recent Warming Reverses Long-Term Arctic Cooling. *Science*, **325**, 1236-1239.

Keeling CD, Chin JFS, Whorf TP (1996) Increased activity of northern vegetation inferred from atmospheric CO_2 measurements. *Nature*, **382**, 146-149.

Keyser AR, Kimball JS, Nemani RR, Running SW (2000) Simulating the effects of climate change on the carbon balance of North American high-latitude forests. *Global Change Biology*, **6**, 185-195.

King JY, Reeburgh WS, Regli SK (1998) Methane emission and transport by arctic sedges in Alaska: Results of a vegetation removal experiment. *Journal of Geophysical Research*, **103**, D00052.

Klein E, Berg EE, Dial R (2005) Wetland drying and succession across the Kenai Peninsula Lowlands, south-central Alaska. *Canadian Journal of Forest Research*, **35**, 1931-1941.

Klinger LF (1996) The myth of the classic hydrosere model of bog succession. *Arctic and Alpine Research*, **28**, 1-9.

Koerselman W, Beltman B (1988) Evapotranspiration from fens in relation to Penman's potential free water evaporation (E_0) and pan evaporation. *Aquatic Botany*, **31**, 307-320.

Korhola A (1992) Mire induction, ecosystem dynamics and lateral extension on raised bogs in the southern coastal area of Finland. *Fennia*, **170**, 25-94.

Korhola A (1995) Lake terrestrialization as a mode of mire formation: A regional review. *Publications of the National Board of Waters and the Environment*, **207**, 11-21.

Krapu GL, Talent LG, Dwyer TJ (1979) Marsh nesting by mallards. *Wildlife Society Bulletin*, **7**, 104-110.

Kratz TK, DeWitt CB (1986) Internal factors controlling peatland-lake ecosystem development. *Ecology*, **67**, 100-107.

Kroger R, Holland MM, Moore MT, Cooper CM (2007) Plant senescence: A mechanism for nutrient release in temperate agricultural wetlands. *Environmental Pollution*, **146**, 114-119.

Laine J, Silvola J, Tolonen K *et al.* (1996) Effect of water-level drawdown on global climatic warming: Northern peatlands. *Ambio*, **25**, 179-184.

Mackay JR (1992) Lake stability in an ice-rich permafrost environment: Examples from the Western Arctic coast. In: *Aquatic Ecosystems in Semi-arid Regions: Implications for Resource Management. N.H.R.I. Symposium Series 7* eds(Robarts RD & Bothwell ML), pp. 1-26, Environment Canada, Saskatoon.

Manderscheid LV (1965) Significance Levels. 0.05, 0.01, or ?. *Journal of Farm Economics,* **47**, 1381-1385.

Manley W, Kaufman D (2002) Alaska PaleoGlacier Atlas: Boulder, CO, Institute of Arctic and Alpine Research (INSTAAR), University of Colorado.

McGuire AD, Sitch S, Clein JS, *et al.* (2000) Carbon balance of the terrestrial biosphere in the twentieth century: Analyses of CO_2, climate, and land use effects with four process-based ecosystem models. *Global Biogeochemical Cycles*, **15**, 183-206.

Minkkinen J, Korhonen R, Savolainen I, Laine J (2002) Carbon balance and radiative forcing of Finnish peatlands 1900-2100 – the impact of forestry drainage. *Global Change Biology*, **8**, 785-799.

Myneni RB, Keeling CD, Tucker CJ, Asrar G, Nemani RR (1997) Increased plant growth in the northern high latitudes from 1981-1991. *Nature*, **386**, 698-702.

Nelson FE, Shiklomanov NI, Mueller GR (1999) Variability of active-layer thickness at multiple spatial scales, north-central Alaska, USA. *Arctic, Antarctic, and Alpine Research*, **31**, 158-165.

Nichols DS, Brown JM (1980) Evaporation from a sphagnum moss surface. *Journal of Hydrology*, **48**, 289-302.

Nichols DS, Keeney DR (1972) Nitrogen and phosphorus release from decaying water milfoil. *Hydrobiologia*, **42**, 509-525.

Nicholson BJ, Vitt DH (1994) Wetland development at Elk Island National Park, Alberta, Canada. *Journal of Paleolimnology*, **12**, 19-34.

Oechel WC, Vourlitis GL, Hastings SJ, Zulueta RC, Hinzman L, Kane D (2000) Acclimation of ecosystem CO_2 exchange in the Alaskan Arctic in response to decadal climate warming. *Nature*, **406**, 978-981.

Osterkamp TE (2005) The recent warming of permafrost in Alaska. *Global and Planetary Change,* **49**, 187-202.

Osterkamp TE, Vierek L, Shur Y, Jorgenson MT, Racine T, Doyle A, Boone RD (2000) Observations of thermokarst and its impact on boreal forests in Alaska, USA. *Arctic and Alpine Research,* **32,** 303-315.

Payette S, Delwaide A, Caccianiga M, Beauchemin M (2004) Accelerated thawing of subarctic peatland permafrost over the last 50 years. *Geophysical Research Letters*, **31**, L18208.

Payne BR (1970) Water balance of lake Chala and its relation to groundwater from tritium and stable isotope data. *Journal of Hydrology*, **11**, 47-58.

Pitkanen A, Turunen J, Tolonen K (1999) The role of fire in the carbon dynamics of a mire, eastern Finland. *Holocene*, **9**, 453-462.

Racine CH, Jorgenson MT, Walters JC (1998) In: *Permafrost. Proceedings of the 7th International Conference, Yellowknife,* pp 927-933, Collection Nordicana No 55.

Riordan B, Verbyla D, McGuire AD (2006) Shrinking ponds in subarctic Alaska based on 1950-2002 remotely sensed images. *Journal of Geophysical Research*, **111**, G04002.

Roulet N, Moore T, Bubier J, Lafleur P (1992) Northern fens: methane flux and climatic change. *Tellus*, **44B**, 100-105.

Rouse WR, Douglas MS, Hecky RE, *et al.* (1997) Effects of climate change on the freshwaters of arctic and subarctic North America. In: *Freshwater Ecosystems and Climate Change in North America*, ed (Cushing CE), pp 55-84. John Wiley & Sons, Chichester.

Rutherford RJ, Byers GL (1973) Controlling wetland water by suppressing evaporation. *Canadian Agricultural Engineering*, **15**, 9-11.

SAS institute, Inc. (2003) *SAS 9.1.3 for Windows*, Cary, NC.

Schindler DW, Beaty KG, Fee EJ, *et al.* (1990) Effects of climatic warming on lakes of the central boreal forest. *Science*, **250**, 967-970.

Simpson HJ, Hamza MS, White JWC, Nada A, Awad MA (1987) Evaporative enrichment of deuterium and ^{18}O in arid zone irrigation. In: *Isotope Techniques in Water Resources Development,* pp 241-256.

Serreze MC, Walsh JE, Chapin III FS *et al.* (2000) Observational evidence of recent change in the northern high-latitude environment. *Climatic Change*, **46**, 159-207.

Smith LC, Sheng Y, MacDonald GM, Hinzman LD (2005) Disappearing arctic lakes. *Science*, **308**, 1429.

Smith NV, Saatchi SS, Randerson JT (2004) Trends in high northern latitude soil freeze and thaw cycle from 1988 to 2002. *Journal of Geophysical Research*, **109**, D12101.

Smol JP, Douglas MS (2007) Crossing the final ecological threshold in high arctic ponds. *Proceedings of the National Academy of Sciences*, **104**, 12395-12397.

Solberg KL, Higgins KF (1993) Overwater nesting by ducks in northeastern South Dakota. *The Prairie Naturalist*, **25**, 19-22.

Sturges DA (1968) Evaporation at a Wyoming mountain bog. *Journal of Soil Water Conservation*, **23**, 23-25.

Swanson DK (1996) Susceptibility of permafrost soils to deep thaw after forest fires in interior Alaska, USA, and some ecological implications. *Arctic and Alpine Research,* **28,** 217-227.

Tallis JH (1983) Changes in wetland communities. In: *Ecosystems of the world* ed (Gore AJP), pp 311-347, Elsevier, Amsterdam.

Turner KW, Wolfe BB, Edwards TWD (2010) Characterizing the role of hydrological processes on lake water balances in the Old Crow Flats, Yukon Territory, Canada, using water isotope tracers. *Journal of Hydrology*, **386**, 103-117.

van Everdingen R (1998 revised May 2005) *Multi-language glossary of permafrost and related ground-ice terms*. National Snow and Ice Data Center/World Data Center for Glaciology, Boulder, CO.

Vasander H, Kuusipalo J, Lindham T (1993) Vegetation changes after drainage and fertilization in pine mires. *Suo*, **44**, 1-9.

Vitt DH, Halsey LA, Zoltai SC (1994) The bog landforms of continental western Canada in relation to climate and permafrost patterns. *Arctic and Alpine Research,* **26**, 1-13.

Vörösmarty CJ, Hinzman LD, Peterson BJ, *et al.* (2001) *The Hydrologic Cycle and its Role in Arctic and Global Environmental Change: A Rationale and Strategy for Synthesis Study.* Arctic Research Consortium of the US. 84 pp.

Walker D (1970) Direction and rate in some British post-glacial hydroseres. In: *Studies in the Vegetational History of the British Isles.* eds (Walker D, West RG), pp. 117-139, University Press of Cambridge, Cambridge.

Whiting GJ, Chanton JP (2001) Greenhouse carbon balance of wetlands: Methane emission versus carbon sequestration. *Tellus*, **53B**, 521-528.

Wiens JA (1989) Spatial Scaling in Ecology. *Functional Ecology*, **3**, 385-397.

Woo MK (1986) Permafrost hydrology in North America. *Atmosphere-Ocean*, **24**, 201-234.

Yoshikawa K, Hinzman LD (2003) Shrinking thermokarst ponds and groundwater dynamics in discontinuous permafrost near Council, Alaska. *Permafrost and Periglacial Processes*, **14**, 151-160.

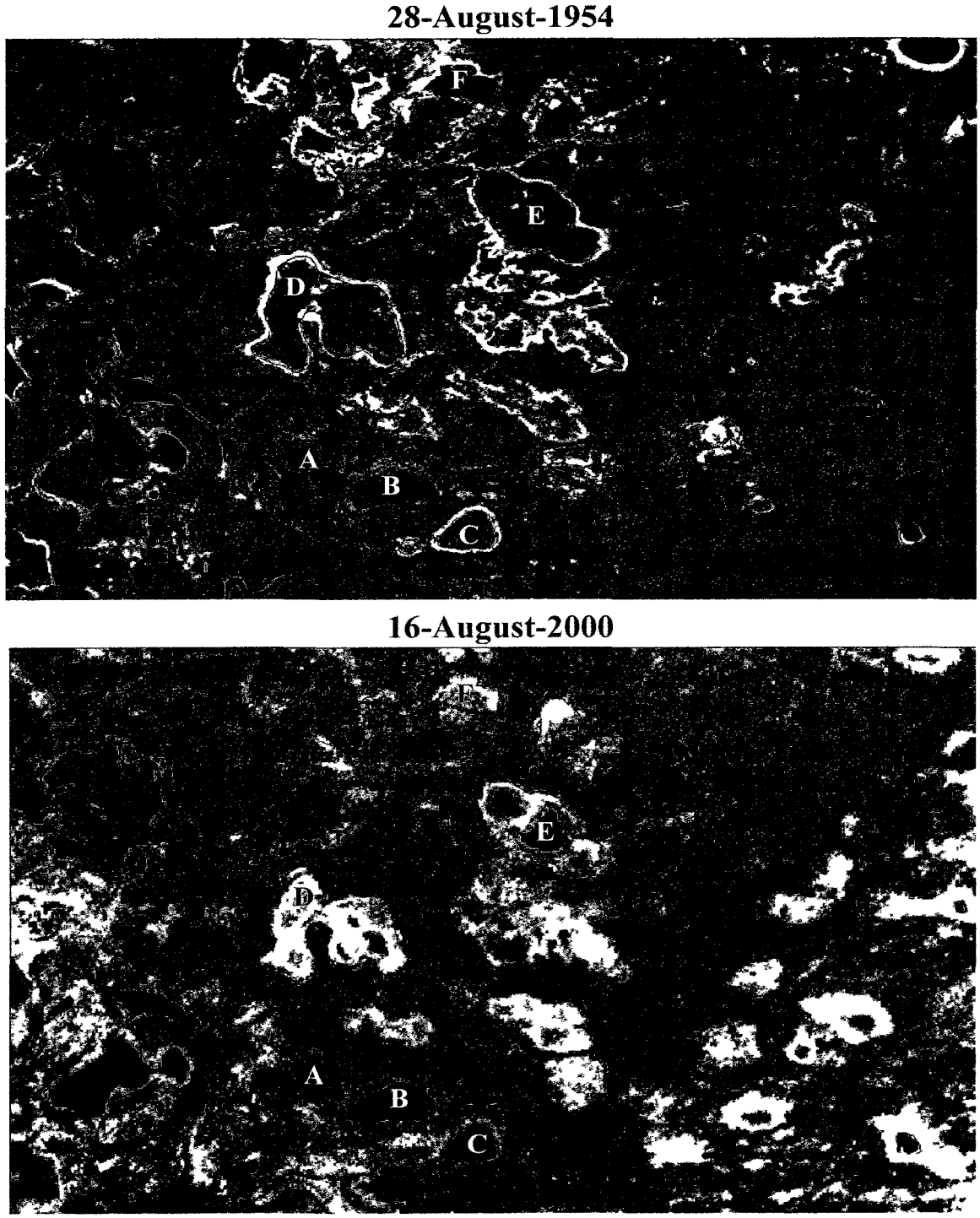

Figure 2.1 Heterogeneous pattern of shrinking lakes in the Yukon Flats East study region. For example, lakes A, B, and C exhibit little change in surface area, while lakes D, E, and F shrank substantially since the 1950s (reproduced from Riordan *et al.* 2006).

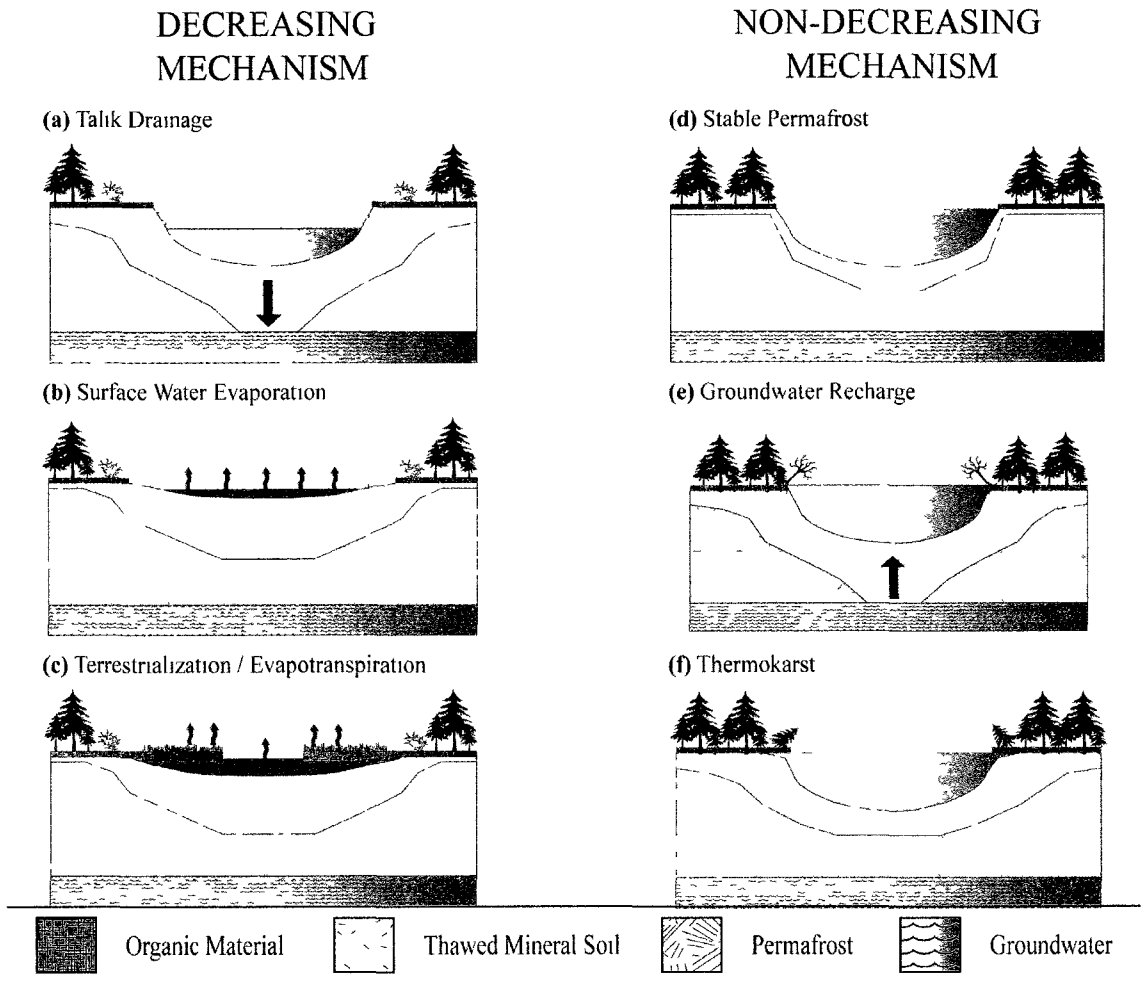

Figure 2.2 Diagrammatic representation of the three decreasing and three non-decreasing mechanisms that were evaluated to explain the fine-scale heterogeneity in decreasing and non-decreasing lakes.

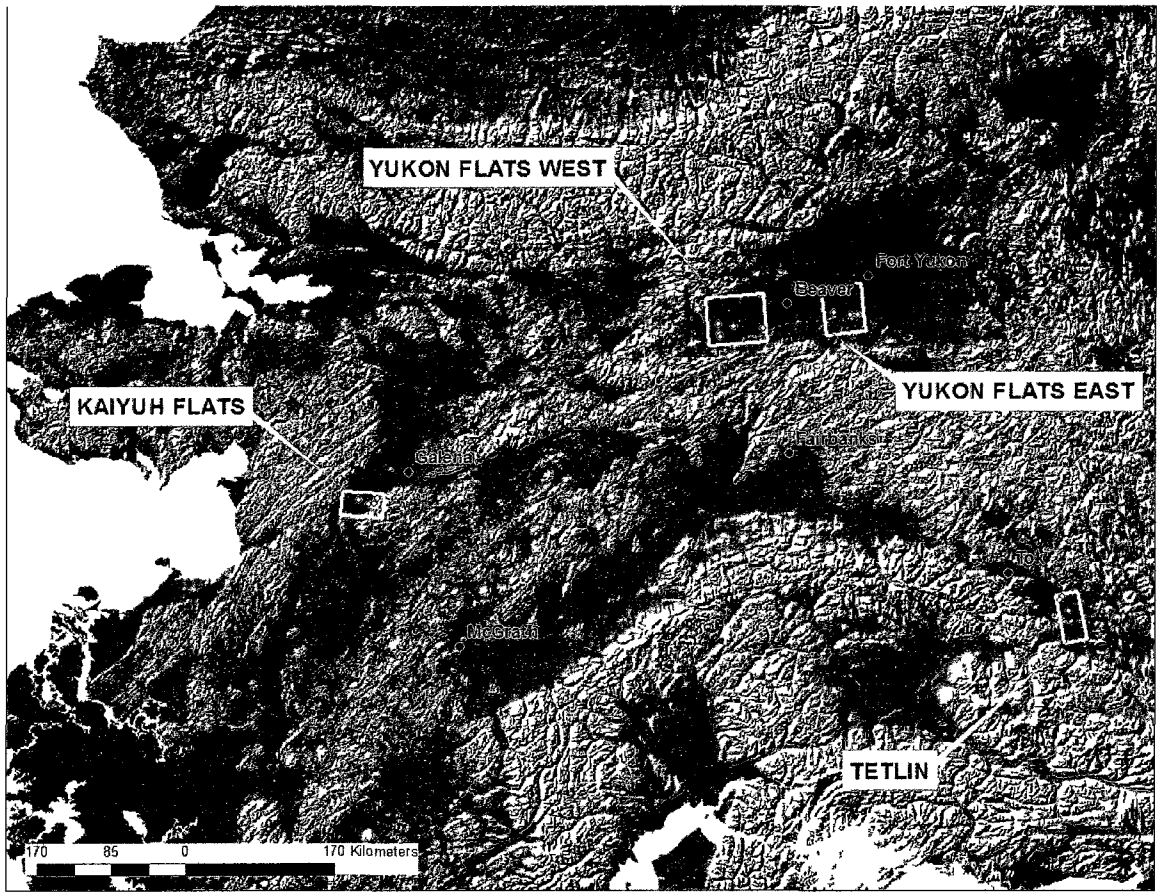

Figure 2.3 Map of Alaska showing boundaries of study areas and the locations of the 15 lake pairs included in this study.

Figure 2.4 Box plots of the difference in nine lake characteristics between paired decreasing and non-decreasing lakes (decreasing minus non-decreasing). Untransformed data are plotted for ease of interpretation. The upper and lower box boundaries are the 75^{th} and 25^{th} percentiles, respectively. The error bars represent the 90^{th} and 10^{th} percentiles. Dots represent outliers that fall outside of the 90^{th} and 10^{th} percentiles. Within the box, the solid line represents the median value and the dotted line represents the mean value. The P-values shown are for the two-tailed paired t-tests of the null hypothesis that the difference between paired decreasing and non-decreasing lakes was zero. Five variables (electrical conductivity, bank slope, floating mat width, thaw depth at shoreline, and thaw depth at forest boundary) required natural log transformation of the raw data before conducting paired t-tests in order to normalize the distributions of paired differences. * indicates experiment-wise significance at the $\alpha = .10$ level using a Holm's sequential Bonferroni correction.

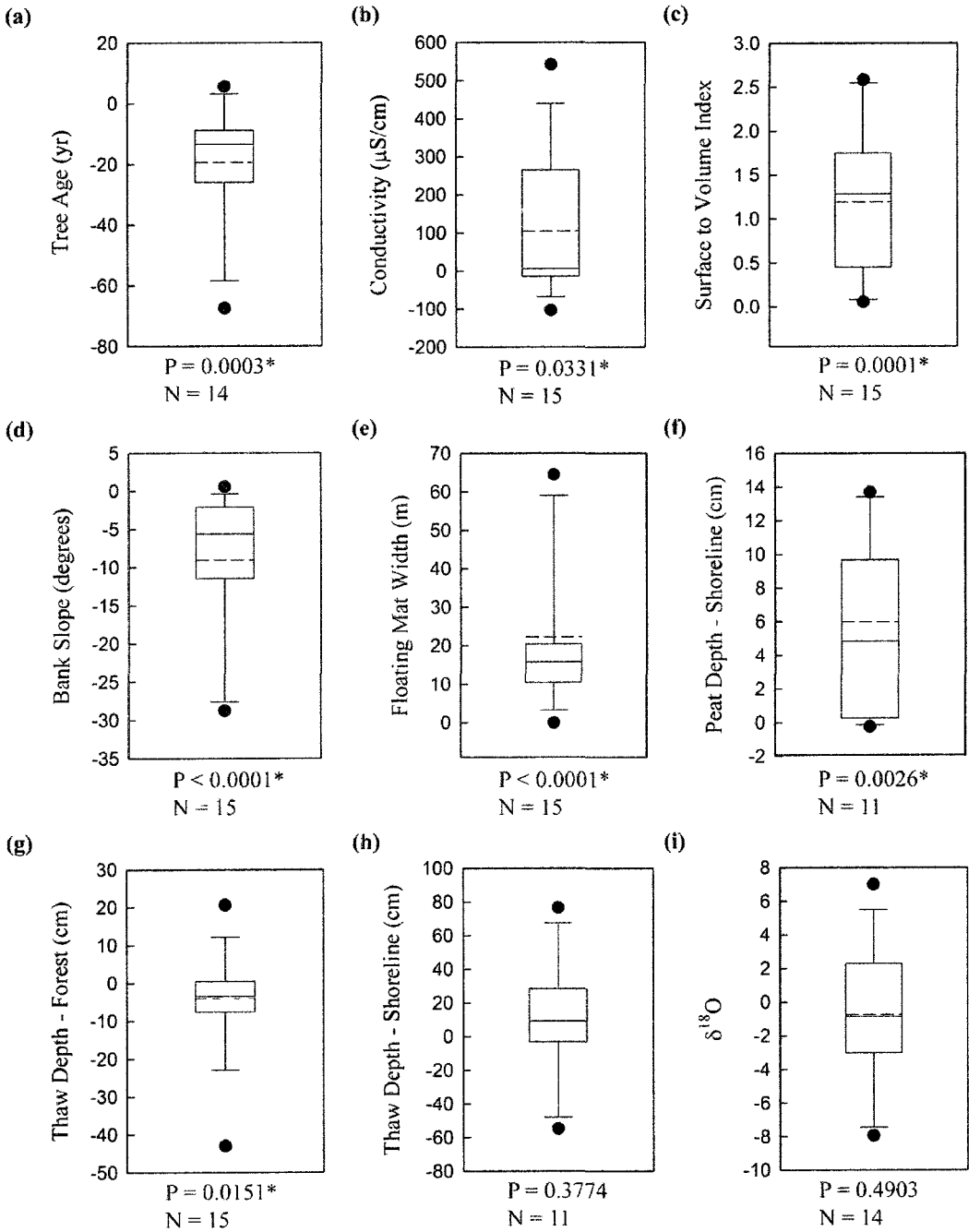
(a)
Tree Age (yr)
20
0
-20
-40
-60
-80
P = 0.0003*
N = 14
(b)
Conductivity (µS/cm)
600
500
400
300
200
100
0
-100
-200
P = 0.0331*
N = 15
(c)
Surface to Volume Index
3.0
2.5
2.0
1.5
1.0
0.5
0.0
P = 0.0001*
N = 15
(d)
Bank Slope (degrees)
5
0
-5
-10
-15
-20
-25
-30
-35
P < 0.0001*
N = 15
(e)
Floating Mat Width (m)
70
60
50
40
30
20
10
0
P < 0.0001*
N = 15
(f)
Peat Depth - Shoreline (cm)
16
14
12
10
8
6
4
2
0
-2
P = 0.0026*
N = 11
(g)
Thaw Depth - Forest (cm)
30
20
10
0
-10
-20
-30
-40
-50
P = 0.0151*
N = 15
(h)
Thaw Depth - Shoreline (cm)
100
80
60
40
20
0
-20
-40
-60
-80
P = 0.3774
N = 11
(i)
δ18O
8
6
4
2
0
-2
-4
-6
-8
-10
P = 0.4903
N = 14

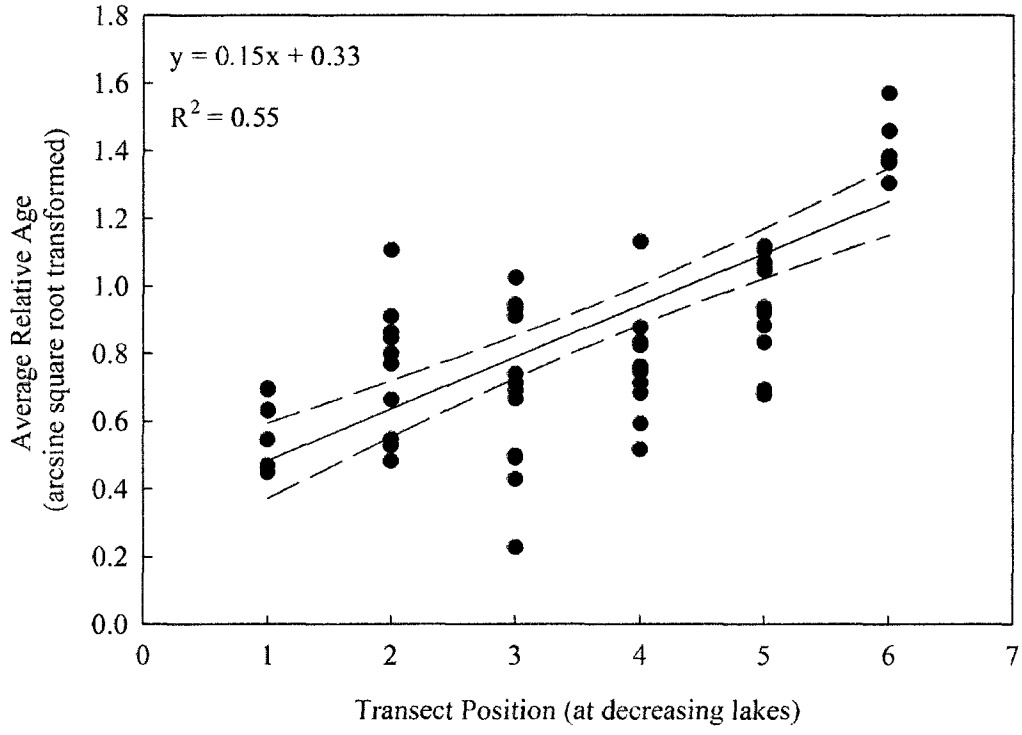

Figure 2.5 Linear regression of arcsine square root transformed average relative tree age against transect position (1 = shoreline, 6 = forest boundary) for decreasing lakes showing 95% confidence intervals.

Table 2.1 Scenario expectations for eight variables used to discriminate between mechanistic scenarios. A '+' indicates that the variable was expected to be greater at the decreasing lake, a '–' indicates that the variable was expected to be lower at the decreasing lake, and a '0' indicates that no difference was expected between paired lakes for the corresponding hypothesis. Blank boxes indicate that the expected direction of the difference was unclear.

	PAIRED LAKE SCENARIO		EXPECTATION AT DECREASING COMPARED TO NON-DECREASING LAKE							
	Decreasing Mechanism	**Non-Decreasing Mechanism**	**$\delta^{18}O$[a]**	**Cond[b]**	**S:V Index[c]**	**Bank Slope[d]**	**Floating Mat[e]**	**Peat Depth[f]**	**Thaw Depth-Shoreline[g]**	**Thaw Depth-Forest[h]**
A	Talik Drainage	Groundwater Recharge	+	-	0	0	0	0	0	0
B	Talik Drainage	Stable Permafrost			-	+	0	0	+	
C	Talik Drainage	Thermokarst			-	+	0	0		
D	Surface Water Evaporation	Groundwater Recharge	+		+	-	0	0	-	
E	Surface Water Evaporation	Stable Permafrost	+	+	+	-	0	0	0	0
F	Surface Water Evaporation	Thermokarst	+	+	+	-	0	0		-
G	Terrestrialization/ Evapotranspiration	Groundwater Recharge	+		+	-	+	+	-	
H	Terrestrialization/ Evapotranspiration	Stable Permafrost	0	+	+	-	+	+	0	0
I	Terrestrialization/ Evapotranspiration	Thermokarst	0	+	+	-	+	+		-

Table 2.1 (Continued) Scenario expectations for eight variables used to discriminate between mechanistic scenarios.

[a] $[(R_{sample} / R_{standard}) - 1] \times 1000‰$, where R is the ratio of oxygen isotopes ($^{18}O/^{16}O$) in sample and standard ocean water, respectively
[b] Electrical conductivity (μS/cm)
[c] Surface to volume index
[d] Bank slope (degrees)
[e] Floating mat width (m)
[f] Peat depth at Shoreline (cm)
[g] Thaw depth at shoreline (cm)
[h] Thaw depth at forest boundary (cm)

Table 2.2 Results from linear regression models of lake area (m^2) against date of image acquisition expressed as day beginning on 1 Jan 1900 for each sampled decreasing (D) and non-decreasing (N) lake. Data for regression models was derived from imagery from at least 6 time periods from the 1950's to 2002. Imagery included black and white aerial photography from the 1950s, color infrared aerial photography from 1977 – 1981, and Landsat TM and ETM+ images from 1991 to 2002. Lakes with significant ($P < 0.05$) negative effects of day on lake area were classified as decreasing. Lakes with significant ($P < 0.05$) positive or non-significant ($P > 0.05$) effects of day on lake area were classified as non-decreasing. Coefficients of variation are shown to demonstrate the degree of interannual variability in lake area for decreasing and non-decreasing lakes.

Refuge / Lake	Slope (m^2/day)	R^2	Coefficient of Variation
YUKON FLATS WEST			
Lake 1D	-19.45	0.864*	0.541
Lake 1N	-	0.341	0.043
Lake 2D	-4.04	0.697*	0.278
Lake 2N	-	0.328	0.026
Lake 3D	-11.16	0.865*	0.338
Lake 3N	-	0.0001	0.032
Lake 4D	-2.09	0.788*	0.272
Lake 4N	-	0.324	0.123
Lake 5D	-7.27	0.874*	0.542
Lake 5N	-	0.006	0.138
YUKON FLATS EAST			
Lake 6D	-0.71	0.910*	0.950
Lake 6N	-	0.533	0.040
Lake 7D	-0.25	0.977*	0.622
Lake 7N	0.37	0.816*	0.058
Lake 8D	-1.13	0.740*	0.824
Lake 8N	-	0.058	0.592

Table 2.2 (Continued) Results from linear regression models of lake area (m^2) against date of image acquisition expressed as day beginning on 1 Jan 1900 for each sampled decreasing (D) and non-decreasing (N) lake.

KAIYUH			
Lake 9D	-0.37	0.885*	0.586
Lake 9N	-	0.042	0.067
Lake 10D	-0.37	0.888*	0.455
Lake 10N	-	0.368	0.166
Lake 11D	-0.17	0.908*	0.244
Lake 11N	-	0.537	0.176
Lake 12D	-0.10	0.993*	0.314
Lake 12N	-	0.286	0.069
TETLIN			
Lake 13D	-0.08	0.909*	0.187
Lake 13N	0.14	0.925*	0.160
Lake 14D	-0.14	0.782*	0.388
Lake 14N	-	0.278	0.197
Lake 15D	-0.33	0.771*	0.386
Lake 15N	-	0.175	0.048

* significant at alpha = 0.05

Table 2.3 Observed results from two-tailed paired t-tests for eight independent variables used to discriminate between mechanistic scenarios of lake area change. Paired t-tests were conducted to test the null hypothesis that the difference between paired decreasing and non-decreasing lakes was zero. When the null hypothesis was rejected, the result (+ or -) was assigned based on the direction of the mean difference between paired decreasing and non-decreasing lakes. A '+' indicates that the variable was significantly greater at the decreasing lake, a '-' indicates that the variable was significantly lower at the decreasing lake, and a '0' indicates that there was no significant difference between paired lakes. Experiment-wise significance was evaluated at $\alpha = .10$ using a Holm's sequential Bonferroni correction.

$\delta^{18}O$[a]	Electrical Conductivity	Surface to Volume Index	Bank Slope	Floating Mat Width	Peat Depth at Shoreline	Thaw Depth at Shoreline	Thaw Depth at Forest Boundary
0	+	+	-	+	+	0	-

[a] $[(R_{sample} / R_{standard}) - 1] \times 1000‰$, where R is the ratio of oxygen isotopes ($^{18}O/^{16}O$) in sample and standard ocean water, respectively

Table 2.4 Conditional probability of each combination (i.e., scenario) of decreasing and non-decreasing mechanisms given observed results.

	PAIRED LAKE SCENARIO				
	Decreasing Mechanism	**Non-Decreasing Mechanism**	**P_{scen} [a]**	**P_{res} [b]**	**Conditional Probability[c]**
A	Talik Drainage	Groundwater Recharge	$1/3^8$	1/3	0.00046
B	Talik Drainage	Stable Permafrost	$1/3^5$	0	0
C	Talik Drainage	Thermokarst	$1/3^4$	0	0
D	Surface Water Evaporation	Groundwater Recharge	$1/3^6$	$1/3^2$	0.01235
E	Surface Water Evaporation	Stable Permafrost	$1/3^8$	$1/3^4$	0.01235
F	Surface Water Evaporation	Thermokarst	$1/3^7$	$1/3^4$	0.03704
G	Terrestrialization/ Evapotranspiration	Groundwater Recharge	$1/3^6$	$1/3^4$	0.11111
H	Terrestrialization/ Evapotranspiration	Stable Permafrost	$1/3^8$	$1/3^7$	0.33333
I	Terrestrialization/ Evapotranspiration	Thermokarst	$1/3^7$	$1/3^7$	1

[a] P_{scen} = random probability of scenario excluding unknown expectations
[b] P_{res} = random probability of the number of results that match the variable expectations for the specified scenario
[c] Conditional probability given results (P_C) = P_{scen}/P_{res} (Casella & Berger 2002)

Appendix 2.1 Data from 15 paired decreasing and non-decreasing lakes in the Alaska boreal forest, 2006-2007. Data were used for general comparisons and to evaluate nine possible combinations of three decreasing and three non-decreasing hypotheses (i.e., scenarios) using paired t-tests of the difference between lake types with Holm's sequential Bonferroni correction.

Id	Lake Type	Latitude	Longitude	Area (ha)[a]	Max Depth (m)[b]	$\delta^{18}O$[c]	Cond (µS/cm)[d]	S V Index[e]	Bank Slope (deg)[f]	Mat (m)[g]	Thaw-Shore (cm)[h]	Thaw-Forest (cm)[i]	Peat (cm)[j]	Tree Age (yr)
1	Decreasing	66 143	-148 069	12 06	0 9	-11 40	262	2 55	9 7	45 0	59 5	11 1	39 3	11 6
	Non-decreasing	66 134	-148 059	7 17	3 2	-11 50	276	0 86	11 4	36 1	81 0	18 8	39 0	24 4
2	Decreasing	66 190	-148 822	9 19	0 5	-8 19	373	3 63	10 3	21 5	126 0	16 3	40 0	13 3
	Non-decreasing	66 199	-148 856	0 68	1 5	-15 18	108	1 04	13 8	5 0	49 5	25 8	39 8	23 3
3	Decreasing	66 222	-149 195	19 24	0 8	-8 66	519	1 81	7 8	55 0	60 8	9 5	40 0	20 6
	Non-decreasing	66 229	-149 186	11 69	1 4	-8 18	148	1 36	19 3	4 4	30 3	14 3	30 3	28 0
4	Decreasing	66 122	-149 198	4 74	1 3	-10 87	247	1 23	10 8	69 0	84 0	12 3	40 0	25 2
	Non-decreasing	66 121	-149 183	0 57	1 3	-14 82	91	1 18	15 8	4 5	61 0	15 0	36 0	24 4
5	Decreasing	66 085	-149 160	7 61	1 0	-14 75	84	1 92	12 4	62 8	40 0	6 3	40 0	19 2
	Non-decreasing	66 081	-149 164	3 47	0 7	-6 80	115	1 82	14 6	7 4	94 8	10 3	31 0	32 0
6	Decreasing	66 174	-145 646	0 15	0 8	-10 77	780	2 17	9 3	15 8	80 0	11 0	40 0	17 9
	Non-decreasing	66 239	-145 744	16 83	3 0	-13 96	238	0 42	17 6	0	69 5	10 5	26 3	42 0
7	Decreasing	66 186	-145 833	0 21	1 4	-18 49	188	1 10	2 2	19 5	59 0	16 8	39 8	30 6
	Non-decreasing	66 193	-145 837	5 52	2 6	-11 55	292	0 52	6 8	4 8	62 3	25 3	40 0	44 4
8	Decreasing	66 230	-146 258	0 48	0 6	-	599	4 00	2 7	0	136 5	9 8	40 0	26 3
	Non-decreasing	66 226	-146 257	0 24	1 7	-	270	1 48	3 7	0	137 8	13 3	27 8	20 7
9	Decreasing	64 453	-157 660	0 27	1 1	-11 41	41	1 43	5 4	9 4	36 5	39 9	36 5	-
	Non-decreasing	64 445	-157 659	1 09	1 7	-11 00	40	0 79	15 0	3 9	27 3	41 5	27 3	-
10	Decreasing	64 397	-157 707	0 52	1 2	-13 50	64	1 94	10 2	26 0	-	34 8	-	38 2
	Non-decreasing	64 399	-157 713	1 02	3 0	-10 39	40	0 56	37 0	10 3	-	30 1	-	52 5
11	Decreasing	64 416	-158 091	0 45	1 6	-12 55	34	1 14	11 6	24 0	128 0	36 0	39 3	30 7
	Non-decreasing	64 416	-158 093	0 68	2 0	-11 29	38	0 81	11 0	4 8	99 5	38 5	34 5	80 2
12	Decreasing	64 382	-157 835	0 19	1 3	-13 52	43	1 74	7 9	25 0	38 7	43 8	38 0	66 5
	Non-decreasing	64 380	-157 829	0 42	2 0	-12 21	38	0 93	18 4	9 3	35 0	37 3	35 0	134 0
13	Decreasing	62 974	-141 876	0 27	0 4	-7 97	159	3 57	27 6	10 5	-	90 3	-	74 0
	Non-decreasing	62 972	-141 878	0 67	1 1	-9 96	87	1 14	33 2	0	-	69 7	-	105 8

Appendix 2.1 (Continued) Data from 15 paired decreasing and non-decreasing lakes in the Alaska boreal forest, 2006-2007.

14	Decreasing	62 942	-141 941	0 12	0 8	-12 66	171	1 93	11 8	20 3	-	49 3	-	60 0
	Non-decreasing	62 947	-141 945	0 84	2 4	-9 67	216	0 65	40 5	0	-	92 3	-	81 5
15	Decreasing	62 821	-141 789	0 36	0 9	-13 62	346	2 06	10 5	31 0	-	44 3	-	42 3
	Non-decreasing	62 826	-141 787	3 37	1 9	-11 17	352	0 76	28 0	10 5	-	48 6	-	55 3

[a] Lake area (hectares) derived from the most current imagery included in this study
[b] Maximum lake depth (m) along transects
[c] $[(R_{sample} / R_{standard}) - 1] \times 1000‰$, where R is the ratio of oxygen isotopes ($^{18}O/^{16}O$) in sample and standard ocean water, respectively
[d] Electrical conductivity (µS/cm)
[e] Surface to volume index
[f] Bank slope (degrees)
[g] Floating Mat Width (m)
[h] Thaw depth at shoreline (cm)
[i] Thaw depth at forest boundary (cm)
[j] Peat depth at shoreline (cm)

Appendix 2.2 Topographical characteristics, climate data, and percent change in lake surface area for the four study areas. Elevation, slope, and aspect derived from Alaska 300m Digital Elevation Model. Climate data and percent change in lake surface area were adapted from Riordan *et al.* 2006. For information on weather station locations and methods used to generate climate and lake area change data see Riordan *et al.* 2006.

	Area Size[a]	Elevation (m)	Slope (degrees)	Aspect (degrees)	Mean Annual Temperature (1971-2000), °C	Mean Precipitation (1971-2000), mm	Trend in Mean Annual Temperature (1939-2002), ° C		Trend in Total Annual PET (1939-2002), mm		% Change in Lake Surface Area[b]
							Slope	P	Slope	P	
Yukon Flats West	107	149	0.75	130	-3.9	193	0.037	0.0005	0.716	0.002	-14
Yukon Flats East	202	159	0.49	133	-3.9	193	0.046	0.0001	0.607	0.009	-18
Kaiyuh	63	75	1.23	123	-2.8	445	0.026	0.003	0.150	0.002	-31
Tetlin	95	594	1.09	141	-4.9	238	0.034	0.0008	0.379	0.064	-4

[a] Units are x 1000 hectares.

[b] Units are hectares of water for closed basin lakes from 1950s to most recent estimate.

Chapter 3: Comparison of three methods for estimating number and area of boreal lakes from TM/ETM+ Landsat imagery[1]

Abstract

We evaluated three methods for the classification of lakes from Landsat imagery (density slicing, classification trees, and feature extraction) by comparing estimates of the number and area of lakes derived from the three classification methods to a validation set of lakes manually delineated from high resolution color infrared (CIR) aerial photography taken within two days of satellite image acquisition. Our objectives were to 1) identify the best spectral band combination for use with the multispectral classification tree and feature extraction methods and 2) compare the performance of the three supervised classification methods. We quantitatively compared the various band combinations and classification methods in terms of 1) the magnitude of bias in lake area estimates, 2) the direction of bias in lake area estimates (i.e., the percentage of lakes with under-estimated lake area), 3) the number of omission and commission errors, and 4) the minimum lake size required for each method to minimize omission and commission errors. Band combinations and classification methods were compared across ten trials in

[1]Roach J, Griffith B, & Verbyla D. Comparison of three methods for estimating number and area of boreal lakes from TM/ETM+ Landsat imagery. Prepared for *Remote Sensing of Environment*.

which two Landsat images (TM/ETM+) were each classified using five different sets of training data derived from lake polygons digitized from CIR aerial photography. Multiple images and training sets were included to ensure that results were not sensor- or training set-dependent. We qualitatively compared the three methods on the basis of efficiency, ease of application, and sensitivity to georeferencing errors. We concluded that the single SWIR Band 5 was the best band for use with the multispectral methods because adding the NIR Band 4 and SWIR Band 7 did not significantly improve results. The density slicing method was the best method for the classification of lake area due to its lower minimum lake size criterion, ability to detect a greater number of lakes, ease of application, consistency, lack of sensitivity to georeferencing errors, and relative lack of directional bias.

Introduction

The detection of change in lake area and number is important in the Arctic and sub-Arctic because lakes are abundant, serve as breeding grounds for millions of migratory waterfowl and shorebirds, and may increase or decrease in size as a result of climate warming (Yoshikawa & Hinzman, 2003; Marsh et al., 2009; Roach et al., 2011). Landsat Thematic Mapper data have been widely used to map lakes and wetlands (Bennett, 1987; Overton, 1997) and to detect changes in lake area (Smith et al., 2005; Plug et al., 2008; Labreque et al., 2009). While Landsat data have provided a powerful tool to detect change in lake area, the data are limited, especially in terms of the temporal coverage. The use of historical aerial photography can increase the temporal scale

beyond the start of Landsat acquisition by 20+ years, while the use of Landsat imagery can increase the sampling frequency and/or spatial extent of a study due to its global spatial coverage, long archival record starting in 1972, and repetitive acquisition every 16 days over a range of seasonally dynamic hydrological conditions. However, inclusion of both aerial photography and satellite imagery in a change detection study can lead to bias in results due to the differences in spatial and spectral resolutions (Ramsey III & Laine, 1997; Brown & Young, 2005; Kennedy et al., 2009).

Previous studies examining lake change that have included both historical aerial photography and satellite imagery have quantified change by manually delineating lakes from both types of imagery (Yoshikawa & Hinzman, 2003; Riordan et al., 2006; Corcoran et al., 2009). Manual delineation is subjective and labor intensive but is often required for lake delineation from aerial photography due to poor spectral reflectance and potential interference from sunglint on a water surface. However, lakes can be mapped from satellite imagery using automated methods such as supervised or unsupervised classification. In order to effectively and efficiently incorporate both historical aerial photography and satellite imagery into the same change detection study, an automated method for satellite image classification that minimizes the bias in estimates of lake area and number when compared to aerial photography of a different spatial and spectral resolution is needed.

Objectives

The goal of this study was to compare three supervised methods of satellite imagery classification (density slicing, classification tree, and feature extraction) relative to reference data from aerial photographs acquired within two days of each satellite overpass. Based on our initial exploratory work and published results (Frazier & Page, 2000), we limited our comparisons to classifications based on the near infrared (NIR) band 4 and short wave infrared (SWIR) bands 5 & 7. Our first objective was to identify the best band combination for lake classification using the multispectral methods. Our second objective was to compare the three classification methods. Both objectives focused on optimal methods for estimation of the number of lakes and the area of lakes. The magnitude and direction of bias in lake number were evaluated by quantifying the number of omission errors (lakes that were present in aerial photography but not classified in Landsat imagery) and the number of commission errors (lakes that were not present in aerial photography and falsely classified in Landsat imagery). The magnitude of bias in lake area was evaluated by calculating mean absolute percent error in lake area estimates for mutually identified lakes (lakes that were present in both aerial photography and classified Landsat imagery, regardless of the lake area in each image type). The direction of bias in lake area was evaluated by calculating the percentages of over- and under-estimated lakes.

Methods

Study Area

Our study area was within Innoko National Wildlife Refuge, an area characterized by a dynamic mosaic of lakes of fluvial and thermokarst origin, extensive fens, bogs, birch and boreal spruce forests. We selected this area to maximize overlap of Thematic Mapper (TM) and Enhanced Thematic Mapper Plus (ETM+) scenes and Color Infrared (CIR) aerial photography and to minimize data gaps resulting from clouds and the malfunctioning scan-line corrector on ETM+ imagery. Within the study area, we randomly located three 10.5 km^2 rectangular frames (Fig. 3.1). Each frame was within a single aerial photograph (Fig. 3.2).

Imagery

Two Landsat images that entirely overlapped the study area were obtained to ensure that results were not date- or sensor-specific (Table 1). We used only NIR band 4 and SWIR bands 5 and 7 for classifications because these bands are the most useful in distinguishing water and non-water (Johnston & Barston 1993; Overton 1997; Frazier & Page, 2000). Digital Numbers (DNs) were converted to Top-Of-Atmosphere (TOA) reflectance (Chander et al., 2009) in order to reduce scene-to-scene variability. Reflectance was then scaled from 0.0 – 0.63 floating point to 0 – 255 integer (1-byte) values. A visual review of visible Band 1 and thermal Band 6 was performed to ensure that local atmospheric variation such as fog, smoke or cirrus clouds were not present.

Color infrared vertical aerial photography was acquired on September 3rd, 2006 by the United States Fish and Wildlife Service (USFWS) (Table 3.1). Each photograph was co-registered to a Landsat ETM+ image using a linear affine transformation model and nearest neighbor re-sampling. Each co-registration model was based on at least 12 well-defined image-based control points and a root mean squared error (RMSE) of less than 15 m. Co-registered photos were 8 km x 8 km in extent and had a pixel size of 0.87 m. Within the three study frames, we manually delineated all lakes that were greater than one 30 m x 30 m Landsat pixel resulting in 220 lake polygons which served as a validation set for comparison to supervised classification results. All geographic data were in the UTM Zone 4N NAD27 map projection.

Classification Methods

Single band density slicing is the simplest of the three methods used. This method uses a threshold value for a single band which discriminates non-water versus water. Frazier & Page (2000) found that density slicing of the SWIR band 5 was moderately better at classifying water than density slicing of the NIR band 4 and the SWIR band 7. With our initial exploratory work, we also found that band 5 was superior to the other five bands for water body delineation. Thus, we considered density slicing of only the single SWIR band 5 in this study.

Our second classification method was classification tree methodology which applies a set of binary partitioning rules to separate pixels into water/non-water classes based on spectral reflectance threshold values. We used CART® software distributed by

Salford Systems to conduct the classification tree methodology. This software considers all possible splitting rules for all predictor variables and uses the Gini method to choose the rule that minimizes the impurity of the two child nodes based on equations and criteria detailed in Breiman et al. (1984). The tree then grows with successive subdivisions until there is no significant decrease in impurity when further divisions are added at which point it is referred to as the 'optimal tree'. For the pruning process we used a 10-fold cross-validation testing procedure to identify the optimal tree based on the misclassification error rate. We defined the optimal tree as the tree that had the smallest number of nodes to avoid over-fitting and a misclassification error rate within 1 standard error of the lowest misclassification error rate of all possible trees to yield high predictive power.

Our third classification method was feature extraction; an object-based classification method that classifies groups of pixels or features rather than individual pixels based on learning algorithms which use information about an object's characteristics and spatial context relative to surrounding features. This approach, referred to as 'foveal vision' (Visual Learning Systems, 2002), is meant to approximate the human visual cognitive process. We used the Feature Analyst™ extension for ArcGIS distributed by Visual Learning Systems to conduct object-based classifications.

Training Data

All training data were derived from aerial photography to serve as a single base training sample for the direct comparison of multiple (i.e. TM/ETM+) image

classifications. Classification methods were trained using five sets of lake training data (Table 3.2). Each set consisted of five lake polygons that were randomly selected from a subset of the validation set of lake polygons manually delineated from CIR aerial photography (Fig. 3.2) that were greater than nine Landsat pixels. We restricted our training polygons to 43 larger lakes because we anticipated potential problems with omission errors for smaller lakes and wanted to ensure that we had sufficient Landsat TM/ETM+ water pixels for supervised classification. The five training sets, each composed of five lake polygons, were randomly selected with replacement from the 43 lake polygons.

For the density slicing approach, the five training sets were used to identify five threshold values to classify water versus non-water pixels for both the TM and ETM+ images resulting in ten density slicing classifications (five for each image). The training data used for the density slicing method were the lake polygons manually delineated from aerial photography (Fig. 3.3a). Threshold values (Table 3.3) were identified by averaging the optimal threshold values for each individual training lake that minimized the difference in total area between the lake area classified from satellite imagery and the lake polygon derived from CIR aerial photography.

The classification tree method required pixel-based training data of scaled reflectance values for each individual water and non-water pixel (Table 3.4). In contrast with the density slicing and feature extraction methods, this method does not use any information about the way that these pixels were arranged into lake polygon features. To generate water pixel data from lake polygons, we selected Landsat TM/ETM+ pixels that

had greater than 50% of their area within each lake polygon (Fig. 3.3b). Non-water pixels for training were identified by randomly selecting an equivalent number of non-water pixels directly surrounding the lake water pixels (Fig. 3.3c).

Similar to the density slicing method, the feature extraction method used polygon-based training data. The feature extraction method used both water and non-water training polygons (Fig. 3.3d). The non-water training polygons were derived from the non-water pixels used with the classification tree method (Fig. 3.3c) by smoothing the non-water pixel boundary with an Exponential Kernel (PAEK) algorithm set to a tolerance of 120 m (Fig. 3.3d).

All classification methods and band combinations considered were trained a total of ten times (Tables 3.5 & 3.6). We conducted supervised classifications using two images and the five sets of training data to ensure that results were not date-, sensor-, or training set-dependent. Controlling for between-training set variability was particularly important in this study because the performance of supervised classification methods can be highly dependent on the particular training set that is used (Foody & Mathur, 2004).

Quantitative Method/Band Combination Comparisons

Evaluation of Method Performance

We evaluated the performance of each supervised classification method in comparison to the validation set of 220 lake polygons from aerial photography. Comparisons between supervised classification results and the validation set of lake polygons were made on a per-lake basis. In order to account for a single lake becoming a

multi-part polygon or multiple lakes becoming a single-part polygon in satellite image classifications, we defined a lake as either the single polygon or group of polygons that intersected the maximum extent of a water body in both the satellite image and manually delineated CIR aerial photograph (Fig. 3.4). This lake definition enabled us to compile datasets that consisted of a list of lakes that were either 1) present in aerial photography but not classified in Landsat imagery (i.e., omission error), 2) not present in aerial photography and falsely classified in Landsat imagery (i.e, commission error), or 3) present in both aerial photography and classified Landsat imagery (i.e., mutually identified lake) and their estimated areas from each image type. We assessed the magnitude and direction of bias in lake number by quantifying the number of omission errors, commission errors, and mutually identified lakes. Because it was important that a lake not only be mutually identified but also yield a minimally biased estimate of lake area, we also evaluated the magnitude of bias in lake area for mutually identified lakes (Fig. 3.5).

The magnitude of bias in lake area was evaluated using a variation of mean absolute percent error described by Tayman et al. (1999) (MAPE). We estimated error using absolute percent error, which is size-independent, instead of absolute error, which tends to over-represent error from large lakes when averaged. Absolute percent error for each lake was calculated by dividing the absolute difference between the lake area classified from satellite imagery and the lake area from the validation set of lake polygons by the lake area from the validation set. Because the underlying distribution for absolute percent error is right skewed and truncated at zero, mean absolute percent error

tends to be subject to 'upward bias' overstating the error represented by some observations, particularly those that have a positive percent error (e.g., over-estimated lakes) vs. a negative percent error (e.g., under-estimated lakes) (Tayman et al., 1999). Thus, we followed procedures developed and verified by Tayman et al. (1999) to obtain an unbiased estimate of mean absolute percent error (MAPE) by 1) using a modified Box-Cox nonlinear transformation to transform skewed error distributions into symmetrical distributions and 2) using a nonlinear quadratic regression relationship to re-express the mean of the transformed absolute percent error distribution back to the original scale of the un-transformed errors so that our re-expressed estimate of mean absolute percent error (MAPE) could be interpreted as a percent error.

Statistical Analyses

We used a two-factor within-subjects analysis of variance (ANOVA) (SAS Institute, Inc. 2003) to compare 1) the performance of the various NIR and SWIR band combinations for the multispectral classification tree and feature extraction methods and 2) the performance of the three classification methods (density slicing, classification trees, and feature extraction). For all ANOVA tests, when a significant (alpha=0.05) main effect was present we used Tukey's Studentized Range Test to control experiment-wise error when making multiple pairwise comparisons (SAS Institute, Inc. 2003).

For our first objective (i.e., to identify the best band combination for methods with multispectral capability), we assessed the effects of band combination (band 5, bands 4 & 5, bands 5 & 7, and bands 4, 5, & 7) and image (TM and ETM+) as the two

within-subjects factors on the number of omissions, the number of commissions, the number of mutually identified lakes, and the magnitude of bias in area estimates for mutually identified lakes (i.e., MAPE) for the classification tree and feature extraction methods (Table 3.5). Thus, this analysis consisted of a total of 40 classifications for five training sets, four band combinations, and two images (i.e., ten classifications for each of the four band combinations considered).

For the second objective (i.e., to identify the best classification method after identifying the optimal band combination for the classification tree and feature extraction methods), we assessed the effects of method (density slicing, classification trees, and feature extraction) and image (TM and ETM+) as the two-within-subjects factors on the number of omissions, the number of commissions, the number of mutually identified lakes, and MAPE (Table 3.6). Thus, this analysis consisted of a total of 30 classifications for five training sets, three methods, and two images (i.e., ten classifications for each of the three methods considered).

Minimum Size Criteria

Methods were also compared on the basis of minimum lake size criteria. Minimum lake size criteria are particularly important in change detection studies that include imagery of different spatial and spectral resolutions. This is because 1) a change from high spatial resolution (e.g. aerial photography) to low spatial resolution (e.g. Landsat imagery) can result in the inability to detect small lakes (i.e., omission errors) and 2) a change in spectral resolution (e.g. from aerial photography to Landsat SWIR

band 5) can result in the false detection of small lakes that may actually be wet, vegetated soil as opposed to open water (i.e., commission errors). Thus, a minimum lake size criterion can be applied in change detection studies to minimize omission and commission errors. Supervised classification methods may differ in their susceptibility to omission and commission errors which may result in differences in their optimal minimum size criteria. The optimal minimum lake size for a classification method may be an important factor for studies interested in detecting change in small lakes or interested in large-scale objectives that may require a larger, more representative sample size.

We defined two minimum size criteria for each method/band combination: 1) the minimum size required to detect all manually delineated CIR lakes (i.e. to avoid all omission errors) and 2) the minimum size required to remove all commission errors with the exception of six large wetland areas that were consistently classified as lakes using all three methods. We chose to not include these latter errors because they were present in all classifications and would not have been critical to our comparison of minimum size criteria amongst the three methods. We defined the optimal minimum size criteria for each method/band combination to be the greater of these two criteria (i.e., the minimum size required to minimize both omission and commission errors). We selected minimum sizes that were midway between each increment in lake size based on 30 m pixels (e.g., 900 m^2 increments of 1350, 2250, 3150, 4050...) in order to have a minimum size scale that was applicable to both the 30 m scale of TM/ETM+ imagery and the continuous scale of CIR aerial photography.

Comparison of Methods After Applying Optimal Minimum Size Criteria

We performed a final comparison of the three classification methods after applying their respective optimal minimum size criteria. In addition, we also removed one lake from our final comparisons which was identified as an outlier in all classifications (i.e., under all treatment conditions) (Fig. 3.6). We defined an outlier to be a lake that had a standardized residual greater than 2 from the linear regression of classified satellite image lake area against CIR lake area for mutually identified lakes. Similar to the six commission errors common to all classifications, this common outlier was consistently over-estimated due to the misclassification of adjacent wet, vegetated areas as open water. Statistical analysis for the final comparison of the three methods was conducted as before using a two-factor within subjects ANOVA and Tukey's Studentized Range Test (SAS Institute, Inc. 2003) to assess the effects of method (density slicing, classification trees, and feature extraction) and image (TM and ETM+) on the number of mutually identified lakes and MAPE (Table 3.3). For this comparison we also considered a third response variable, the percentage of under-estimated lakes, to assess the direction of bias in area estimates for the three classification methods (Fig. 3.5). The ability to identify the direction of bias for a classification method can be helpful when interpreting results from a change detection study in which historical high resolution aerial photography is followed by current lower resolution satellite imagery in a time series. In this type of study, under-estimation of lake area in satellite imagery may lead to the false detection of a negative trend in lake area. When selecting a classification

method, there may be a preference for potential over- or under- estimation of lake area depending on a study's particular objectives.

Qualitative Comparisons

Our qualitative assessment compared the three methods in terms of 1) relative speed (i.e., efficiency) of data preparation, training, and classification, 2) ease of application, and 3) sensitivity to georeferencing errors. Ease of application is an important feature of any long-term monitoring program and our assessment of this characteristic was based primarily on whether specialized software (i.e., not including software used for standard image processing) was required to conduct training or classification. The use of specialized software requires the funds to purchase the software as well as personnel that are trained to use it correctly.

Results

Quantitative Method/Band Combination Comparisons

Comparison of Band Combinations

For the classification tree method, there were no significant (alpha=0.05) main effects for band combination, image, and band combination*image interaction for the number of omissions, number of commissions, number of mutually identified lakes, and MAPE. In fact, eight of the ten classifications (5 training sets x 2 TM/ETM+ images) for the Bands 4 & 5 combination, eight of the ten classifications for the Bands 5 & 7 combination, and seven of the ten classifications for the Bands 4, 5, & 7 combination

identified optimal classification trees that contained only a single splitting rule for Band 5. In correspondence with this result, there also was no difference in the minimum size criteria identified for the four band combinations (Table 3.7). Because spectral bands 4 & 7 did not significantly improve method performance, we concluded that the single band 5 was the optimal band for use with the classification tree method.

There were also no significant (alpha = 0.05) effects for band combination, image, and band combination*image on the number of commissions, number of mutually identified lakes, and MAPE for the feature extraction method. There was a significant (P = 0.045) difference in the number of omission errors between the various feature extraction band combinations. Specifically, the single band 5 method resulted in significantly more omission errors compared to the feature extraction method that used both bands 4 & 5 (P = 0.005) (Table 3.7). However, the feature extraction method with bands 4 & 5 exhibited substantial inconsistency in the number of commission errors across the 10 classifications (5 training sets x 2 TM/ETM+ images) as evidenced by a large standard error (Table 3.4). The presence of large commission errors under some treatment conditions also resulted in a large commission minimum of 27,450 m^2 for the bands 4 & 5 feature extraction method (Table 3.7). This unusually large commission minimum led us to conclude that despite the reduction in omission errors the use of band 4 in conjunction with band 5 did not improve the overall performance of the single band 5 feature extraction method. Thus, we identified the single band 5 as the optimal band for use with the feature extraction method.

Comparison of Three Methods

The among method comparison was conducted for the band 5 density slicing method, the optimal band 5 classification tree method, and the optimal band 5 feature extraction method. There were no significant main effects for image or image*method on the performance variables we considered: number of omissions, number of commissions, number of mutually identified lakes, and MAPE. Thus, we concluded that image type (i.e., sensor or day and time of image acquisition) did not affect the performance of these three methods. There was also no significant difference in the number of commission errors between the three methods (Table 3.7).

There were significant main effects for method on the number of omissions ($P = 0.014$), number of mutually identified lakes ($P = 0.004$), and MAPE ($P = 0.036$). The classification tree method had significantly more omissions and significantly fewer mutually identified lakes compared to the feature extraction method ($P = 0.019$ and $P = 0.008$, respectively) (Table 3.7). Thus, we concluded that the classification tree method performed worse than the feature extraction method in terms of the number of omissions and the number of mutually identified lakes. There were no significant differences between the density slicing method and either the classification tree or the feature extraction method in terms of the number of omissions and the number of mutually identified lakes. Although there was a significant main effect for method on MAPE, none of the pair-wise comparisons were statistically significant.

Minimum Size Criteria

The optimal minimum lake sizes for the density slicing, band 5 classification tree, and band 5 feature extraction methods were 5850 m^2, 8550 m^2, 8550 m^2, respectively (Tables 3.7 & 3.8). Thus, the density slicing method was better at classifying small lakes compared to the classification tree and feature extraction methods.

Comparison of the Three Methods After Applying Minimum Size Criteria

After applying the optimal minimum size criteria to their respective methods and removing one common outlier (Fig. 3.6), the only significant difference between methods was in the number of mutually identified lakes ($P < 0.0001$) (Table 3.8) which was most likely due to the application of different minimum size criteria to the three classification methods. The density slicing method resulted in significantly more mutually identified lakes compared to both the classification tree ($P = 0.0002$) and the feature extraction ($P = 0.0005$) methods (Table 3.8). There was no significant difference in the number of mutually identified lakes between the classification tree and feature extraction methods. Similar to our results before applying minimum size criteria, there were no significant differences in MAPE between the three classification methods. There were also no significant main effects for image or image*method on the number of mutually identified lakes and MAPE indicating the performance of these three methods was not dependent upon image type. Although there were no significant main effects for image, method or image*method on the percentage of under-estimated lakes, the direction of bias for density slicing was closer to parity than for either other method (Table 3.8).

Qualitative Comparisons

The three supervised methods we considered (density slicing, classification tree, and feature extraction) differed in the relative speed and efficiency of the various stages of the training and classification process (Table 3.9). Preparation of single-class polygon training data for the density slicing method was categorized as relatively fast compared to the preparation of multi-class (i.e., water/non-water) training data for the classification tree and feature extraction methods. Training data preparation was considered to be the slowest for the classification tree method which required the conversion of high resolution polygon data to 30 m pixel data organized in a format suitable for use outside of a GIS environment (Fig. 3.3). Training speed for the density slicing method was categorized as slow compared to the other two methods because training required a greater number of steps to identify the optimal threshold for each training lake. In contrast, once training data were created and put into the correct format, training for the classification tree and feature extraction methods were carried out quickly and efficiently with the CART® and Feature Analyst™ software.

Classification speed for the density slicing and feature extraction methods were classified as fast because they functioned seamlessly within the ArcGIS environment (Table 3.9). In contrast, the classification tree method generated individual pixel classification results that required translation back into a GIS environment for spatial analyses. The density slicing method may have been the least sensitive of the three methods to geo-referencing errors in the training dataset. The classification tree and feature extraction methods used training data to interpret spectral data on a per-pixel

basis. In contrast, the density slicing method used a per-lake training approach which selected individual lake thresholds that minimized the difference in area between the classified lake and the training lake. Thus, the density slicing method only required that the training data and underlying imagery to be classified were correctly paired on a lake-to-lake basis in comparison to the classification tree and feature extraction methods which required accurate pairing on a pixel-to-pixel basis.

Discussion

Consistent with the results of other work (Frazier & Page, 2000), we found that the NIR Band 4 and SWIR Band 7 did not significantly improve either the classification tree or the feature extraction methods. Thus, we concluded that the single infrared Band 5 was the optimal band for use with all three methods. Our comparisons of the three methods indicated that density slicing of the single Band 5 was the best method for the classification of lake area from Landsat imagery, particularly when high resolution aerial photography is included in a change detection study.

Our quantitative comparisons clearly identified the classification tree method as the worst of the three methods because it resulted in significantly more omission errors and significantly fewer mutually identified lakes compared to the feature extraction method (Table 3.7). Although there were no significant quantitative differences between the density slicing and feature extraction methods before applying the minimum size criteria, the feature extraction method tended to perform worse in terms of the number of commission errors (Table 3.7). Differences in the number of commission errors between

the three methods were not statistically significant due the large standard error for the feature extraction method which indicated substantial inconsistency in the number of commission errors depending on the training set that was used. Thus, the performance of the feature extraction method may be highly dependent on training data selection compared to the density slicing method which performed more consistently (i.e., had a relatively low standard error) across the five different training sets.

The density slicing method allowed the smallest minimum lake size criterion to reduce omission and commission errors which resulted in a significantly greater number of mutually identified lakes compared to the classification tree and feature extraction methods (Table 8). The inclusion of small lakes in a change detection study is important because 1) it increases the sample size, and 2) it increases the range of lake sizes for which results will be applicable. Small lakes can make up a large proportion of lakes (Downing et al., 2006) and their inclusion can enhance the ability to draw regional-scale conclusions. In addition to reducing the number of omission and commission errors, the application of a minimum size criterion also resulted in substantial decreases in MAPE for all three methods (Tables 3.7 & 3.8). The identification of a larger optimal minimum size criterion for the feature extraction and classification tree methods compared to the density slicing method (Table 3.8) was driven primarily by omission errors (Table 3.7). Specifically, the classification tree and feature extraction methods tended to omit larger lakes than the density slicing method.

The density slicing method also tended to be less biased towards under-estimating lake area compared to the classification tree and feature extraction methods (Table 3.8).

Thus, the density slicing method may be least likely to falsely detect a negative trend in lake area in a change detection study where historical high resolution aerial photography is followed by current lower resolution satellite imagery in a time series. If a negative trend in lake area is detected using the density slicing method, there can be greater confidence that the direction of the trend is correct in comparison to a trend detected using either the classification tree or feature extraction methods.

Our qualitative comparisons also identified the density slicing method as the best method because it employed a simple threshold rule that can be easily applied to classify Landsat imagery in any GIS environment. Because it does not require specialized software, the density slicing method had the greatest ease of application of the three methods (Table 3.9). The qualitative strengths of the density slicing method make it the preferred method for a long-term monitoring program since the monitoring of lake area and ability to share data between agencies and individuals is not dependent on having access to a specific type and version of software.

Our analyses for all three methods identified six large-sized commission errors (i.e., lakes that appeared in satellite image classifications that were not present in CIR aerial photography) and one common outlier that resulted from wet, vegetated areas being misclassified as open water. While we can identify the effect that these commission errors will have on the direction of bias for a change detection study, there may still be a need to improve the overall performance of imagery classification by removing these misclassified areas from the change detection analysis. When historical or current high resolution aerial photography is available, the appearance or unusually

large growth of a lake in lower resolution Landsat SWIR band 5 may be indicative of potential misclassified areas. Further careful visual inspection of aerial photography (e.g., dark, textured areas tend to be indicative of wet, vegetated surfaces) may help to identify these areas as misclassifications for removal from the analysis. When high resolution aerial photography is not present, visual inspection of other Landsat spectral bands may be helpful to identify misclassified areas to be masked out of the analysis.

In this study, we derived all training data from polygons manually delineated from high resolution aerial photography. The use of high resolution training data has been shown to improve classification of low resolution imagery (Swain, 2007) and may serve as an important link between imagery of different spectral and spatial resolutions within the same change detection study. When same-day high resolution imagery is not available, it may be possible to derive training data from high resolution imagery from a different time period for lakes that have not changed in area between the time periods of interest. While there is some level of subjectivity in identifying lakes that are stable between different types of imagery, we propose that the alternative of directly delineating training polygons from low resolution imagery would involve much greater subjectivity and would not provide a potentially important link between different types of imagery in a change detection study.

We propose that the benefits gained from density slicing in terms of minimum lake size criterion, the number of mutually identified lakes, ease of application, consistency, sensitivity to georeferencing errors, and direction of bias make it the best operational method for the detection and monitoring of past and future changes in lake

area using Landsat imagery. The density slicing method is a simple and accurate tool that can be used across a variety of research and land management fields to estimate lake area at large spatial and temporal scales.

Acknowledgments

We thank Steve Ewest, Matthew Balasz, and Garrett Altmann for help with image processing, Jeremy Jones and Jennifer Harden for manuscript reviews, and Eric J. Taylor for administrative and funding support. We thank Karen Murphy and Steve Kovach at Innoko National Wildlife Refuge for providing high resolution CIR aerial photography. Funding was provided by USGS, FWS, and a UAF Graduate School Thesis Completion Fellowship. Any use of trade names is for descriptive purposes only and does not imply endorsement by the U.S. Government.

References

Bennett, M.W.A. (1987). Rapid monitoring of wetland water status using density slicing. *Proceedings of the 4th Australasian Remote Sensing Conference*, September 14-18, Adelaide, pp. 682-691.

Breiman, L., Friedman, J.H., Olshen, R.A., & Stone, C.J. (1984). *Classification and regression trees*. Monterey, CA: Wadsworth.

Brown, L., & Young, K.L. (2005). Assessment of three mapping techniques to delineate lakes and ponds in a Canadian high arctic wetland complex. *Arctic*, 59, 283-293.

Chander, G., Markham, B.L., & Helder, D.L. (2009). Summary of current radiometric calibration coefficients for Landsat MSS, TM, ETM+, and EO-1 ALI sensors. *Remote Sensing of Environment*, 113, 893–903.

Corcoran, R.M., Lovvorn, J.R., & Heglund, P.J. (2009). Long-term change in limnology and invertebrates in Alaskan boreal wetlands. *Hydrobiologia*, 620, 77-89.

Downing, J.A., Prairie, Y.T., Cole, J.J., Duarte, C.M., Tranvik, L.J., Striegl, R.G., McDowell, W.H., Kortelainen, P., Caraco, N.F., Melack, J.M., & Middelburg, J.J. (2006). The global abundance and size distribution of lakes, ponds, and impoundments. *Limnology and Oceanography*, 51, 2388-2397.

Foody, G.M., & Mathur, A. (2004). Toward intelligent training of supervised image classifications: directing training data acquisition for SVM classification. *Remote Sensing of Environment*, 93, 107-117.

Frazier, P.S., & Page, K.J. (2000). Water body detection and delineation with Landsat TM data. *Photogrammetric Engineering & Remote Sensing*, 66, 1461-1467.

Johnston, R., & Barson, M. (1993). Remote sensing of Australian wetlands: An evaluation of Landsat TM data for inventory and classification. *Australian Journal for Marine and Freshwater Research*, 44, 235-252.

Kennedy, R.E., Townsend, P.A., Gross, J.E., Cohen, W.B., Bolstad, P., Wang, Y.Q., & Adams, P. (2009). Remote sensing change detection tools for natural resource managers: Understanding concepts and tradeoffs in the design of landscape monitoring projects. *Remote Sensing of Environment*, 113, 1382-1396.

Labrecque, S., Lacelle, D., Duguay, C.R., Lauriol, B., & Hawkings, J. (2009). Contemporary (1951–2001) evolution of lakes in the Old Crow Basin, northern Yukon, Canada: Remote sensing, numerical modeling, and stable isotope analysis. *Arctic*, 62, 226-238.

Marsh, P., Russell, M., Pohl, S., Haywood, H., & Onclin, C. (2009). Changes in thaw lake drainage in the Western Canadian Arctic from 1950 to 2000. *Hydrological Processes*, 23, 145-158.

Overton, I. (1997). *Satellite Image Analysis of River Murray Floodplain Inundation*, NRMS Project R6045, Murray-Darling Basin Commission, Adelaide, 12p.

Plug, L.J., Walls, C., & Scott, B.M. (2008). Tundra lake changes from 1978 to 2001 on the Tuktoyaktuk Peninsula, western Canadian Arctic. *Geophysical Research Letters*, 35, L03502.

Ramsey III, E.W., & Laine, C.L. (1997). Comparison of Landsat Thematic Mapper and high resolution photography to identify change in complex coastal wetlands. *Journal of Coastal Research*, 13, 281-292.

Riordan, B., Verbyla, D., & McGuire, A.D. (2006). Shrinking ponds in subarctic Alaska based on 1950-2002 remotely sensed images. *Journal of Geophysical Research*, 111, G04002.

Roach, J., Griffith, B., Verbyla, D., & Jones, J. (2011). Mechanisms influencing changes in lake area in the Alaskan boreal forest. *Global Change Biology*, **17**, 2567-2583.

SAS institute, Inc. (2003) *SAS 9.1.3 for Windows*, Cary, NC.

Smith, L.C., Sheng, Y., MacDonald, G.M., & Hinzman, L.D. (2005). Disappearing arctic lakes. *Science*, 308, 1429.

Swain, J.J. (2007). *The effect of spatial resolution on an object-oriented classification of downed timber.* MS Thesis, North Carolina State University, Raleigh, NC, 52 pp.

Tayman, J., Swanson, D.A., & Barr, C.F. (1999) In search of the ideal measure of accuracy for subnational demographic forecasts. *Population Research and Policy Review*, 18, 387-409.

Visual Learning Systems (2002). *The Feature Analyst™ Extension for ArcView® and ArcGIS™*. Overwatch Systems, LTD.

Yoshikawa, K., & Hinzman, L.D. (2003). Shrinking thermokarst ponds and groundwater dynamics in discontinuous permafrost near Council, Alaska. *Permafrost and Periglacial Processes*, 14, 151-160.

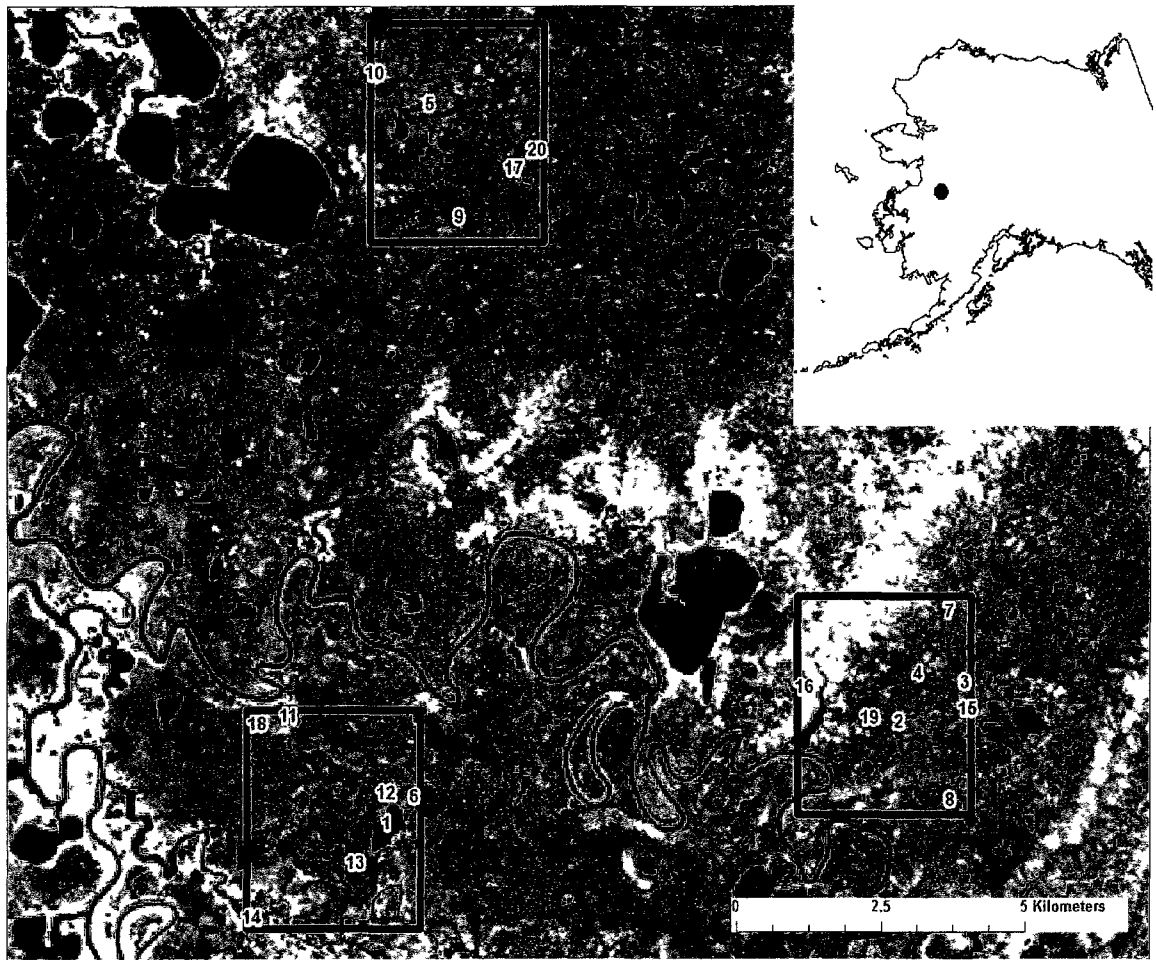

Figure 3.1 Location of study area within Innoko National Wildlife Refuge, Alaska overlaid on Landsat TM imagery. Black rectangles indicate boundaries of three 10.5 km^2 study frames. Number labels 1-20 indicate lakes that were used as training data. Lakes were randomly selected with replacement in groups of five for each of the five training data sets A-E. Training Set A was composed of Lakes 1-5. Training Set B was composed of Lakes 6-10. Training Set C was composed of Lakes 11-15. Training Set D was composed of Lakes 2, 7, & 15-16. Training Set E was composed of Lakes 6, 10, & 18-20.

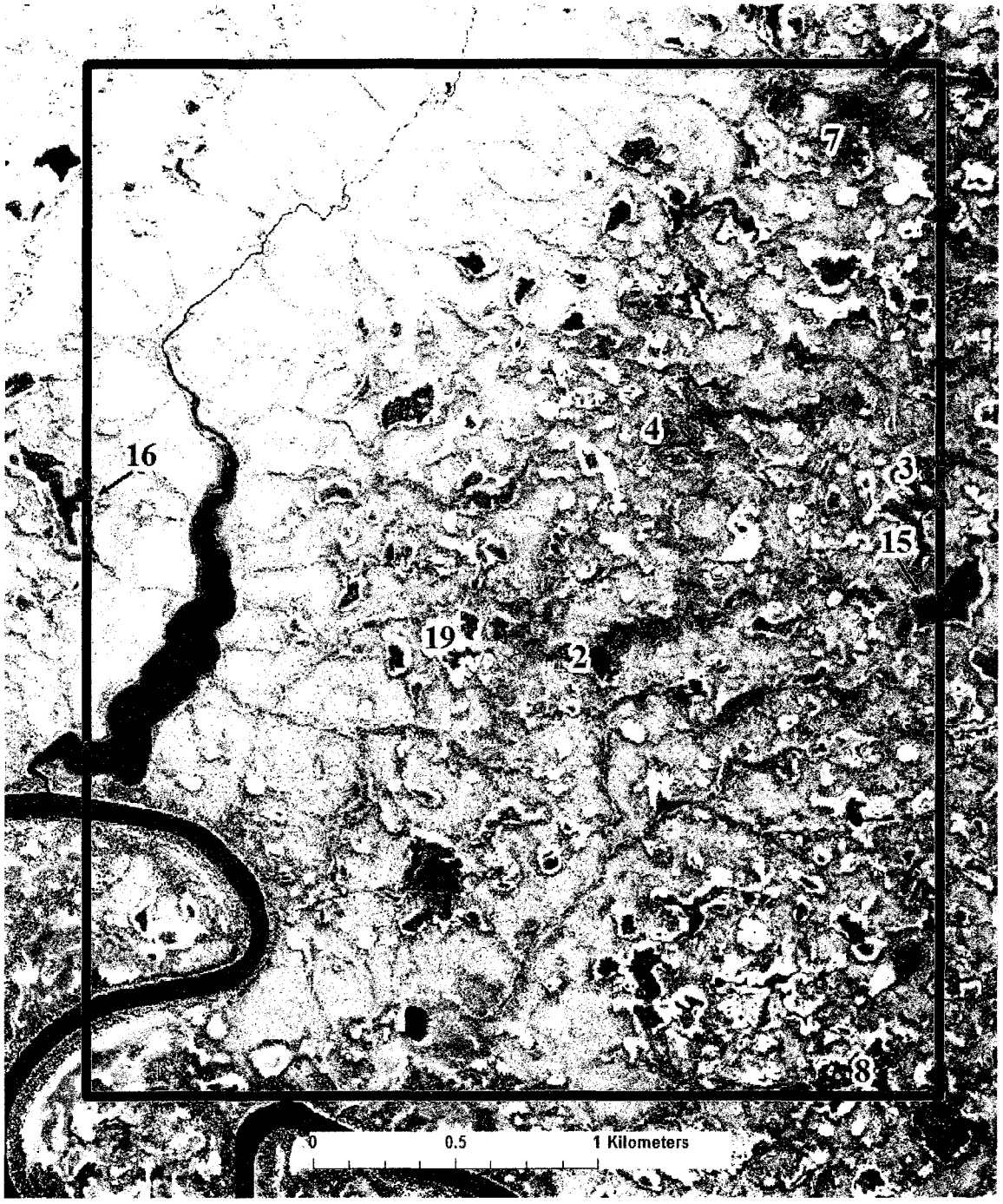

Figure 3.2 Close-up of southeastern study frame showing manually digitized lake polygons overlaid on CIR aerial photography. Number labels indicate lakes that were randomly selected with replacement for each of the five training data sets A-E.

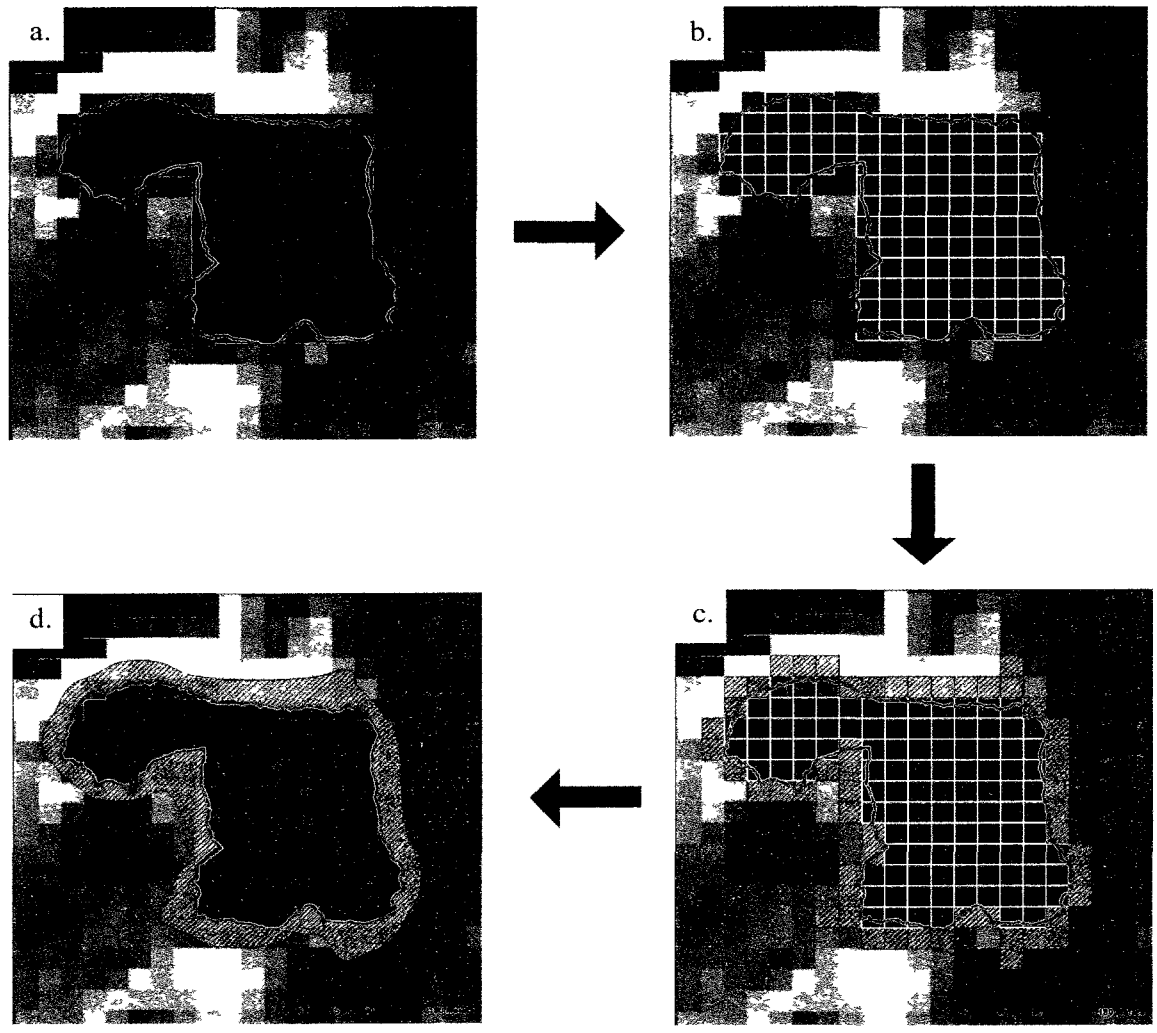

Figure 3.3 Example of workflow to prepare training data for the three methods. Image shown is Landsat ETM+ band 5. (a) Cyan outline is the lake shoreline digitized from CIR aerial photography for Training Lake 11 in Training Set C. For the density slicing method, each lake polygon was used to determine the pixel threshold value that resulted in the closest agreement between classified water pixel lake area and the lake polygon area. (b) Conversion of a lake polygon to water pixel training data used with the classification tree method. Each polygon was converted to water pixels by selecting pixels that had greater than 50% of their area within the manually delineated lake boundary. (c) Creation of non-water pixel training data used with the classification tree method. Non-water pixel training data was created by randomly selecting an equivalent number of surrounding non-water pixels as water pixels. (d) Conversion of non-water pixel training data in (c) to non-water training polygon used with the feature extraction method. Water polygon training data used with the feature extraction method was the same as the original lake boundary manually delineated from CIR aerial photography and used with the density slicing method shown in (a).

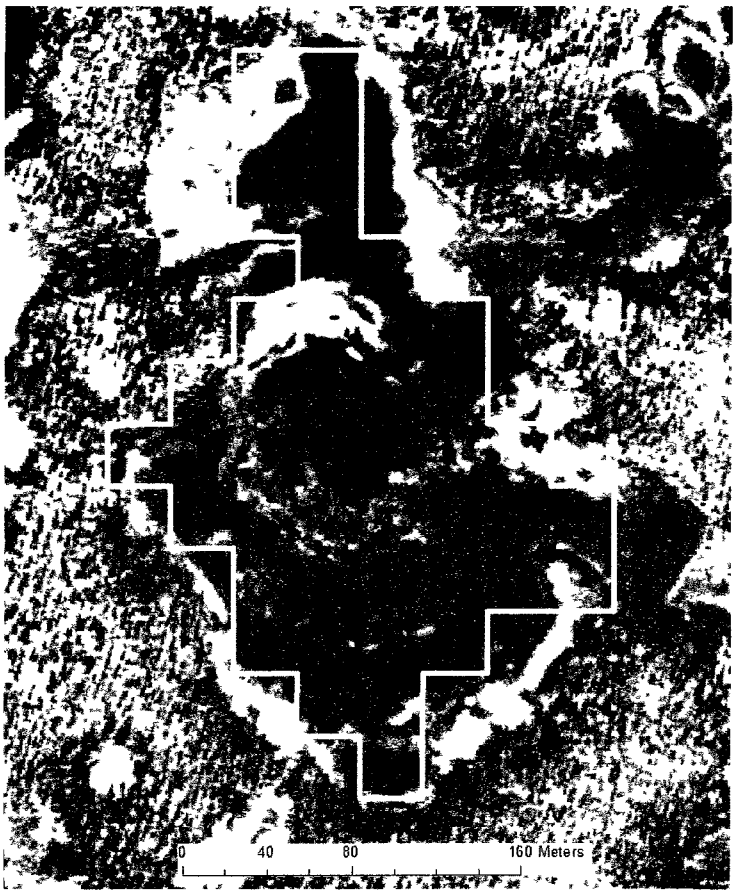

Figure 3.4 Example of a multipart lake. The white outline represents results from a supervised classification. All individual lake polygons that intersect this outline are considered to be parts of the lake. This lake definition enabled us to assess the magnitude of bias in lake area estimates for each supervised classification.

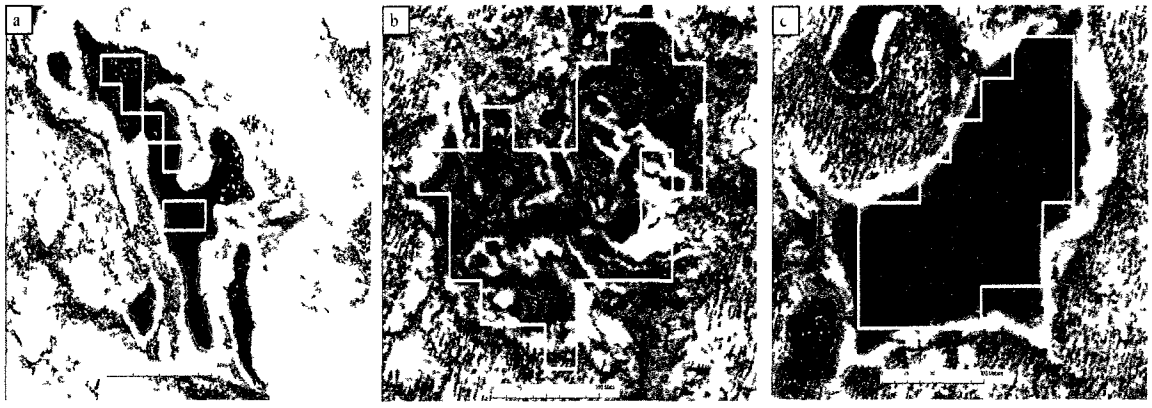

Figure 3.5 Examples of the magnitude and direction of bias in lake area for mutually identified lakes that resulted from supervised classifications. White outlines are examples of results from supervised classifications. (a) Under-estimated lake, (b) Over-estimated lake, (c) Lake with small amount of bias in area estimate.

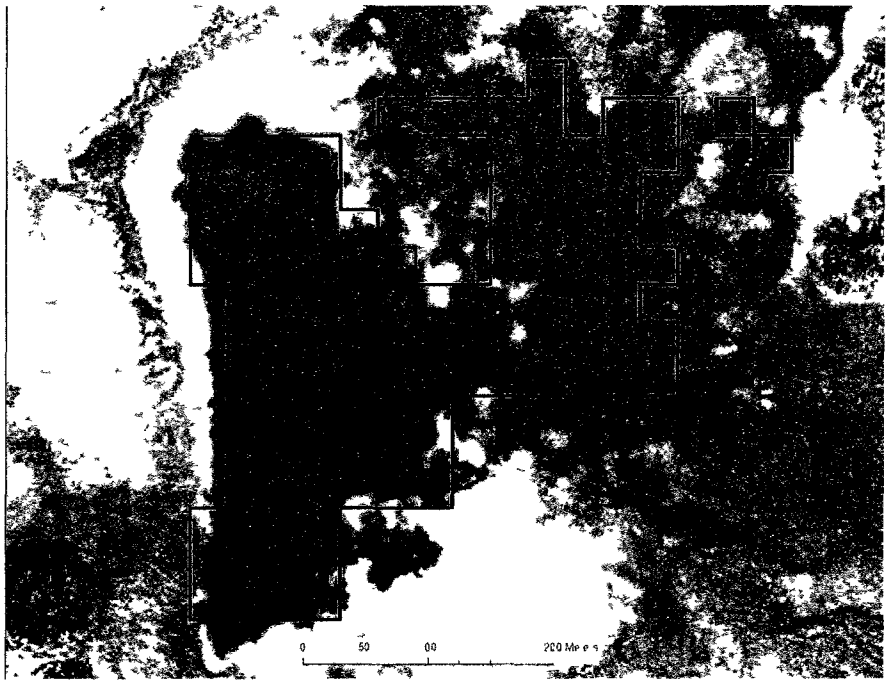

Figure 3.6 Common outlier resulting from all classifications for all three methods overlaid on CIR aerial photography. The black outline represents results from one supervised classification. This lake was consistently over-estimated due to the misclassification of adjacent wet, vegetated areas as open water.

Table 3.1 Acquisition dates and resolution of Landsat imagery and CIR aerial photography.

Image Type	Row	Path	Acquisition Date	Resolution
Color Infrared Aerial Photography (3 frames)	N/A	N/A	9/3/2006	0.87 m
Landsat TM	76	16	9/4/2006	30 m
Landsat ETM+	75	16	9/5/2006	30 m

Table 3.2 Mean (standard error) spectral reflectance values for water and non-water pixels across training sets and for each TM and ETM+ scene.

Training Set	Band 4				Band 5				Band 7			
	TM Image		ETM+ Image		TM Image		ETM+ Image		TM Image		ETM+ Image	
	Water	Non-water	Water	Non-water	Water	Non-water	Water	Non-water	Water	Non-water	Water	Non-water
1	23.4 (0.88)	71.0 (1.06)	24.2 (0.78)	75.6 (1.02)	9.1 (0.45)	41.4 (0.61)	9.8 (0.46)	45.1 (0.67)	6.3 (0.26)	23.3 (0.35)	4.7 (0.21)	21.1 (0.32)
2	24.1 (1.29)	74.8 (1.02)	25.0 (0.92)	79.0 (0.99)	8.9 (0.45)	33.3 (0.55)	9.3 (0.49)	36.1 (0.67)	6.0 (0.25)	19.0 (0.29)	4.6 (0.23)	16.9 (0.29)
3	28.0 (1.09)	63.2 (1.75)	29.8 (1.05)	66.7 (1.63)	13.0 (0.62)	38.1 (0.82)	13.9 (0.66)	41.7 (0.91)	8.9 (0.36)	21.5 (0.39)	6.5 (0.32)	19.6 (0.39)
4	35.4 (1.69)	62.6 (1.75)	37.6 (1.45)	65.8 (1.48)	17.6 (0.88)	36.4 (1.92)	17.4 (0.91)	38.7 (1.17)	10.7 (0.46)	20.1 (0.55)	8.1 (0.41)	17.8 (0.53)
5	23.6 (1.13)	73.2 (1.34)	24.0 (1.03)	77.9 (1.17)	8.2 (0.53)	31.0 (0.60)	8.9 (0.55)	33.6 (0.67)	5.7 (0.31)	18.0 (0.32)	4.4 (0.26)	15.7 (0.31)

Table 3.3 SWIR Band 5 at-sensor spectral reflectance threshold values used for density slicing classifications. Pixels with values less than the threshold value were classified as water.

Training Set	TM Image	ETM+ Image
1	26	27
2	23	24
3	28	30
4	26	26
5	24	27

Table 3.4 Total number of water and non-water pixels used as training data for the classification tree method. Half of the total number of pixels for each training set were water pixels and half were non-water pixels. The classification tree method classified pixels as water or non-water using a set of binary partitioning rules derived from spectral reflectance values for these water and non-water training pixels. The classification tree method was evaluated for four different band combinations: band 5, bands 4 & 5, bands 5 & 7, and bands 4, 5, & 7.

Training Set	# Water and Non-water Pixels
1	696
2	580
3	468
4	212
5	496

Table 3.5 Layout for two-factor within-subjects repeated measures design to identify the best band combination for the classification tree and feature extraction methods. Each training data set consisted of five lakes randomly selected from 43 lake polygons manually delineated from CIR aerial photography that were greater than 9 Landsat pixels in size. A total of 40 classifications were conducted for five training sets, four band combinations, and two images. The four band combinations used were: B_1 = band 5, B_2 = bands 4 & 5, B_3 = bands 5 & 7, and B_4 = bands 4, 5, & 7. The two images classified were: I_1 = TM and I_2 = ETM+. This experimental design was used to assess the effects of band combination and image type on the number of omissions, the number of commissions, the number of mutually identified lakes, and the magnitude of bias in area estimates for mutually identified lakes (i.e., MAPE).

TRAINING SET	TREATMENT							
	TM Image:				ETM+ Image:			
1	B_1I_1	B_2I_1	B_3I_1	B_4I_1	B_1I_2	B_2I_2	B_3I_2	B_4I_2
2	B_1I_1	B_2I_1	B_3I_1	B_4I_1	B_1I_2	B_2I_2	B_3I_2	B_4I_2
3	B_1I_1	B_2I_1	B_3I_1	B_4I_1	B_1I_2	B_2I_2	B_3I_2	B_4I_2
4	B_1I_1	B_2I_1	B_3I_1	B_4I_1	B_1I_2	B_2I_2	B_3I_2	B_4I_2
5	B_1I_1	B_2I_1	B_3I_1	B_4I_1	B_1I_2	B_2I_2	B_3I_2	B_4I_2

Table 3.6 Layout for two-factor within-subjects repeated measures design to identify the best method for classification of lakes from Landsat imagery. Each training data set consisted of five lakes randomly selected from 43 lake polygons manually delineated from CIR aerial photography that were greater than 9 Landsat pixels in size. A total of 30 classifications were conducted for five training sets, three methods, and two images. The three methods considered were: M_1 = density slicing, M_2 = classification tree, and M_3 = feature extraction. The two images classified were I_1 = TM and I_2 = ETM+. This experimental design was used to assess the effects of method and image type on the number of omissions, the number of commissions, the number of mutually identified lakes, the magnitude of bias in area estimates for mutually identified lakes (i.e., MAPE), and the direction of bias (i.e., percentage of under-estimated lakes).

TRAINING SET	TREATMENT					
	TM Image:			ETM+ Image:		
1	M_1I_1	M_2I_1	M_3I_1	M_1I_2	M_2I_2	M_3I_2
2	M_1I_1	M_2I_1	M_3I_1	M_1I_2	M_2I_2	M_3I_2
3	M_1I_1	M_2I_1	M_3I_1	M_1I_2	M_2I_2	M_3I_2
4	M_1I_1	M_2I_1	M_3I_1	M_1I_2	M_2I_2	M_3I_2
5	M_1I_1	M_2I_1	M_3I_1	M_1I_2	M_2I_2	M_3I_2

Table 3.7 Band and method comparisons in terms of the number of omission errors, the minimum lake size to minimize omission errors, the number of commission errors, the minimum lake size to minimize commission errors, the number of mutually identified lakes, and the magnitude of bias in area estimates for mutually identified lakes (i.e., MAPE). The optimal band combination used for method comparisons are highlighted in grey. Entries for # omissions, # commissions, # mutually identified lakes, and mean absolute percent error (MAPE) are the mean (standard error) of the 10 classifications (5 training sets x 2 TM/ETM+ images) run for each method. All band and method comparisons were made within columns. Matching superscripts within columns denote that the two entities were significantly different using a two-way within-subjects analysis of variance (ANOVA) and Tukey's studentized range test to maintain experiment-wise error (alpha=0.05) (SAS Institute, Inc. 2003). We did not use the convention of common superscripts for entities that are not significantly different for ease of results presentation.

METHOD/ BAND	# OMISSIONS	SIZE (m^2) TO MINIMIZE OMISSIONS	# COMMISSIONS	SIZE (m^2) TO MINIMIZE COMMISSIONS	# MUTUALLY IDENTIFIED LAKES	MEAN ABSOLUTE PERCENT ERROR (MAPE)[a]
Density Slicing						
5	51.8 (5.68)	4050	39.8 (6.29)	5850	131.5 (4.26)	27.3 (1.32)
Classification Tree						
5	84.0[B] (11.48)	8550	25.0 (5.08)	4950	109.4[A] (8.29)	34.9 (2.95)
4, 5	86.6 (11.06)	8550	25.8 (5.68)	4950	107.7 (8.25)	36.1 (2.67)
5, 7	82.7 (11.75)	8550	28.4 (6.06)	4950	110.4 (8.56)	34.6 (2.99)
4, 5, 7	85.0 (11.47)	8550	30.0 (6.76)	4950	109.3 (8.79)	35.7 (2.76)

Table 3.7 (Continued) Band and method comparisons in terms of the number of omission errors, the minimum lake size to minimize omission errors, the number of commission errors, the minimum lake size to minimize commission errors, the number of mutually identified lakes, and the magnitude of bias in area estimates for mutually identified lakes (i.e., MAPE).

Feature Extraction						
5	46.8[A,B] (6.34)	8550	179.5 (74.91)	5850	149.8[A] (5.45)	27.2 (1.47)
4, 5	39.8[A] (6.94)	5850	336.7 (163.99)	27450	150.2 (6.20)	27.4 (2.97)
5, 7	56.4 (10.96)	9450	229.3 (118.39)	13050	141.9 (8.65)	31.4 (2.40)
4, 5, 7	41.0 (7.92)	9450	399 (158.59)	50850	152.9 (5.14)	31.9 (1.68)

[a] Mean absolute percent error (MAPE) is an estimate of the magnitude of bias in area estimates. Absolute percent error for each lake was calculated by dividing the absolute difference between the lake area classified from satellite imagery and the lake area from the validation set of lake polygons by the lake area from the aerial photography validation set. We followed procedures described by Tayman et al. (1999) to transform skewed percent error distribution and then re-express the mean of the transformed absolute percent error distribution back to the original scale of the un-transformed errors so that our re-expressed estimate of mean absolute percent error (MAPE) could be interpreted as a percent error.

Table 3.8 Method comparisons after applying optimal minimum size criteria and removing a common outlier in terms of the optimal minimum lake size criterion, the number of mutually identified lakes, mean absolute percent error (MAPE), and the direction of bias as estimated by the percentage of under-estimated lakes. Entries for mutually identified lakes, mean absolute percent error (MAPE), and % under-estimated lakes are the mean (standard error) of the 10 classifications (5 training sets x 2 images (TM/ETM+)) for each method. All comparisons were made within columns. Matching superscripts within columns denote that the two entities were significantly different using a two-way within-subjects analysis of variance (ANOVA) and Tukey's studentized range test to maintain experiment-wise error (alpha=0.05) (SAS Institute, Inc. 2003). We did not use the convention of common superscripts for entities that are not significantly different for ease of results presentation.

METHOD	OPTIMAL MINIMUM SIZE (m^2)	# MUTUALLY IDENTIFIED LAKES	MEAN ABSOLUTE PERCENT ERROR (MAPE)	DIRECTION OF BIAS: % UNDER-ESTIMATED LAKES
Density Slicing (Band 5)	5850	$44.0^{A, B}$ (1.01)	14.9 (0.71)	52.7 (2.66)
Classification Tree (Band 5)	8550	27.1^{A} (1.41)	17.9 (1.70)	67.6 (5.90)
Feature Extraction (Band 5)	8550	29.8^{B} (0.92)	12.2 (1.22)	63.8 (6.85)

[a] Mean absolute percent error (MAPE) is an estimate of the magnitude of bias in area estimates. Absolute percent error for each lake was calculated by dividing the absolute difference between the lake area classified from satellite imagery and the lake area from the validation set of lake polygons by the lake area from the aerial photography validation set. We followed procedures described by Tayman et al. (1999) to transform skewed percent error distribution and then re-express the mean of the transformed absolute percent error distribution back to the original scale of the un-transformed errors so that our re-expressed estimate of mean absolute percent error (MAPE) could be interpreted as a percent error.

Table 3.9 Qualitative comparison of the performance of the three supervised classification methods.

	Density Slicing	Classification Tree	Feature Extraction
EFFICIENCY:			
Training Data Preparation Speed	Fast	Slow	Moderate
Training Speed	Slow	Fast	Fast
Classification Speed	Fast	Slow	Fast
EASE OF APPLICATION:			
Use of Specialized Software	No	Yes	Yes
SENSITIVITY TO GEOREFERENCING ERRORS	Low	High	High

Chapter 4: Temporal trends in lake area in Alaskan National Wildlife Refuges[1]

Abstract

The objectives of this study were 1) to use improved methods to estimate and compare historical trends in lake area across ten study areas in eight Alaskan National Wildlife Refuges based on aerial photography and satellite imagery and 2) to identify potential relationships between study area trends and landscape characteristics to elucidate potential underlying mechanisms. Using a multi-scale hierarchical approach, annual and within-summer trends were estimated at two temporal scales, a long-term scale (since ~1948) and a shorter recent scale (since ~1985), and at two spatial scales: broad-scale estimates were obtained for ten study areas and finer-scale estimates were obtained for ~23,000 individual lakes within these study areas. Across the ten study areas, lakes overall were decreasing in size. Seven of the ten study areas had significant long-term declines in lake area and five study areas had significant recent declines. The average rate of change across study areas was -1.07 % per year for the long-term records and -0.80 % per year for the recent records. The presence of net declines in lake area statewide and for several study areas suggests that, while there was

[1]Roach J, Griffith B, Ver Hoef J & Verbyla D. Temporal trends in lake area in Alaskan National Wildlife Refuges. *Prepared for Global Change Biology.*

substantial among-lake heterogeneity in trends at scales as small as 3 km, a dynamic equilibrium in lake area may not be present. Study areas with decreasing trends in lake area tended to have a predominantly non-fluvial surficial geology, coarser-grained sandy soils, and fewer lakes in zones with thermokarst features compared to study areas with negligible or increasing trends. Coarse-grained sandy soils may promote decreasing lake area due to better drainage, while finer-grained silty soils may be more susceptible to large subsidence events due to higher ice contents (i.e., thermokarst), which may promote lake expansion. Study areas with decreasing trends also tended to have smaller lakes, which may have been more susceptible to decreasing lake area than larger lakes due to shallower bathymetries and warmer water temperatures.

Introduction

Lakes and wetlands are a predominant land-cover type on the sixteen National Wildlife Refuges in Alaska and serve as breeding grounds for global populations of waterfowl and shorebirds that migrate annually from more southerly parts of North America, South America, Asia, and Australia. Refuge lakes and wetlands support local populations of fish, mammals, and birds that are important subsistence resources for local indigenous groups. Northern peatlands are also important stores of global carbon and changes in lake area and/or peatland extent could have a large effect on the global storage and emission of radiative gases such as carbon dioxide and methane (Laine *et al.* 1996; Walter *et al.* 2006). The maintenance of Alaskan lake and peatland ecosystems and their

associated biodiversity and storage of carbon is critical to the sustainability of high latitude and global social and ecological systems.

Broad-scale losses in lake number and area have been identified in the Arctic and sub-Arctic boreal forest during the past ~50 years (Smith *et al.* 2005; Riordan *et al.* 2006; Labrecque *et al.* 2009), and these changes have been coincident with a warming climate and increased water deficit (Oechel *et al.* 2000; Barber *et al.* 2000). However, these previous estimates have not adequately accounted for within- and among-year variability in order to isolate linear trends that are essential for the projection of future change and potential implications for the global carbon budget and fish and wildlife habitats. This is especially important in the Alaskan boreal forest where inter- and intra-annual variability in lake area can be substantial and, if not accounted for, could be mistaken for long-term change.

An understanding of the spatial processes and mechanisms associated with change at multiple scales can also enhance spatial and temporal projections of future change by identifying lakes, regions, and refuges that may be most susceptible to change. Recent studies have suggested a range of climate-related mechanisms for changes in lake area in northern regions including permafrost degradation (Yoshikawa & Hinzman 2003; Smith *et al.* 2005), increased evapotranspiration (Klein *et al.* 2005; Smol & Douglas 2007; Labrecque *et al.* 2009), and terrestrialization (i.e., peatland development) (Payette *et al.* 2004; Roach *et al.* 2011), which could be related to a number of lake and landscape

characteristics such as lake size and bathymetry, soil type and origin, permafrost extent and ice content, and mean air temperature and total precipitation.

Permafrost has a large influence on hydrological properties in the Arctic and sub-Arctic by acting as an aquiclude that prevents surface water and sub-permafrost groundwater interactions. When permafrost underneath lakes thaws, interactions between surface water and sub-permafrost groundwater systems may largely depend on soil drainage properties and the direction of hydraulic gradients, which can lead to either drainage (Yoshikawa & Hinzman 2003) or groundwater recharge of lakes (Kane & Slaughter 1973). In particular, coarse-grained sandy soils promote drainage (Burn 2002), while fine-grained silty soils can act as an aquiclude similar to permafrost, thus, promoting surface water ponding. Permafrost degradation can also lead to a reduction in lake area by increasing water infiltration into a deepening active layer, which can affect surface and subsurface flow (Brabets & Walvoord 2009) and the amount of run-off reaching lake systems. The degradation of ice-rich permafrost (i.e., thermokarst), commonly found in fine-grained silty soils (Jorgenson & Osterkamp 2005), can also lead to either increases (Jorgenson *et al.* 2001; Roach *et al.* 2011) or decreases (MacDonald *et al.* 2011) in lake area. Although permafrost degradation has been associated with both decreases and increases in lake area, net decreases in lake area have been observed predominantly in discontinuous permafrost regions that have more unstable permafrost, while increases or negligible changes have been found in continuous permafrost regions (Smith *et al.* 2005; Riordan *et al.* 2006).

An important first step to understanding the mechanisms and spatial processes underlying lake area trends is the identification of spatial heterogeneity in trends at multiple scales. In this study, a multi-scale hierarchical approach was used to obtain explicit statistical estimates of annual and within-summer trends at two temporal scales, a long-term scale (since ~1948) and a shorter recent scale (since ~1985), and at two spatial scales, a broad study area-scale and an individual lake scale. Broad-scale estimates were obtained for ten study areas located in eight Alaskan National Wildlife Refuges spanning longitudinal and latitudinal gradients of ~1000 km (Fig. 4.1) and finer-scale estimates were obtained for ~23,000 individual lakes within these study areas. Using improved statistical methods for the estimation of lake area change, our objective was to compare temporal trends in lake area among the ten study areas 1) to facilitate prioritization of research and management programs and 2) to identify potential relationships between annual trends in lake area and landscape characteristics to elucidate potential mechanisms for among-study area heterogeneity in trends.

Materials and Methods

Study Areas

Temporal trends in lake area were estimated for ten study areas within eight Alaskan National Wildlife Refuges in boreal and tundra ecozones: Tetlin, Yukon Flats, Kanuti, Selawik, Koyukuk, Innoko, Togiak, and Becharof (Fig. 4.1). In the Yukon Flats National Wildlife Refuge we used three study areas (West, Central, and East) due to the

presence of a wide longitudinal gradient (~ 200 km) within this refuge and preliminary suggestions of differential lake trends along this longitudinal gradient. Study area boundaries were delineated to 1) contain North American Waterfowl Breeding Pair Survey (BPS) transects (Hodges *et al.* 1996) that had the most complete and temporally consistent (i.e., imagery acquired during a single year and season) coverage of historical aerial photography, 2) maximize overlap with National Wildlife Refuge lands of particular value to wildlife populations and other ongoing studies identified through consultations with USFWS land managers, and 3) maximize overlap of cloud-free satellite imagery. Study areas contained BPS waterfowl survey transects because they have been surveyed since 1957 (Hodges *et al.* 1996) and may provide the opportunity in the future to link lake area and waterfowl abundance trends.

Imagery

We analyzed two types of imagery: aerial photography and Landsat sensor imagery. Digital vertical aerial photographs and Landsat TM/ETM+ scenes were obtained from the United States Geological Survey (USGS) Earth Resources Observation and Science (EROS) Center, Sioux Falls, South Dakota. The USGS EROS historical film archives were acquired from a wide variety of sources including USGS, U.S. Air Force, Army Map Service, U.S. Navy, and Alaska High-Altitude Aerial Photography (AHAP).

Because the manual delineation of lake polygons from aerial photography is time- and labor-intensive, the use of historical aerial photography was restricted to lakes that

intersected a 200 m wide buffer on either side of the 26 km long BPS waterfowl survey transects (Fig. 4.2). A 200 m buffer was used for lake selection because this was the distance from the BPS flight paths within which bird observations were recorded (Hodges *et al.* 1996).

The inclusion of historical aerial photography extended the temporal record for the on-transect lake population beyond the start of Landsat TM acquisition in 1984 (Table 4.1). The earliest aerial photographs were acquired from 1948-1953 for all study areas with the exception of the Kanuti and Selawik study areas which had aerial photograph records starting in 1970 and 1978, respectively. The temporal records for the on-transect lake population that included historical aerial photography were referred to as long-term records, while the temporal records for the off-transect lake population that included only Landsat imagery were referred to as recent records.

Six overlapping TM/ETM+ scenes were obtained for each study area. A visual review of visible Band 1 and thermal Band 6 was performed to ensure that local atmospheric variation such as fog, smoke or cirrus clouds, which can erroneously inflate Band 5 spectral reflectance, were not present. If atmospheric interference was present, the image was removed and replaced with a new image. With the exception of the Kanuti study area, each time series of six TM/ETM+ scenes included three early season (pre-July 10) and three late season (post-July 10) scenes. The Kanuti study area time series included four late season scenes and only two early season scenes due to early

season cloud interference. The inclusion of imagery from a range of dates (Table 4.1) within the summer season enabled the estimation of within-summer trends in lake area.

Image Processing

The short wave infrared (SWIR) Band 5 was used to classify water from TM/ETM+ scenes because this band is the most useful in discriminating water from non-water pixels (Chapter 3; Johnston & Barson 1993; Frazier & Page 2000). Digital Numbers (DNs) were converted to Top-Of-Atmosphere (TOA) reflectance (Chander *et al.* 2009) in order to reduce scene-to-scene variability. Reflectance was then scaled from 0.0 – 0.63 floating point to 0 – 255 integer (1-byte) values.

Multiple aerial photographs were required to encompass all transect lakes and were clipped to extents that included lakes that intersected a 200 m buffer around each transect (Fig. 4.2). Each study area was defined by the area of complete overlap of six TM/ETM images that included BPS transects. One or two (Fig. 4.2) unique series of six overlapping TM/ETM+ scenes were required to completely cover each study area. Thus, each time series (Table 4.1) was encompassed by a unique spatial extent (Fig. 4.2) and TM/ETM+ scenes were clipped to these spatial extents.

Each clipped aerial photograph and satellite image was co-registered to the UTM NAD27 map projection using a linear affine transformation model and nearest neighbor re-sampling. The statewide coverage of 1:63,360 topographic maps (http://agdc.usgs.gov/geodata) was used as a source for control points. Because each of

the six images within a time series was clipped to the same extent with pixels aligned throughout the series, a single co-registration model was used for each extent/time series (Fig. 4.2). This ensured a consistent spatial alignment throughout each satellite image time series thus removing between satellite image positional error as a source of bias in the time series analysis. Each satellite image co-registration model was based on at least 30 control points and a root mean squared error (RMSE) of less than 23 m. Co-registered clipped Landsat TM/ETM+ images ranged in size from 579 km^2 to 4842 km^2 and had a pixel size of 30 m. Each clipped aerial photograph co-registration model was based on at least 10 control points and a density of at least 0.5 points per km^2 and a root mean squared error (RMSE) of less than one pixel which ranged from 0.6 to 12.1 m. Co-registered clipped aerial photographs ranged in size from 0.3 km^2 to 39.5 km^2.

Lake Polygon Creation

Lake polygons were manually delineated from aerial photography because poor spectral resolution and interference from sunglint on water surfaces prevented the use of automated methods. Water was classified from TM and ETM+ images using supervised density slicing with SWIR Band 5 spectral reflectance integer values (Chapter 3). This method used a threshold value for a single band to discriminate water from non-water pixels. A unique threshold value was identified for each image by comparing classified lake area to the associated lake polygons derived from the aerial photography for three to five lakes that did not change in size between the aerial photography and Landsat image.

When a large number of potential training lakes were available for threshold determination, five lakes were chosen so that they represented a range of lake sizes and covered the widest spatial extent.

Density slicing resulted in a binary raster image of water and non-water which was then converted to polygon features. A visual inspection of polygons and imagery was conducted to identify rivers and wetlands that were misclassified as lake water pixels. The misclassification of wetlands as open water can be particularly problematic when classifying water and non-water from TM/ETM+ imagery (Chapter 3). Because wetlands often tend to be ephemeral within and among years, one useful indicator of potentially misclassified lake polygons is the presence of a large lake polygon or unusually large growth of a lake polygon at a certain location in only one image in a time series. Visual inspection of areas such as these can often identify boundaries between lakes and surrounding wetland areas that were not able to be detected using an automated classification approach. Once identified, these rivers and misclassified wetland polygons or partial polygons were masked from all six images within a time series. Classified images were also visually inspected for the presence of clouds and cloud shadows. If clouds or cloud shadows interfered with the classification of a lake's area, the lake area for that image was labeled as no data.

Preparation of Lake Polygon Data for Trend Analysis

In order to perform a statistical analysis using lakes as sample units, lake polygon data were summarized into discrete entities that could be tracked through time. To account for a single lake becoming a multi-part polygon or multiple lakes coalescing into a single polygon within a time series, we defined a lake sample unit as either the single polygon or group of polygons that intersected the combined maximum extent of a water body throughout the time series (Fig. 4.3). Thus, if a lake split into multiple parts in a subsequent image, its area was the sum of the areas of each individual part. This lake definition enabled the area of lake sample units to be monitored through time so that our final dataset consisted of a list of lakes and their total multi-part or single-part area in each image within a time series.

Once polygons were organized into lake sample units, a lower detection limit of 5850 m^2 was applied to minimize potential omission and commission errors that could result when comparing imagery of different spatial and spectral resolutions (Chapter 3). Lakes that were less than 5850 m^2 in all aerial photographs and TM/ETM+ images were removed from the analysis. If a lake was larger than 5850 m^2 in at least one image it was retained and if its area fell below 5850 m^2 in one or more time periods these values were substituted with a constant that was half the detection limit (i.e., 2925 m^2). Substitution with a constant is a practice commonly used with data below a detection limit (Helsel 2005). In a similar manner, all islands less than 5850 m^2 were also removed and were, thus, classified as water. Islands larger than 5850 m^2 were classified as land.

Statistical Analysis of Temporal Trends

Repeated measures regression models with lakes as sample units were used to estimate study area trends in lake area (SAS Institute, Inc. 2008). Log-transformed lake area (m^2) was the dependent variable ($Y_{i,j}$ for the *j*th repeated measurement of the *i*th lake). Natural log transformation was required to normalize the right skewed distributions. All models included year as an independent variable to estimate annual trends in lake area. Inclusion of a day-of-summer independent variable to estimate within-summer trends in lake area was assessed using a p-value of 0.05. To obtain separate equations for on-transect long-term trends and off-transect recent trends, we pooled variances from on- and off-transect lake populations by including an indicator variable (a 0 or 1) for lakes on- or off-BPS transects along with all interactions between the transect variable and the main effects that entered into each model (i.e., year and day-of-summer). By pooling variances from the on- and off-transect lake populations, we were able to increase the statistical power to detect long-term trends for on-transect lake populations which had small sample sizes.

We used a random coefficient model that allowed for overall fixed effects in year and day-of-summer and random variations from those effects for each individual lake, while testing and adjusting for any transect effect. The model may be written as,

$$Y_{i,j} = A_i + \tau_k I_i + \beta t_{i,j} + (\tau\beta)_k t_{i,j} + B_i t_{i,j} + \theta d_{i,j} + (\tau\theta)_k d_{i,j} + T_i d_{i,j} + Z_{i,j} + e_{ij} \qquad (1)$$

where A_i is a random intercept for the *i*th lake, τ_k is a fixed effect for on or off transect, I_i is an indicator variable (a 0 or 1) for the *i*th lake being on or off transect, β is an

overall slope (fixed effect) for year, $t_{i,j}$ is the year for the *j*th repeated measurement for the *i*th lake, $(\tau\beta)_k$ is an interaction (fixed effect) that allows for separate slopes on or off transect, B_i is a random deviation from the overall and transect interaction slope for year for the *i*th lake, θ is an overall slope (fixed effect) for day-of-summer, $(\tau\theta)_k$ is an interaction (fixed effect) that allows for separate slopes on or off transect, $d_{i,j}$ is the day of summer for the *j*th repeated measurement for the *i*th lake, T_i is a random deviation from the overall and transect interaction slope for day-of-summer for the *i*th lake, and $Z_{i,j}$ is a temporally autocorrelated random error, and e_{ij} is an independent random error. The temporal autocorrelation was assumed to follow an exponential autocovariance model,

$$\text{cov}(Z_{i,j}, Z_{i',j'}) = \sigma_Z^2 \exp(-|u_{i,j} - u_{i',j'}| / \rho) \quad (2)$$

where $u_{i,j}$ is days since the earliest image date in each time series for the *j*th repeated measurement of the *i*th lake. Year ($t_{i,j}$) and day-of-summer ($d_{i,j}$) variables were coded as years or days since the earliest year or day of image acquisition for each time series and were divided by 100 to enable model convergence. The full random effects model (eq. 1) had six covariance parameters: $\text{var}(A_i) = \sigma_A^2$, $\text{var}(B_i) = \sigma_B^2$, $\text{var}(T_i) = \sigma_T^2$, $\text{var}(e_{ij}) = \sigma_e^2$, and σ_Z^2 and ρ for the autocovariance model. The parameters of the random effects model (eq. 1) were estimated by setting the covariance parameters for intercept ($\text{var}(A_i)$), year ($\text{var}(B_i)$), and day-of-summer ($\text{var}(T_i)$) to be equal to the

variances of the respective intercept, year, and day-of-summer effects from individual lake regression models,

$$Y_{i,j} = \alpha_i + \beta_i t_{i,j} + \theta_i d_{i,j} + e_{ij} \quad (3)$$

where α_i is an intercept for the *i*th lake, β_i is a slope for year for the *i*th lake, and θ_i is a slope for day-of-summer for the *i*th lake, and e_{ij} is an independent random error. We set the covariance parameter estimates to be equal to the variances of these individual lake fixed effects because the restricted maximum likelihood estimates of these parameters were unrealistically small, under-estimating the variance among individual lake intercepts and model slopes.

To identify individual lake equations, variances for all lakes in each study area (i = 1,.., n) were pooled into a single regression model by including indicator variables for each lake and all interactions between the indicator variables and the main effects (i.e., year and day-of-summer),

$$Y_{i,j} = \alpha + (\lambda_1 I_1 + ... + \lambda_{n-1} I_{n-1}) + \beta t_{i,j} + ((\lambda\beta)_1 t_{1,j} + ... + (\lambda\beta)_{n-1} t_{n-1,j}) + \theta d_{i,j} + ((\lambda\theta)_1 d_{1,j} + ... + (\lambda\theta)_{n-1} d_{n-1,j}) + e_{ij} \quad (4)$$

where α is the intercept, λ_i is a fixed effect for the *i*th lake, I_i is an indicator variable for the *i*th lake, β is an overall slope for year, $t_{i,j}$ is the year for the *j*th repeated measurement for the *i*th lake, $(\lambda\beta)_i$ is an interaction term that allows for a separate slope for the *i*th lake, θ is an overall slope for day-of-summer, $(\lambda\theta)_i$ is an interaction term that allows for a separate slope for the *i*th lake, $d_{i,j}$ is the day of summer for the *j*th repeated

measurement for the *i*th lake, and e_{ij} is an independent random error. All models included year as an independent variable. Day-of-summer was included as an independent variable if it entered into the study area repeated measures model (Eq. 1).

Interpretation of Statistical Model Coefficients

Year slopes from all models were estimates of the geometric percent change in average lake area per year (Flanders *et al.* 1992) and henceforth will be referred to as annual rates of change. Day-of-summer slopes from all models were estimates of the geometric percent change in average lake area per day of the summer (Flanders *et al.* 1992) and henceforth will be referred to as within-summer rates of change.

Comparison of On- and Off-Transect Trends

Significance of the transect*year ($(\tau\beta)_k$) and transect*day-of-summer ($(\tau\theta)_k$) interaction terms (Eq. 1) indicated that long-term (i.e., on-transect) and recent (i.e., off-transect) rates of change in average lake area were significantly different. These differences in on- and off-transect rates of change could be due either to 1) an increase or decrease in rates of change after ~1985, 2) an enhanced ability to detect trends of a smaller magnitude with the longer temporal record for lakes on the transects, or 3) the small on-transect lake population may not have been representative of the larger off-transect lake population in terms of trends. In contrast, non-significance of interaction terms may have been due to the small on-transect sample sizes reducing the power of the

tests or may indicate that rates of change were consistent for both the recent and long-term temporal records.

To identify whether a non-representative on-transect sample may have been a source of differences between on- and off-transect lake populations, rates of change were compared between the two populations during the same time period (i.e., for the recent post-1985 records) using Equation 1. Significant differences between on- and off-transect lake populations (i.e., significant $(\tau\beta)_k$ or $(\tau\theta)_k$ terms) during the same time period would indicate that the on-transect lake population may not have been representative of the larger off-transect lake population in terms of temporal trends.

To further explore the potential representativeness of the on-transect lake population in terms of lake size, we tested the hypothesis that on-transect lakes may have been larger on average compared to the off-transect lake population because transects preferentially sample larger objects. One-tailed t-tests were used to test whether the difference in average lake size between on- and off-transect lake populations was significantly greater than zero for each study area.

Spatial Heterogeneity in Individual Lake Annual Trends

Five trend classes were defined based on the combined distribution of individual lake annual rates of change from all ten study areas. Trend class threshold values were selected to yield a relatively equitable distribution of lakes among the five classes. The negligible trend class contained lakes that had annual rates of change within the 20th

percentile centered on zero of the combined lake distribution. The remaining lakes with negative annual rates of change were split into two equal sized groups and assigned to small and large decreasing trend classes. In a similar manner, the remaining lakes with positive annual rates of change were split into two equal sized groups and assigned to small and large increasing trend classes.

Each lake was assigned an ordinal value of 1 through 5 based on its trend class (1 = large decrease, 2 = small decrease, 3 = negligible, 4 = small increase, 5 = large increase) and the Moran's I statistic was used to evaluate whether high or low trend class values were clustered, dispersed, or randomly distributed across each study area. Calculation of the Moran's I statistic in ArcGIS generates z-scores and p-values to test the null hypothesis that trend classes were randomly spatially distributed. A fixed distance band approach was used with multiple distance bands in increments of 1000 m starting at the distance where every lake has at least one neighbor and ending with the distance where at least one lake has every other lake as a neighbor. The distance band that resulted in the highest z-score (highest degree of clustering) was then used to calculate Moran's I. This distance band is informative because it is the scale at which clustering and its associated underlying spatial characteristics are most pronounced.

Temporal Variability in Lake Area

Coefficients of variation in lake area (standard deviation / mean) were used to characterize temporal variability in lake area for individual lakes. These individual lake

coefficients of variation were then averaged to estimate overall temporal variability in lake area for each study area. Coefficients of variation include all potential sources of temporal variability in lake area including annual trends, inter-annual variability, and intra-annual variability. In order to reduce the influence of large annual trends on coefficients of variation, our estimations of coefficients of variation were restricted to lakes within the small decrease, small increase, and negligible annual trend classes.

Two classes of lakes, fluctuating and non-fluctuating, were identified based on the combined distribution of lake coefficients of variation from the three trend classes for all ten study areas. Fluctuating lakes were lakes that had coefficients of variation within the upper 25^{th} percentile of this distribution. Using a similar approach to that used for trend classes, the Moran's I statistic was calculated to identify whether fluctuating lakes tended to be clustered and the scale at which clustering was most pronounced. Characterizing among- and within-study area heterogeneity in coefficients of variation in lake area may elucidate potential mechanisms underlying large fluctuations in lake area. An understanding of these underlying mechanisms may highlight important biological differences between fluctuating and non-fluctuating lakes (e.g., water chemistry, wildlife biodiversity).

Spatial Distribution of Individual Lake Annual Trends and Fluctuating Lakes

Ordinary kriging (ArcGIS) was conducted to provide a visual representation of the spatial distribution and degree of clustering of individual lake annual trend classes

(i.e., large decrease, small decrease, negligible, small increase, and large increase) and individual lake temporal variability (i.e., fluctuating and non-fluctuating lakes). Ordinary kriging was applied to trend class values 1 through 5 and to an indicator variable (0 or 1) for fluctuating or non-fluctuating lakes to maintain consistency with the approach used to calculate the Moran's I statistic. The spatial autocorrelation was assumed to follow an exponential autocovariance model. Model parameters were optimized using the standard optimization procedure within the Geostatistical Wizard, which uses cross validation to minimize the mean square error with a focus on the estimation of the range parameter. A standard single sector search neighborhood was used to make predictions with a minimum of eight and a maximum of 20 nearest neighbors.

Study Area Characteristics and Annual Trends in Lake Area

Statistical Analysis

Study area geophysical, topographical, climatic, and lake size and density characteristics were summarized to explore potential explanations for among-study area differences in recent annual lake area trends. To identify potential relationships between study area characteristics and the direction of annual trends in lake area, study areas were assigned to either decreasing or non-decreasing (i.e., increasing/negligible) groups based on recent annual rates of change for the off-transect lake populations and one-tailed t-tests were used to evaluate whether the difference in mean characteristics between the two groups was significantly greater than or less than zero. These analyses were

restricted to the recent trends estimated for off-transect lake populations because they contained the vast majority of lakes in each study area. *A priori* hypotheses for the expected direction of the difference in mean values between decreasing and non-decreasing groups were tested and are detailed in the following sections. Categorical characteristics (e.g., surficial geology) were converted to continuous variables based on these *a priori* hypotheses (e.g., percentage of lakes with fluvial surficial geology). With a small sample size of ten study areas and a high potential for correlation among the various study area characteristics, it was not possible to conduct multivariate analyses. Thus, due to the large number of multiple comparisons, statistical significance was not assigned to individual results. Instead we present P-values and discuss those that were < 0.10 that may be of interest for exploratory purposes and future hypothesis testing only. Study area within-summer rates of change and coefficients of variation in lake area were initially qualitatively compared to study area characteristics to identify potential relationships for further quantitative analysis.

Geophysical Characteristics

Geophysical characteristics such as permafrost extent and ice content, surficial geology, and soil type and grain size can have large influences on lake drainage properties and subsurface groundwater interactions (Jorgenson & Osterkamp 2005; Burn 2002). Statewide maps were used to assess surficial geology, permafrost extent and ice

content, soil texture, thermokarst features, and landform type (Jorgenson *et al.* 2008; Johnson *et al.* unpublished data).

A revision of the statewide surficial geology map of Karlstrom (1964) by Jorgenson *et al.* (2008) was used. This revision had ten categories at its broadest level of organization: coastal, fluvial, eolian loess, eolian sand, glacial moraines and drift, glacio-fluvial, glacio-lacustrine, glacio-marine, mountain alluvium and colluvium, and undifferentiated alluvium and colluvium. Because fluvial surficial geology tends to be associated with poorly drained fine-grained soils, we hypothesized that study areas with increasing or negligible annual trends in lake area would have a greater percentage of lakes with fluvial surficial deposits than study areas with decreasing trends in lake area. Similarly, we hypothesized that study areas with decreasing annual trends in lake area would have a greater percentage of lakes with better-drained coarse-grained sandy soils.

Because fine-grained soils also tend to have higher permafrost ice content (Jorgenson & Osterkamp 2005) and, thus, tend to be more susceptible to thermokarst events, we hypothesized that study areas with increasing or negligible annual trends in lake area would have a greater percentage of lakes located in areas with moderate to high ice content and thermokarst features. Thermokarst features included troughs, sinks, pits, slumps, gullies, and water tracks (Jorgenson *et al.* 2008). Previous studies have identified thermokarst as a mechanism for increasing or negligible changes in lake area (Payette *et al.* 2004; Jorgenson & Osterkamp 2005; Roach *et al.* 2011) in contrast to terrestrialization (i.e., expanding vegetation into open water with a potential trajectory

towards peatland development) as a mechanism for decreasing lake area (Payette *et al.* 2004; Roach *et al.* 2011). Thus, we hypothesized that study areas with increasing or negligible annual trends in lake area may have a greater percentage of lakes with a woody wetland landform type (Johnson *et al.*, unpublished data) that may be more susceptible to thermokarst formation while study areas with decreasing annual trends may have a greater percentage of lakes with a herbaceous wetland landform (Johnson *et al.* unpublished data) type that may be more susceptible to terrestrialization.

Permafrost extent was derived from a rule-based model that incorporated mean annual air temperatures and surficial deposit types (Jorgenson *et al.* 2008) and included the following categories: continuous (90-100%), discontinuous (50-90%), sporadic (10-50%), and isolated (0-10%). Greater rates of decline in lake area have been found in discontinuous permafrost regions compared to continuous permafrost regions (Smith *et al.* 2005; Riordan *et al.* 2006). Discontinuous permafrost regions are more susceptible to permafrost thawing (Osterkamp & Romanovsky 1999), which can cause a decrease in lake water levels through 1) increased water infiltration into a deepening active layer which can affect surface and subsurface flow (Brabets & Walvoord 2009) and the amount of run-off reaching lake systems or 2) talik expansion which can lead to removal of the permafrost aquiclude underneath lakes and drainage to groundwater systems in the presence of a negative hydraulic gradient (Yoshikawa & Hinzman 2003). Thus, we hypothesized that study areas with decreasing annual trends in lake area would have a greater percentage of lakes in discontinuous, sporadic, and isolated permafrost.

Topography

Mean elevation and elevation-relief ratios were assessed using a 300 m Alaska digital elevation model. Elevation-relief ratios are an approximation of the hypsometric integral used to describe the topographical distribution of a land area (Pike & Wilson 1971). They were calculated for each study area using the following equation:

$$\text{Elevation-relief Ratio} = \frac{\text{Mean Elevation} - \text{Minimum Elevation}}{\text{Maximum Elevation} - \text{Minimum Elevation}}$$

Low values occur in terrain characterized by isolated relief features standing above extensive level surfaces typical of surface runoff-dominated drainages. Lake area in this type of terrain may be largely influenced by spring snowmelt. Higher values describe broad, somewhat level surfaces broken by occasional depressions that may be more typical of groundwater influenced terrain (Pike & Wilson 1971; Luo 2002). Lake area in this latter type of terrain may be influenced by inter- and intra-annual variability in the water table, subsurface flow, and overland flow in connected streams and rivers. We hypothesized that study areas with increasing or negligible annual trends in lake area would have more relief features and runoff-dominated drainages (i.e., higher mean elevation and lower elevation-relief ratios).

The United States Geological Society (USGS) 1:2,000,000 Digital Line Graphs (DLG) dataset and a subset of major rivers from this dataset compiled by Alaska Department of Natural Resources were used to estimate mean distance from lakes to major rivers and streams for each study area. The shortest straight line distance from lake centroids to the nearest stream or river was estimated using ArcGIS. Proximity of lakes

to rivers may be indicative of lake connections to surface or subsurface flow and fluvial landscape characteristics. Similar to our expectations for fluvial surficial geology and soil texture, we hypothesized that study areas with negligible or increasing annual trends in lake area would have lakes located closer to rivers and streams.

Ecoregion

Study area ecoregeions were assessed using the Unified Ecoregions of Alaska (Nowacki *et al.* 2001) classification, which consists of hierarchical levels of ecosystem classification based on regional climate, topography, vegetation, and geology. Level I generally follows climatic gradients and consists of the polar, boreal, and maritime ecoregions. Level II is a finer scale of ecoregion division consisting of nine classes: Arctic Tundra, Bering Tundra, Bering Taiga, Intermontane Boreal, Alaska Range Transition, Aleutian Meadows, Coastal Rainforests, Coast Mountains Transition, and Pacific Mountains Transition. Previous studies have documented declines in lake area in the boreal ecoregion which encompasses the eastern Yukon River Basin (Riordan *et al.* 2006; Corcoran *et* al. 2009; Anderson *et al.* 2010).

Climate

Study area climatic characteristics were assessed using 2-km grid Scenarios Network for Alaska Planning (SNAP) historical Climate Research Unit (CRU) data (http://www.snap.uaf.edu/downloads/alaska-climate-datasets). Seasonal and annual

mean temperature and total precipitation data were averaged across all 2-km grids within each study area. Seasonal and annual mean temperatures were averaged from 1950-2009 and total precipitation was averaged from 1950-2006. Seasons were summer (June, July, and August), fall (September, October, and November), winter (December, January, and February), and spring (March, April, and May). Because previous studies have identified declines in lake area primarily in continental climates of the boreal forest (Riordan *et al.* 2006; Corcoran *et* al. 2009; Anderson *et al.* 2010), we hypothesized that study areas with decreasing annual trends in lake area would have warmer summer mean temperatures, cooler fall, winter, and spring mean temperatures, and lower seasonal and annual total precipitation.

Lake Size and Density Characteristics

Study area-scale lake size and density characteristics were summarized using the average size of lakes across all time periods included in each study area analysis. Large lakes were defined as greater than 10 hectares (ha). Small lakes were defined as less than 1 ha. Limnetic ratio ((Total lake area / Total study area) x 100%) was used to describe areal lake extent and lake density was used to describe lake abundance. Because small lakes tend to be shallower and, thus, may be more susceptible to losses in lake area (Roach *et al.* 2011), we hypothesized that study areas with decreasing annual trends in lake area would have a smaller mean lake area, a greater percentage of small lakes, and a smaller percentage of large lakes.

Results

Annual Trends in Lake Area

Magnitude and Direction

At the statewide scale, most lakes and most study areas had decreasing annual trends in lake area (Tables 4.2 & 4.3). Seven of the ten study areas had significantly decreasing long-term trends in lake area (Table 4.4, Fig. 4.4a). For the recent temporal records, which constituted the vast majority of lakes in each study area, five study areas had significant decreasing trends, four study areas had non-significant trends, and one study area had a significant increasing trend in lake area (Table 4.4, Fig. 4.4a). The average rate of change across study areas was -1.07% per year for the long-term records and -0.80% per year for the recent records (Table 4.4). The average rate of change across individual lakes was nearly identical at -1.07% and -0.72% for the long-term and recent records, respectively (Table 4.2). The average cumulative percent reduction in lake area across study areas was 41% for the long-term records and 14% for the recent records (Table 4.4).

Comparison of Long-term and Recent Annual Trends

At the statewide scale, there was a tendency for rates of decline to be lower for the recent temporal records compared to the long-term records (Table 4.4). This may be mostly attributable to the Tetlin, Becharof, and Koyukuk study areas which were the only study areas to have significantly different long-term and recent rates of change and,

specifically, had significant long-term declines in lake area but non-significant recent trends (Table 4.4, Fig. 4.4a). These differences in rates of change were likely not due to a non-representative on-transect sample because on- and off-transect rates of change were not significantly different when compared at the *same* temporal scale (Table 4.5, Fig. 4.5a).

Innoko was the only study area to have significantly different on- and off-transect trends at the *same* temporal scale (i.e., since ~1985) (Table 4.5, Fig. 4.5a) suggesting that the on-transect lake population may not have been representative of the larger study area in terms of annual trends. In Innoko, lakes on the transects were significantly larger than lakes off of the transects (~ 5 times larger) (Table 4.6). However, eight of the remaining nine study areas that had representative on-transect lake populations in terms of annual trends (Table 4.5, Fig. 4.5a) also had significantly larger lakes on the transects (Table 4.6). Thus, in Innoko, lakes on the transects may not have been representative of lakes off of the transects for reasons besides differences in lake size.

Within-Study Area Spatial Heterogeneity

There was a large degree of among-lake heterogeneity in annual trends (Fig. 4.6) in all ten study areas (Table 4.2, Figs. 4.7 & 4.8), which included substantial decreases (Fig. 4.9) and increases (Fig. 4.10) in lake area. Yukon Flats East was the most variable in individual lake annual rates of change (standard deviation = 4.9) and Becharof was the least variable (standard deviation = 1.8) (Table 4.2, Fig. 4.7). The distribution of all

individual lake annual rates of change in the ten study areas as well as the distributions of individual lake annual rates of change in several study areas had skew values of less than -0.5 indicating substantially left-skewed distributions with a long tail to the left representing very large decreases in area for some individual lakes, while the majority of data had more moderate rates of change (Table 4.2, Fig. 4.7).

The threshold values for annual rates of change used to assign lakes to the five trend classes were: less than -1.6486 for large decreases, less than -0.2534 for small decreases, less than 0.2551 for negligible change, less than 1.099 for small increases, and greater than 1.099 for large increases. Moran's I values were positive and statistically significant (alpha = 0.05) for all ten study areas indicating that lakes in high or low trend classes tended to be spatially clustered at scales ranging from 3 to 22 km (Table 4.3, Fig. 4.8). Maximum clustering of individual lake annual trends occurred at scales (i.e., distance bands) of less than or equal to 10 km in eight study areas suggesting fine-scale heterogeneity both in trends and their underlying mechanisms (Table 4.3, Fig. 4.8). In the Selawik (Fig. 4.8f) and Togiak (Fig. 4.8i) study areas, maximum clustering occurred at comparatively large scales of 22 km suggesting broader scale underlying spatial processes in these areas (Table 4.3).

Among-Study Area Spatial Heterogeneity

Study area trends were variable: the Yukon Flats Central study area had the largest rate of decline for both the long-term and recent temporal records and the Yukon

Flats West study area had the only significant increasing trend for the recent temporal record. The among-study area spatial heterogeneity in recent annual trends was associated with a number of likely correlated variables. The five study areas with decreasing recent annual trends tended to have a smaller percentage of lakes with a fluvial surficial geology, a greater average distance of lakes to rivers and streams, a greater percentage of lakes with a coarse-grained sandy soil texture, and a smaller percentage of lakes with thermokarst features compared to the five study areas with negligible or increasing annual trends (Tables 4.7 & 4.8). Study areas with decreasing annual trends in lake area also tended to have a smaller mean lake size, a greater percentage of lakes in herbaceous wetlands, and a smaller percentage of lakes in woody wetlands (Tables 4.7 & 4.9). No relationships between annual trends and study area climatic characteristics were found (Table 4.10).

Within-Summer Trends in Lake Area

Magnitude and Direction

At the statewide scale, most lakes and most study areas had decreasing within-summer trends in lake area (Table 4.2, Fig. 4.11). The day-of-summer independent variable entered into nine of the ten study area regression models (Table 4.4). Of these nine, seven had significant decreasing within-summer trends and two had significant increasing within-summer trends for the recent temporal records (Table 4.4, Fig. 4.4b). The average rate of change across study areas was -0.16% per day-of-summer for both

the long-term and recent temporal records (Table 4.4). The average cumulative percent reduction in lake area during the summer across study areas was 13% for both the long-term and recent temporal records (Table 4.4).

Comparison of Long-term and Recent Within-Summer Trends

With the exception of Selawik, within-summer trends were not significantly different between the long-term and recent temporal records (Table 4.4, Fig. 4.4b). In Selawik, on- and off-transect within-summer trends were significantly different at the *same* temporal scale (i.e., since ~1985) (Table 4.5, Fig. 4.5b) suggesting that the on-transect lake population may not have been representative of the larger study area in terms of within-summer trends. Similar to Innoko, lakes on the transects were significantly larger than lakes off of the transects in Selawik (~ 2 times larger) (Table 4.6). However, seven of the remaining eight study areas that had representative on-transect lake populations in terms of within-summer trends (Table 4.5, Fig. 4.5b) also had significantly larger lakes on the transects (Table 4.6). Thus, in Selawik, lakes on the transect may not have been representative of lakes off of the transects for reasons besides differences in lake size.

Within-Study Area Spatial Heterogeneity

There was a large degree of among-lake heterogeneity in within-summer trends in all of the ten study areas (Table 4.2). Yukon Flats East was the most variable in

individual lake within-summer rates of change (standard deviation = 1.1) and Becharof was the least variable (standard deviation = 0.3) (Table 4.2). The distribution of all individual lake within-summer rates of change in the ten study areas as well as the distributions of individual lake within-summer rates of change in several study areas had skew values of less than -0.5 indicating substantially left-skewed distributions characterized by some lakes with very large within-summer decreases in area while the majority of data had more moderate rates of change (Table 4.2).

Coefficients of Variation: Temporal Variability in Lake Area

Within-Study Area Spatial Heterogeneity

Coefficients of variation for individual lakes ranged greatly and included a number of lakes that had very large changes in area between images (Figs. 4.11 & 4.12). Lakes with coefficients of variation greater than 0.21 (i.e., upper 25th percentile) were classified as fluctuating lakes. The percentage of fluctuating lakes was greatest in Innoko and Yukon Flats Central and was lowest in Togiak (Table 4.11).

Moran's I values were positive and statistically significant (alpha = 0.05) for all ten study areas indicating that fluctuating lakes tended to be spatially clustered (Table 4.11, Fig. 4.13). In general, the scale of maximum clustering of fluctuating lakes (Table 4.11, Fig. 4.13) tended to be greater than that observed for trend class values (Table 4.3, Fig. 4.8) suggesting that mechanisms underlying temporal variability in lake area may occur at broader scales than those underlying annual trends in lake area. Maximum

clustering occurred at scales of greater than 15 km in eight study areas (Table 4.11). In contrast, maximum clustering occurred at comparatively small scales of 4 km and 6 km in Yukon Flats West (Fig. 4.13c) and Innoko (Fig. 4.13h), respectively, suggesting finer scale underlying spatial processes for temporal variability in lake area in these study areas (Table 4.11).

Among-Study Area Spatial Heterogeneity

Togiak had the lowest mean coefficient of variation in lake area and Yukon Flats Central had the greatest (Table 4.11, Fig. 4.14). Our qualitative comparisons of study area mean coefficients of variation in lake area with study area characteristics highlighted potential relationships between high coefficients of variation and fluvial landscape characteristics. Specifically, the seven study areas with the greatest mean coefficients of variation (Fig. 4.14) had the largest percentages of lakes with fluvial surficial geology of the ten study areas (Table 4.7) and these seven were all located in the boreal ecoregion (Table 4.8) which largely overlaps the Yukon River Basin. We also found that the four study areas with the largest mean coefficients of variation in lake area (Fig. 4.14) had the largest percentages (i.e., 97-100%) of lakes in unstable permafrost types (i.e., discontinuous, sporadic, and isolated) (Table 4.7). In addition, study area mean coefficient of variation was inversely related to study area mean distance of lakes to major rivers (Fig. 4.15).

Discussion

This work is the first to account for inter-annual and intra-annual variability when estimating annual trends in lake area at both the study area and individual lake scales. Inter-annual variability was accounted for by including a sufficient number of images to use regression models to estimate linear trends while intra-annual variability was accounted for by including a day-of-summer term in regression models to reduce bias in annual trend estimates. Within-summer (May to September) trends in lake area were substantial in some study areas (Figs. 4.4b & 4.11) and, if not explicitly accounted for, could have been mistaken for annual trends.

Annual Trends in Lake Area

Magnitude and Direction

The presence of net declines in lake area statewide and for several study areas suggests that, at these scales, a dynamic equilibrium in lake area may not be present. The formation, growth, and fen-bog succession of thermokarst lakes via terrestrialization have been described as stages of a cyclical process involving alternating phases of permafrost degradation and regeneration as peat accumulates and insulates the ground surface (Drury 1956; Luken & Billings 1983; Zoltai 1993; Payette *et al.* 2004). If increasing, stable, and decreasing trends of individual lakes are different phases of a natural cyclical process, we would expect there to be a net balance in lake area change (i.e., negligible trend). However, our findings suggest that disequilibrium may be present statewide and for some

study areas. A warming climate may have accelerated terrestrialization while slowing or preventing the regeneration of permafrost required to complete the cycle (i.e., form new lakes), and tipped the balance toward a net loss in lake area and a net gain in terrestrial peatland or forested ecosystems.

Temporal Heterogeneity: Comparison of Long-term and Recent Annual Trends

The presence of significant long-term declines in lake area since ~1948 but non-significant recent trends in the Tetlin, Becharof, and Koyukuk study areas (Fig. 4.4a) may indicate a recent slowing of, or recovery from, long-term declining trends. One plausible explanation for a shift in rates of lake area change after ~1985 is the shift from a strong to a weak Aleutian Low after 1985 (Clegg & Hu 2010). Shifts in the intensity and position of the Aleutian Low have been associated with changes in lake area (Anderson *et al.* 2007; Clegg & Hu 2010). A weak westerly Aleutian Low corresponds to increased moisture delivery into interior Alaska, particularly during the winter, and has been correlated with increased winter precipitation in Bettles and increased lake water levels in the southern Brooks Range (Clegg & Hu 2010) and to increased snow accumulation in the Wrangell-St. Elias Range (Rupper *et al.* 2004). The Tetlin, Becharof, and Koyukuk study areas receive snowmelt runoff from and the Wrangell-St. Elias, the Aleutian, and the Brooks Ranges, respectively, and, thus, may have been particularly responsive to shifts in the Aleutian Low climate pattern.

Continued monitoring of lake area change in these study areas could clarify whether the direction and/or magnitude of lake area trends has shifted since ~1985 or whether these differences in rates may be due to the inability to detect a smaller rate of change with a shorter temporal record. If shifts in rates after ~1985 are present, paleoclimatic investigations may elucidate the potential involvement of multidecadal climate patterns.

Non-significant differences between long-term and recent annual trends in the Yukon Flats Central, Kanuti, and Selawik study areas (Table 4.4, Fig. 4.4a) suggest consistent rates of decline in these study areas. In the Togiak, Yukon Flats West, and Yukon Flats East study areas, long-terms trends were also not significantly different from recent trends (Table 4.4, Fig. 4.4a) but were also not significantly different from zero. Thus, these non-significant tests likely occurred because these study areas had the smallest number of lakes intersecting the transects of the ten study areas (< 35 lakes in each case) reducing the power of the tests.

Spatial Heterogeneity

Statewide Among-Study Area Spatial Heterogeneity

The majority of study area long-term annual trends were decreasing but recent study area trends were spatially heterogeneous (Fig. 4.4a), which was consistent with previous studies that identified heterogeneous regional lake area trends in Siberia (Smith *et al.* 2005) and in Alaska (Riordan *et al.* 2006). Five study areas had significant

decreasing recent trends in lake area and five study areas had negligible or increasing recent trends. Our first-order analysis of these ten study area trends with various spatial characteristics highlighted potential sources of statewide among-study area heterogeneity. The lack of an association with climatic gradients (Table 4.10) suggests that substrate, land cover or other finer-scale spatial processes may be the primary influence on among-study area heterogeneity in trends.

Our findings suggested that study areas with a predominantly non-fluvial surficial geology and coarser-grained sandy soils may be most susceptible to net decreasing annual trends in lake area (Table 4.7). This increased susceptibility may be either a direct result of these better drainage properties (Burn 2002) or may be due to correlated properties associated with different lake area change mechanisms. For example, in addition to their poor drainage properties, fine-grained soils also tend to have greater ice content and, thus, tend to be more susceptible to ground subsidence and the development of thermokarst features as permafrost thaws (Jorgenson & Osterkamp 2005), which have been associated with increasing or negligible changes in lake area (Roach *et al.* 2011). Consistent with this, study areas with increasing or negligible changes in lake area tended to have a greater percentage of lakes in zones with thermokarst features (Table 4.7) and a larger mean lake area compared to study areas with decreasing trends in lake area (Table 4.9). This larger mean lake area may be indicative of larger subsidence events during the formation of thermokarst lakes. A smaller degree of subsidence in smaller, shallower lakes in study areas with decreasing trends may provide propitious conditions for

terrestrialization and fen/bog peatland development (Payette *et al.* 2004; Roach *et al.* 2011). The predominance of herbaceous wetlands in study areas with decreasing trends (Table 4.7) may also reflect enhanced susceptibility to terrestrialization.

Regional Among-Study Area Spatial Heterogeneity

While our results highlight some potential sources of statewide among-study area heterogeneity, it may also be informative to consider heterogeneity within regions that encompass multiple study areas. For example, within the Yukon Flats, recent study area annual trends ranged from significantly increasing in the West, to significantly decreasing in the Central study area, to insignificant changes in the East. Of the three study areas, the West region is unique in that it is located north of the Yukon River, has predominantly silty poorly drained soils, continuous permafrost with a higher ice content, and more thermokarst features compared to the other two Yukon Flats study areas (Table 4.7), which may all contribute to increasing lake area. In contrast, the Central study area has predominantly sandy, and more easily drained, soils of Eolian origin (Table 4.7).

There were also differences in recent study area annual trends between Togiak and Becharof which are both located in a maritime Bering taiga ecoregion (Table 4.8). Specifically, Becharof had negligible recent annual trends while Togiak had significant decreasing annual trends in average lake area (Table 4.4, Fig. 4.4a). Of the characteristics we considered, the main difference between these two study areas was their dominant soil types and surficial geology. Becharof has rocky soils characterized

by moraine and glacial drifts while Togiak has predominantly old marine and alluvial sandy soils (Table 4.7). However, the effect of these different geologies on rates of lake area change is unclear.

Within-Study Area Spatial Heterogeneity

The presence of non-random heterogeneity in the magnitude and direction of individual lake annual trends (Table 4.2, Figs. 4.8) suggests a relationship between trends and concomitant spatial heterogeneity in lake and/or landscape characteristics. Characteristics that may be correlated with spatial heterogeneity in individual lake annual trends include permafrost stability and/or ice content which effect soil water holding capacity and the degree of ground subsidence when permafrost thaws (Jorgenson & Osterkamp 2005), soil type, grain, and origin which can effect soil drainage properties (Burn 2002), the direction of sub-surface hydraulic gradients which can become important once a permafrost aquiclude thaws leading to either sub-permafrost groundwater recharge (Kane & Slaughter 1973) or drainage (Yoshikawa & Hinzman 2003) of lakes, the presence of surface connections to nearby streams and rivers which can periodically recharge lakes, and lake bathymetry which may be associated with relative susceptibility to evaporation, talik formation, and terrestrialization (Roach *et al.* 2011). Lake bathymetry has been identified as an important factor in among-lake heterogeneity in trends with shallow lakes susceptible to terrestrialization and

comparatively deeper lakes susceptible to thermokarst and increasing or negligible changes in lake area (Roach *et al.* 2011).

Future field-based studies should be conducted to test and verify whether the potential sources of among-study area heterogeneity identified here using coarse-scale maps (i.e., surficial geology/ soil type) also apply to among lake heterogeneity in trends within study areas. For example, soil type and texture may be correlated with lake bathymetry and may vary at a similar scale as among-lake heterogeneity in trends (Table 4.3) or relative lake bathymetry may be a source of among-lake heterogeneity within a single soil type/texture. A better understanding of the spatial processes underlying among-study area and among-lake heterogeneity in trends will improve spatial and temporal projections of future change and will enable the identification of lakes and refuges that may be most susceptible to change.

Within-Summer Trends in Lake Area

Significant net declines in lake area during the summer months in seven study areas (Fig. 4.4b) highlights the importance of spring recharge events or the length of the growing season as controls on lake water levels in these areas. In contrast, there may be different controls on seasonal variability in Yukon Flats West and Becharof that had increasing trends in lake area during the summer months. For example, the presence of poorly drained silty soils and predominantly continuous permafrost in Yukon Flats West (Table 4.7) may cause lakes to retain more water from large rain storms that typically

occur late in the summer in interior Alaska. In Becharof, within-summer increasing trends in lake area may have been due to late season precipitation and snow melt from higher elevations that may further compounding increases in lake area that typically occur following spring snowmelt in early June (Susan Savage, Becharof National Wildlife Refuge, pers. comm.).

Temporal Variability in Lake Area

Lakes with large fluctuations in area (Fig. 4.12) both within- and among-years are highly dynamic habitats that may support unique assemblages of invertebrate, fish, and waterfowl species (Kratz *et al.* 1997). The seven study areas with the largest mean coefficients of variation in lake area were located in the Yukon River Basin of the boreal forest ecoregion (Table 4.8) and were associated with a number of fluvial landscape characteristics (Table 4.7; Fig. 4.15) while the three study areas with the lowest mean coefficients of variation were located outside of the Yukon River Basin. The spatial distribution of fluctuating lakes also appears to follow major river drainages in several study areas (Fig. 4.13). This suggests that lake area fluctuations may be predominantly fed by surface or subsurface flow connected to the groundwater table and nearby river networks. Study areas with large mean coefficients of variations also tended to have patchy and more unstable permafrost (Fig. 4.14, Table 4.7) which may further promote groundwater interactions (Kane & Slaughter 1973; Yoshikawa & Hinzman 2003). In contrast, non-fluctuating lakes may be predominantly fed by precipitation.

Groundwater fed lakes tend to have greater concentrations of silica and cations such as calcium and magnesium (Kratz *et al.* 1997) which can affect the types of species present in aquatic systems. For example, snails and crayfish are limited by calcium (Capelli & Magnuson 1983) and a high silica concentration can lead to more prominent sponge spicules, thus making them more desirable prey species (Frost 1991). Groundwater fed lakes also tend to have greater fish species richness compared to precipitation fed lakes (Kratz *et al.* 1997). Groundwater fed and precipitation fed lakes may also respond differently to drought conditions (Kratz *et al.* 1997). Drought conditions have been associated with a decrease in ion concentrations in groundwater-fed lakes due to reduced runoff and cation inputs and increased ion concentrations in precipitation-fed lakes due to the evapoconcentration of ions (Webster *et al.* 1996; Kratz *et al.* 1997).

Priorities for Future Research

The long-term net declines in average lake area identified in seven study areas and the recent net declines identified in five study areas may have substantial implications for wildlife habitats and for the global carbon balance. Drying of northern peatlands has been associated with a net decrease in radiative forcing due to decreased methane emissions which offset increased carbon dioxide emissions from the same drying peatlands (Laine *et al.* 1996). In contrast, terrestrialization (i.e., expanding floating mat vegetation into open water) has been identified as a mechanism for

decreasing lake area in the Alaskan boreal forest (Roach *et al.* 2011), which may lead to peatland development and have the opposite effect on methane and carbon dioxide emissions (i.e., increase and decrease, respectively). Terrestrialization may also provide negative feedbacks to climate warming by increasing albedo as open water becomes covered by floating mat vegetation. Future research could clarify the effects of net declines in lake area on carbon balance by identifying the mechanisms involved (e.g., terrestrialization vs. drainage or evaporation) and estimating their net effect on radiative forcing including both gas emissions and albedo responses.

Future work should also focus on identifying the relative habitat qualities of increasing, decreasing, and stable lakes for invertebrate, avian, mammal, and fish species. This information may clarify the ability of the fine-scale (3-22 km) heterogeneity in trends to provide broad-scale system resiliency. For example, clusters of stable or increasing lakes may provide suitable habitat alternatives for species displaced from nearby clusters of shallow, shrinking lakes. The suitability of these alternative habitats will depend on the similarity of stable and increasing lake characteristics (e.g., water chemistry, invertebrates) to shallow, shrinking lake characteristics.

Acknowledgements

We thank Steve Ewest, Matthew Balasz, and Garrett Altmann for help with image processing, Eric J. Taylor for administrative and funding support, and Jennifer Harden and Jeremy Jones for constructive reviews which substantially improved this manuscript.

Funding was also provided by USGS, FWS, and a UAF Graduate School Thesis Completion Fellowship. Any use of trade names is for descriptive purposes only and does not imply endorsement by the U.S. Government.

References

Anderson LA, Abbott MB, Finney BP, Burns SJ (2007) Late Holocene moisture balance variability in the southwest Yukon Territory, Canada. *Quaternary Science Reviews*, **26**, 130-141.

Anderson L, Guldager N, Finney BP (2010) Wetlands of the Yukon Flats Alaska: influence of hydrogeographic setting on climate sensitivity and sediment records of past climate-induced hydrologic change. *Proceedings of the 40th International Arctic Workshop*, March 10-12, Winter Park, CO.

Barber VA, Juday GP, Finney BP (2000) Reduced growth of Alaskan white spruce in the twentieth century from temperature-induced drought stress. *Nature*, **405**, 668-673.

Brabets TP, Walvoord MA (2009) Trends in streamflow in the Yukon River Basin from 1944 to 2005 and the influence of the Pacific Decadal Oscillation. *Journal of Hydrology*, **371**, 108-119.

Burn CR (2002) Tundra lakes and permafrost, Richards Island, western Arctic coast, Canada. *Canadian Journal of Earth Sciences*, **39**, 1281-1298.

Capelli GM, Magnuson JJ (1983) Morphoedaphic and biogeographic analysis of crayfish distribution in northern Wisconsin. *Journal of Crustacean Biology*, **3**, 548-564.

Chander G, Markham BL, Helder, DL (2009) Summary of current radiometric calibration coefficients for Landsat MSS, TM, ETM+, and EO-1 ALI sensors. *Remote Sensing of Environment*, **113**, 893–903.

Clegg BF, Hu FS (2010) An oxygen-isotope record of Holocene climate change in the south-central Brooks Range, Alaska. *Quaternary Science Reviews*, **29**, 928-939.

Corcoran RM, Lovvorn JR, & Heglund PJ (2009). Long-term change in limnology and invertebrates in Alaskan boreal wetlands. *Hydrobiologia*, **620**, 77-89.

Drury WH (1956) *Bog Flats and Physiographic Processes in the Upper Kuskokwim River Region, Alaska* eds (Rollins RC, Foster RC), pp 130, The Gray Herbarium of Harvard University, Cambridge.

Flanders WD, DerSimonian R, Freedman DS (1992) Interpretation of linear regression models that include transformations or interaction terms. *Annals of Epidemiology*, **2**, 735-744.

Frazier PS, Page KJ (2000) Water body detection and delineation with Landsat TM data. *Photogrammetric Engineering & Remote Sensing*, **66**, 1461-1467.

Frost TM (1991) Porifera. In: *Ecology and Classification of North American Freshwater Invertebrates* eds (Thorp JH, Covich AP), pp. 95-124, Academic Press, New York.

Helsel DR (2005) More than obvious: better methods for interpreting nondetect data. *Environmental Science & Technology*, **39**, 419A-423A.

Hodges JI, King JG, Conant B, Hanson HA (1996) Aerial surveys of waterbirds in Alaska 1957-94: population trends and observer variability. National Biological Service Information and Technology Report 4. 24 pp.

Johnston R, Barson M (1993) Remote sensing of Australian wetlands: An evaluation of Landsat TM data for inventory and classification. *Australian Journal for Marine and Freshwater Research*, **44**, 235-252.

Jorgenson MT, Racine CH, Walter JC, Osterkamp TE (2001) Permafrost degradation and ecological changes associated with a warming climate in central Alaska. *Climate Change*, **48**, 551-579.

Jorgenson MT, Osterkamp TE (2005) Response of boreal ecosystems to varying modes of permafrost degradation. *Canadian Journal of Forest Research*, **35**, 2100-2111.

Jorgenson MT, Yoshikawa K, Kanveskiy M, Shur YL, Romanovsky V, Marchenko S, Grosse G, Brown J, Jones B (2008) Permafrost characteristics of Alaska. In: *Proceedings of the Ninth International Conference on Permafrost*, 29 June – 3 July 2008, Fairbanks, Alaska eds (Kane DL, Hinkel KM), pp. 121-122, Institute of Northern Engineering, University of Alaska Fairbanks.

Kane DL, Slaughter CW (1973) Recharge of a central Alaska lake by subpermafrost groundwater. In: *Permafrost. Proceedings of the 2nd International Conference, Yakutsk* eds (Pewe TL, MacKay JR), pp 458-462, North American Contribution, National Academy of Sciences, Washington, DC.

Karlstrom TNV (1964) *Surficial geology of Alaska*. U.S. Geological Survey, Miscellaneous Geologic Investigations Map I-357, 1:1,584,000 scale.

Klein E, Berg EE, Dial R (2005) Wetland drying and succession across the Kenai Peninsula Lowlands, south-central Alaska. *Canadian Journal of Forest Research*, **35**, 1931-1941.

Kratz TK, Webster KE, Bowser CJ, Magnusen JJ, Benson BJ (1997) The influence of landscape position on lakes in northern Wisconsin. *Freshwater Biology*, **37**, 209-217.

Labrecque S, Lacelle D, Duguay CR, Lauriol B, Hawkings J (2009). Contemporary (1951–2001) evolution of lakes in the Old Crow Basin, northern Yukon, Canada: Remote sensing, numerical modeling, and stable isotope analysis. *Arctic*, **62**, 226-238.

Laine J, Silvola J, Tolonen K, *et al.* (1996) Effect of water-level drawdown on global climatic warming: Northern peatlands. *Ambio*, **25**, 179-184.

Luken JO, Billings WD (1983) Changes in bryophyte production associated with a thermokarst erosion cycle in a subarctic bog. *Lindbergia*, **9**, 163-168.

Luo W (2002) Hypsometric analysis of Margaritifer Sinus and origin of valley networks. *Journal of Geophysical Research*, **107**, doi:10.1029/2001JE001500.

MacDonald LA, Turner KW, Balasubramaniam AM, Wolfe BB, Hall RI, Sweetman JN (2011) Tracking hydrological responses of a thermokarst lake in the Old Crow Flats (Yukon Territory, Canada) to recent climate variability using aerial photographs and paleolimnological methods. *Hydrological Processes*, doi: 10.1002/hyp.8116.

Nowacki GJ, Spencer P, Fleming M, Brock T, Jorgenson T (2001) *Unified Ecoregions of Alaska*, U.S. Geological Survey, Open-File Report 02-297.

Oechel WC, Vourlitis GL, Hastings SJ, Zulueta RC, Hinzman L, Kane D (2000) Acclimation of ecosystem CO_2 exchange in the Alaskan Arctic in response to decadal climate warming. *Nature*, **406**, 978-981.

Osterkamp TE, Romanovsky VE (1999) Evidence for warming and thawing of discontinuous permafrost in Alaska. *Permafrost and Periglacial Processes*, **10**, 17-37.

Payette S, Delwaide A, Caccianiga M, Beauchemin M (2004) Accelerated thawing of subarctic peatland permafrost over the last 50 years. *Geophysical Research Letters*, **31**, L18208.

Pike RJ, Wilson SE (1971) Elevation–relief ratio, hypsometric integral, and geomorphic area–altitude analysis. *Geological Society of America Bulletin*, 8, 1079–84.

Riordan B, Verbyla D, McGuire AD (2006) Shrinking ponds in subarctic Alaska based on 1950-2002 remotely sensed images. *Journal of Geophysical Research*, **111**, G04002.

Roach J, Griffith B, Verbyla D, Jones J (2011) Mechanisms influencing changes in lake area in the Alaskan boreal forest. *Global Change Biology*, **17**, 2567-2583.

Rupper S, Steig E, Roe G (2004) The relationship between snow accumulation at Mt. Logan, Yukon, Canada, and climate variability in the North Pacific. *Journal of Climate*, **17**, 4724-4739.

Smith LC, Sheng Y, MacDonald GM, Hinzman LD (2005) Disappearing arctic lakes. *Science*, **308**, 1429.

Smol JP, Douglas MS (2007) Crossing the final ecological threshold in high arctic ponds. *Proceedings of the National Academy of Sciences*, **104**, 12395-12397.

Walter KM, Zimov SA, Chanton JP, Verbyla D, Chapin III FS (2006) Methane bubbling from Siberian thaw lakes as a positive feedback to climate warming. *Nature*, **443**, 71-75.

Webster KE, Kratz TK, Bowser CJ, Magnusen JJ, Rose WJ (1996) The influence of landscape position on lake chemical responses to drought in northern Wisconsin. *Limnology and Oceanography*, **41**, 977-984.

Yoshikawa K, Hinzman LD (2003) Shrinking thermokarst ponds and groundwater dynamics in discontinuous permafrost near Council, Alaska. *Permafrost and Periglacial Processes*, **14**, 151-160.

Zoltai SC (1993) Cyclic development of permafrost in the peatlands of Northwestern Alberta, Canada. *Arctic and Alpine Research*, **25**, 240-246.

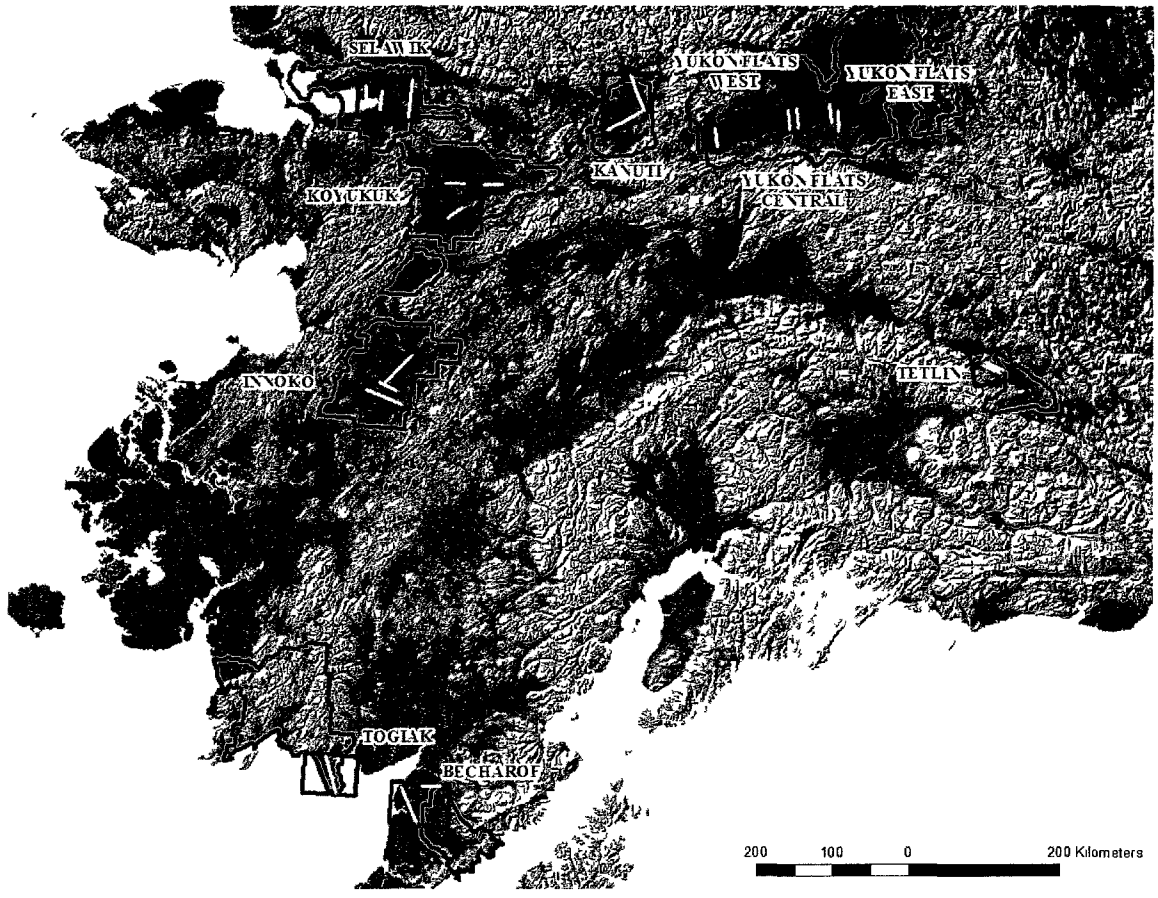

Figure 4.1 Map showing boundaries of ten study areas located in eight Alaskan National Wildlife Refuges. Study area boundaries are shown in red and refuge boundaries are shown in black. National Wildlife Refuges were Tetlin, Yukon Flats, Kanuti, Selawik, Koyukuk, Innoko, Togiak, and Becharof where temporal trends in lake area were estimated. White lines indicate the locations of the North American Waterfowl Breeding Pair Survey (BPS) transects used in this study. Aerial photography was used to extend the temporal records of lakes intersecting these waterfowl survey transects to as early as 1948.

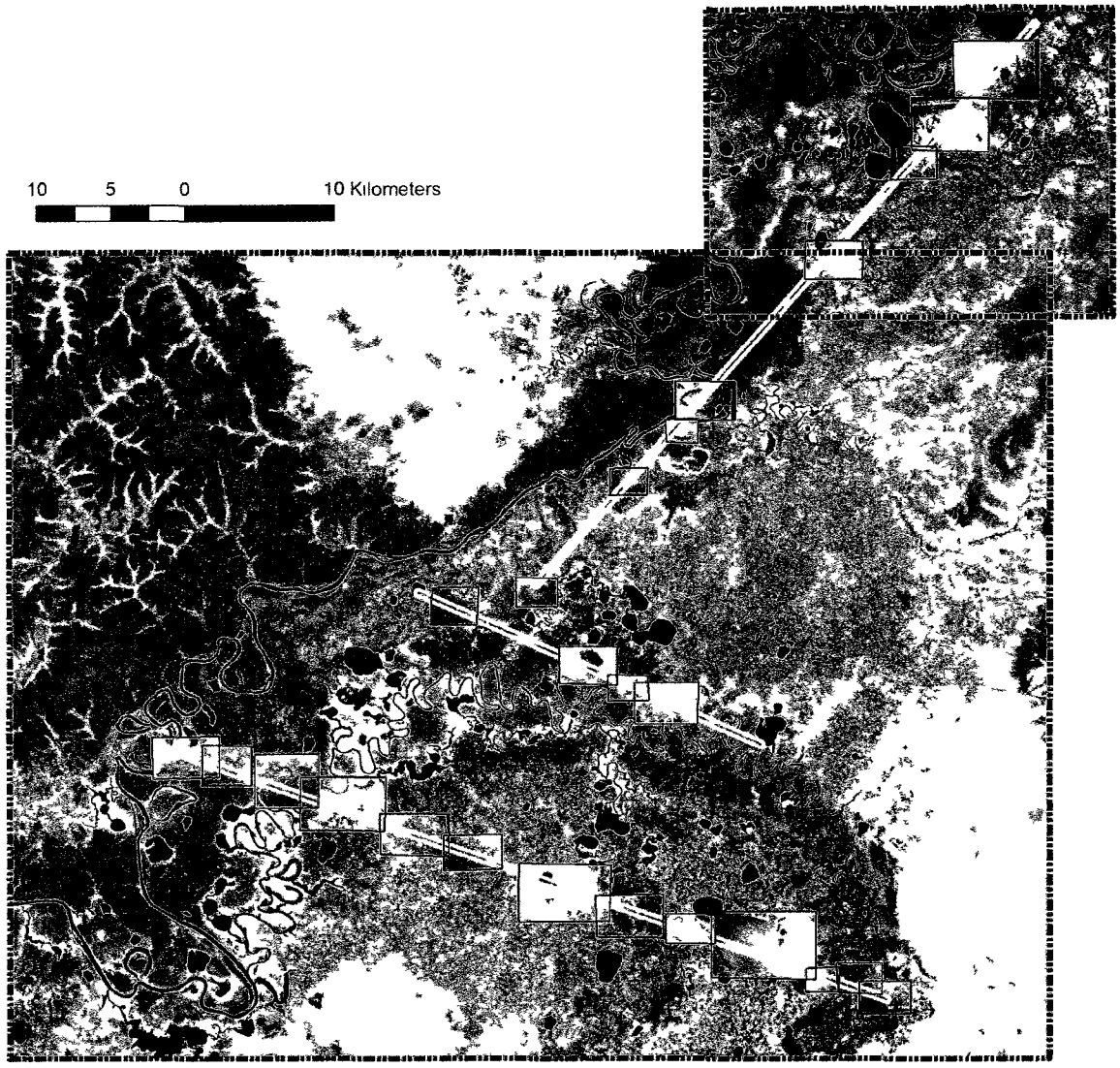

Figure 4.2 Clipped black and white aerial photographs from 1953 and Landsat extents from 2008 and 2009 used in the Innoko study area time series. Aerial photos were clipped (outlined in black) so that they encompassed all lakes that intersected a 200 m buffer on either side of the North American Waterfowl Breeding Pair Survey (BPS) transects shown in white Aerial photos were only processed for portions of transects that had intersecting lakes Two clipped Landsat extents (broken line) were used to encompass the five transects in the Innoko study area and a complete series of six Landsat images was obtained for each extent yielding two complete series of Landsat images for the Innoko study area Lakes that overlapped both extents were assigned to only one extent for analysis

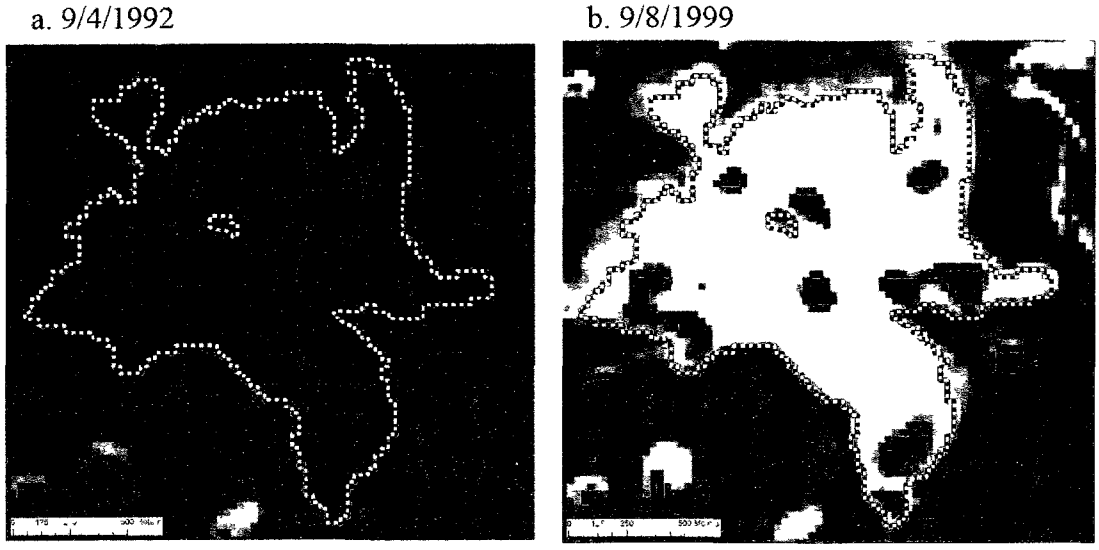

Figure 4.3 Example of the definition of a lake sample unit for a lake in the Yukon Flats Central study area. This lake consisted of multiple polygons and a single polygon during different time periods. The lake sample unit was the combined maximum extent of the lake throughout the time series (black and white dotted line)

Figure 4.4 Year (a) and day-of-summer (b) slopes from repeated measures regression models for ten study areas representing geometric percent change in average lake area (m^2) per year and per day of the summer, respectively. Slopes are presented separately for long-term and recent (i.e., since ~1985) temporal trends. Natural log-transformed lake area (m^2) was the dependent variable. All models included year as an independent variable and inclusion of the day-of-summer variable was assessed using backwards model selection with p-value to remove of 0.05. The Innoko study area was the only study area that did not have a day-of-summer term enter into its regression model. Year and day-of-summer variables were coded as years or days since the earliest year or day of image acquisition for each time series and then divided by 100. To obtain separate equations for long-term and recent (i.e., since ~1985) trends, we pooled variances from on- and off-transect lake populations by including an indicator variable for lakes on- or off-transects (i.e., long-term vs. recent temporal trends) along with all interactions between the transect variable and the main effects that entered into each model (i.e., year and day-of-summer). Regression slopes were compared between long-term and recent temporal records for each study area to identify whether long-term rates of change increased and decreased since ~1985.

a.

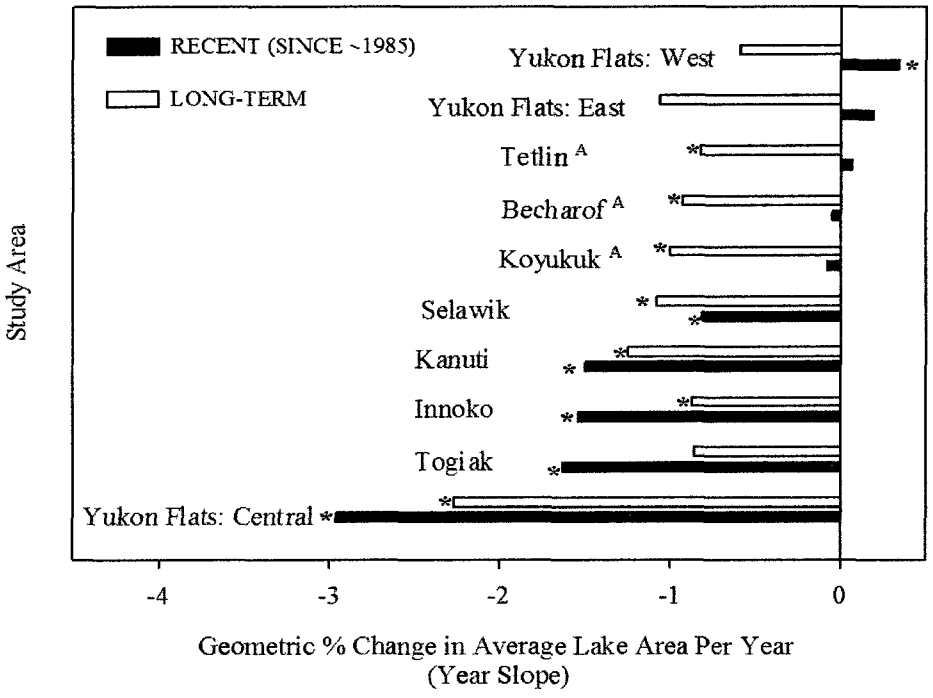

b.

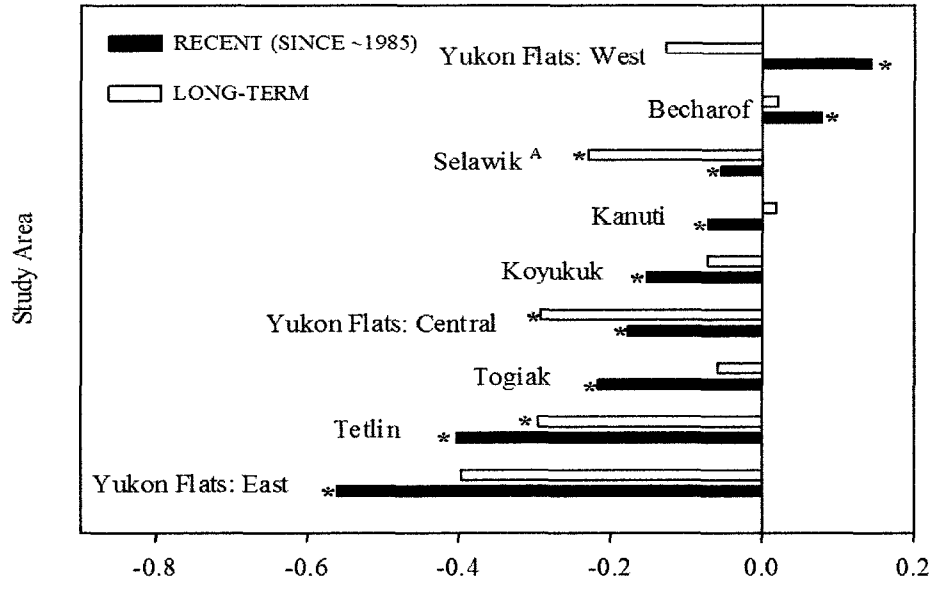

*significantly different from zero at alpha = 0.05
A recent and long-term trends significantly different at alpha = 0 05

Figure 4.5 Year (a) and day-of-summer (b) slopes from repeated measures regression models on the same temporal scale (i.e., since ~1985) for ten study areas representing geometric percent change in average lake area (m^2) per year and per day of the summer, respectively. Slopes are presented separately for on- and off-transect recent (i.e., since ~1985) temporal trends. Natural log-transformed lake area (m^2) was the dependent variable. All models included year as an independent variable and inclusion of the day-of-summer variable was assessed using backwards model selection with a p-value to remove of 0.05. The Innoko study area was the only study area that did not have a day-of-summer term enter into its regression model. Year and day-of-summer variables were coded as years or days since the earliest year or day of image acquisition for each time series and then divided by 100. To obtain separate equations for on- and off- transect trends, we pooled variances from on- and off-transect lake populations by including an indicator variable for lakes on- or off- transects along with all interactions between the transect variable and the main effects that entered into each model (i.e., year and day-of-summer). Regression slopes were compared between on- and off-transect lake populations on the same temporal scale for each study area to identify if the trends of the smaller on-transect lake population were representative of the trends of the larger off-transect lake population.

a.

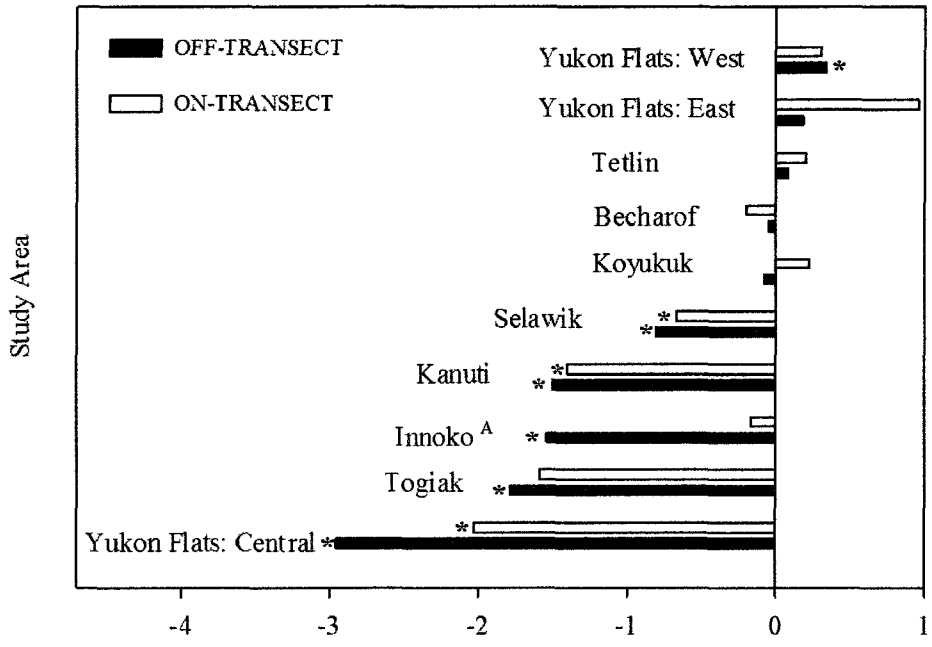

b.

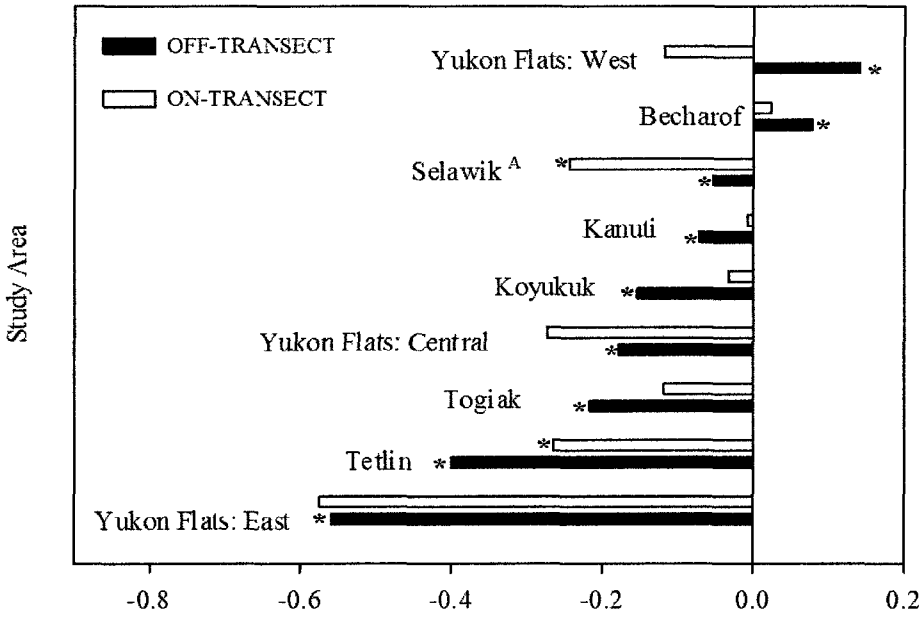

*significantly different from zero at alpha = 0.05
A on- and off-transect trends significantly different at alpha = 0.05

a 6/15/1986

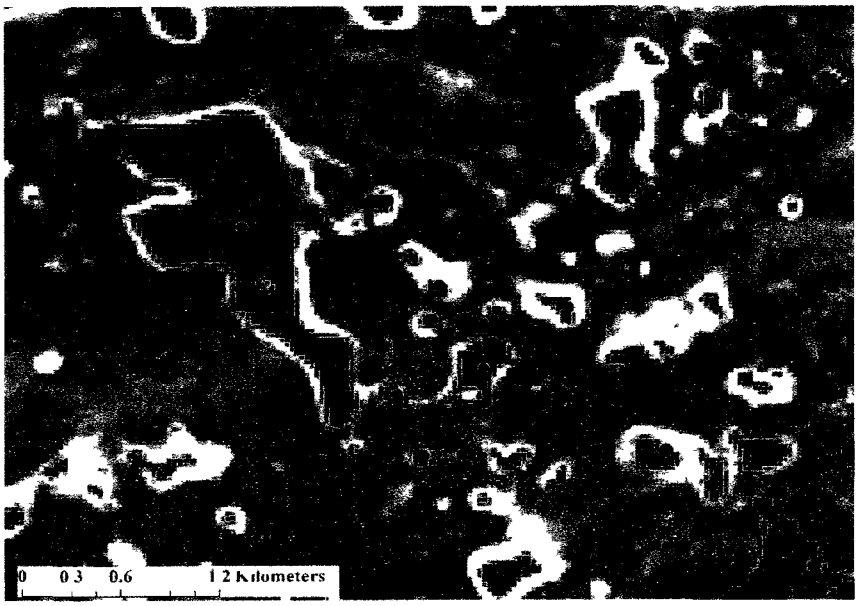

b. 8/30/2008

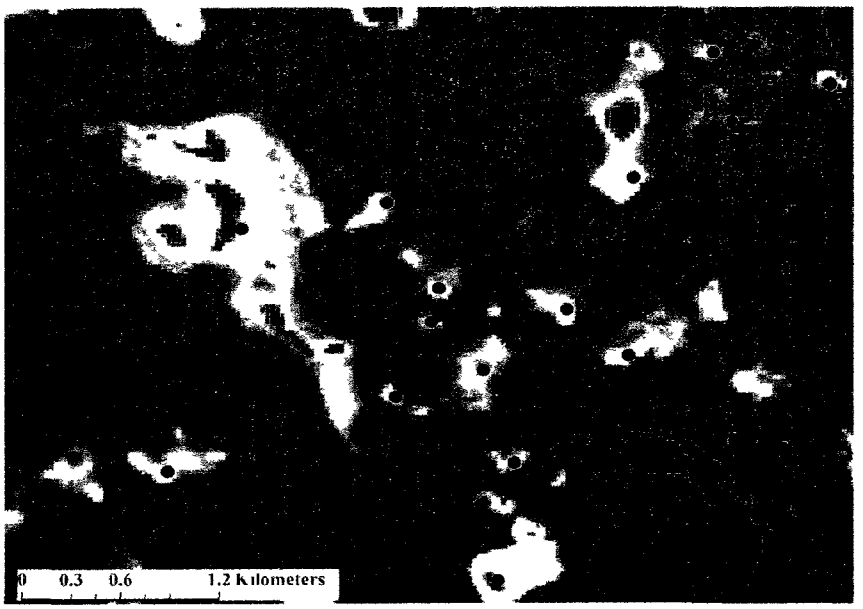

Figure 4.6 Time series of images from 1986 and 2008 demonstrating heterogeneity in the direction of individual lake annual trends in the Yukon Flats Central study area. Lakes marked with a red dot had decreasing trends and lakes marked with blue dots had increasing trends in area.

Figure 4.7 Frequency histograms of individual lake annual rates of change (i.e., year slopes) for lakes with long-term and recent temporal records for ten study areas (a-j). Dotted and solid lines connect the p-values from tests that the year slopes were different from zero for lakes with long-term and recent temporal records, respectively. P-values were only plotted for lakes that had the same number of images in their time series for simplicity.

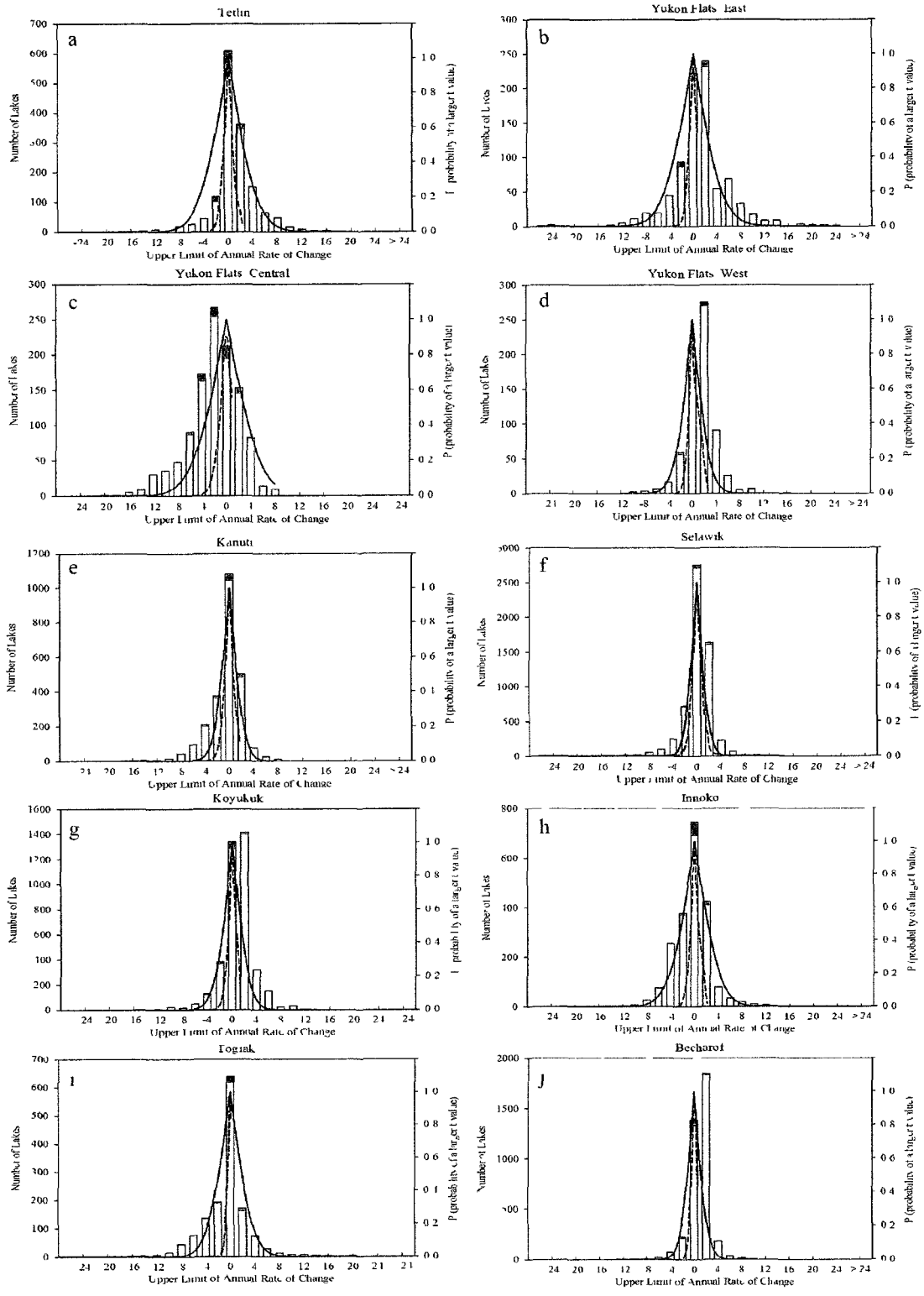
Tetlin
a
Yukon Flats East
b
Yukon Flats Central
c
Yukon Flats West
d
Kanuti
e
Selawik
f
Koyukuk
g
Innoko
h
Togiak
i
Becharof
j
Number of Lakes
P (probability of a larger t value)
Upper Limit of Annual Rate of Change
Recent Temporal Records
Long-term Temporal Records
Significance of Recent Annual Rates of Change
Significance of Long-term Annual Rates of Change

Figure 4.8 Maps showing the spatial distribution of lake trend classes in ten study areas (a-j). Ordinary kriging was used to provide a visual representation of the spatial distribution and degree of clustering of individual lake annual trend classes (i.e., large decrease, small decrease, negligible, small increase, and large increase). Trend classes were defined based on the combined distribution of individual lake annual rates of change (i.e., year slopes) from all ten study areas and were assigned values one through five starting with the large decrease class and ending with the large increase trend class. Ordinary kriging was applied to these trend class values. White lines are North American Waterfowl Breeding Pair Survey (BPS) transects.

a. Tetlin

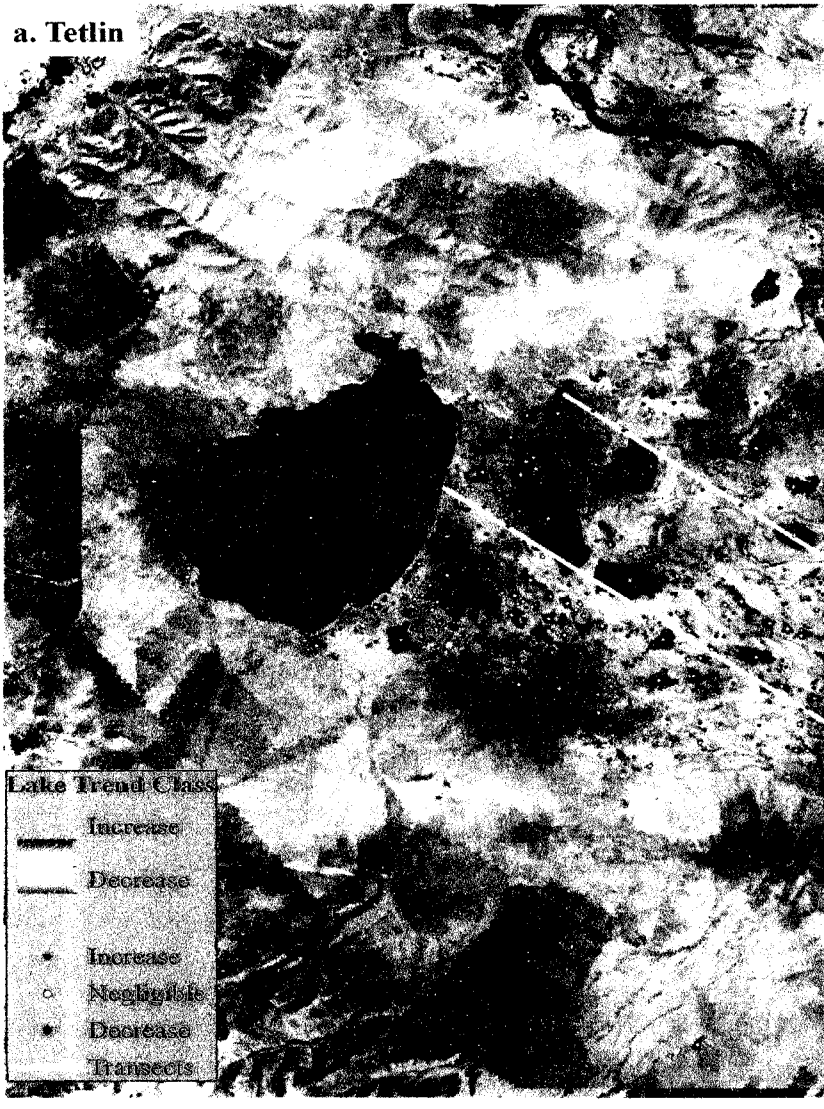
Lake Trend Class
Increase
Decrease
Increase
Negligible
Decrease
Transects

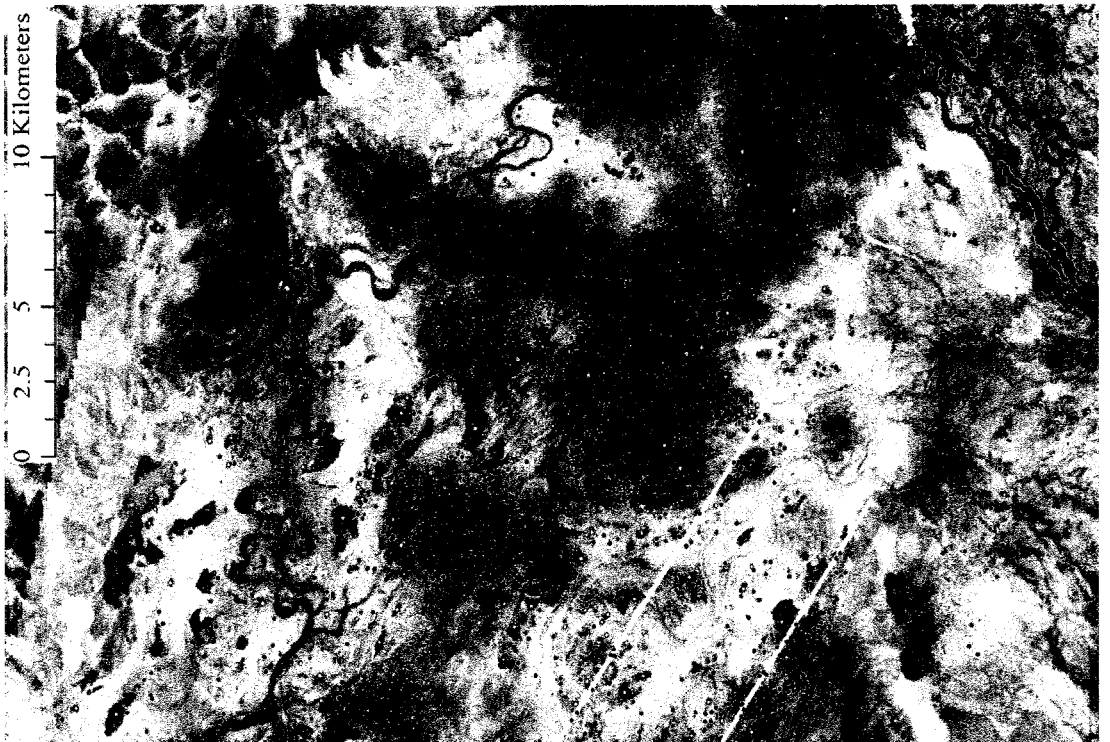
0
2.5
5
10 Kilometers

Figure 4.8 (Continued) Maps showing the spatial distribution of lake trend classes in ten study areas (a-j).

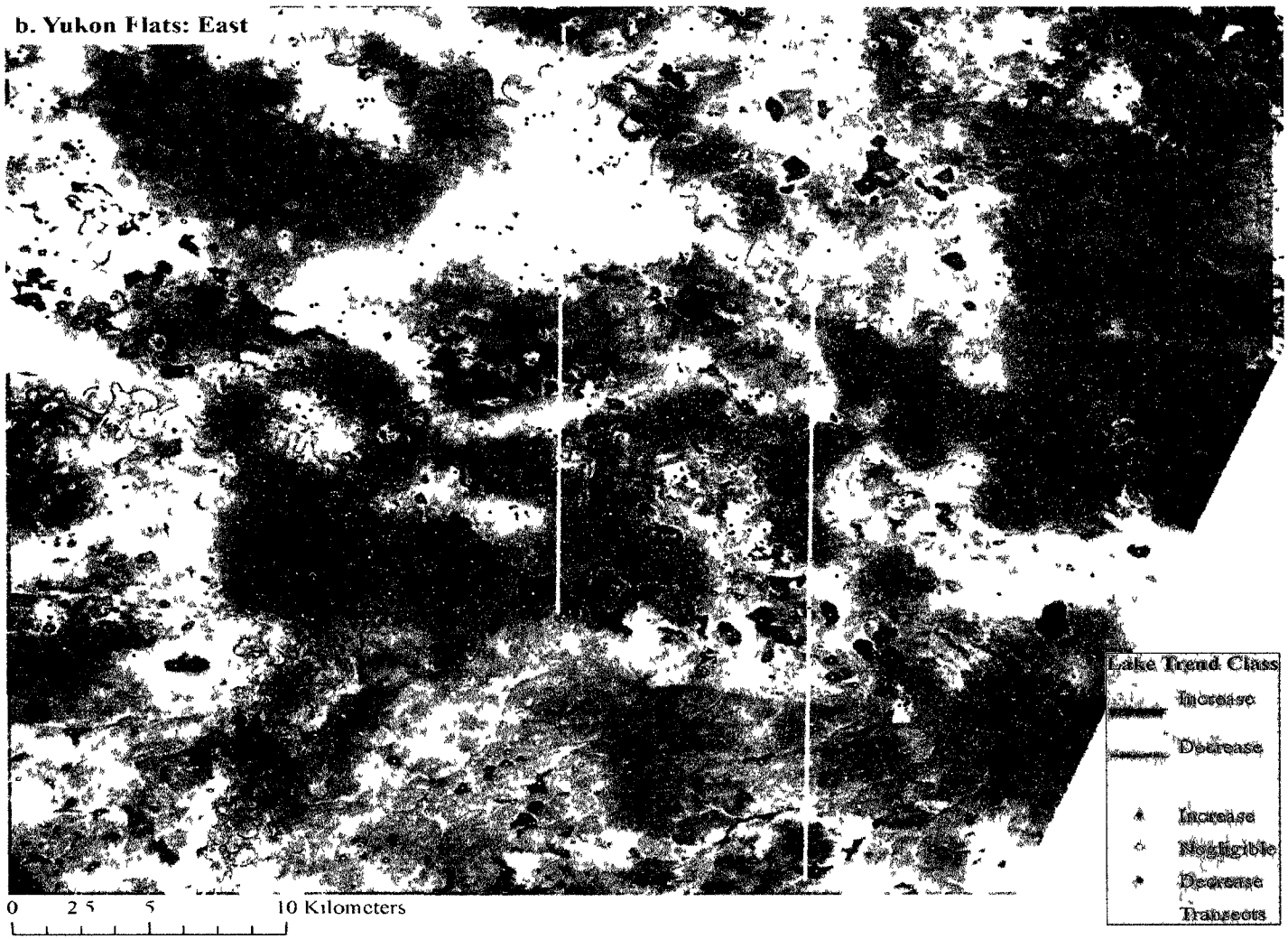

Figure 4.8 (Continued) Maps showing the spatial distribution of lake trend classes in ten study areas (a-j).

c. Yukon Flats: Central

Figure 4.8 (Continued) Maps showing the spatial distribution of lake trend classes in ten study areas (a-j).

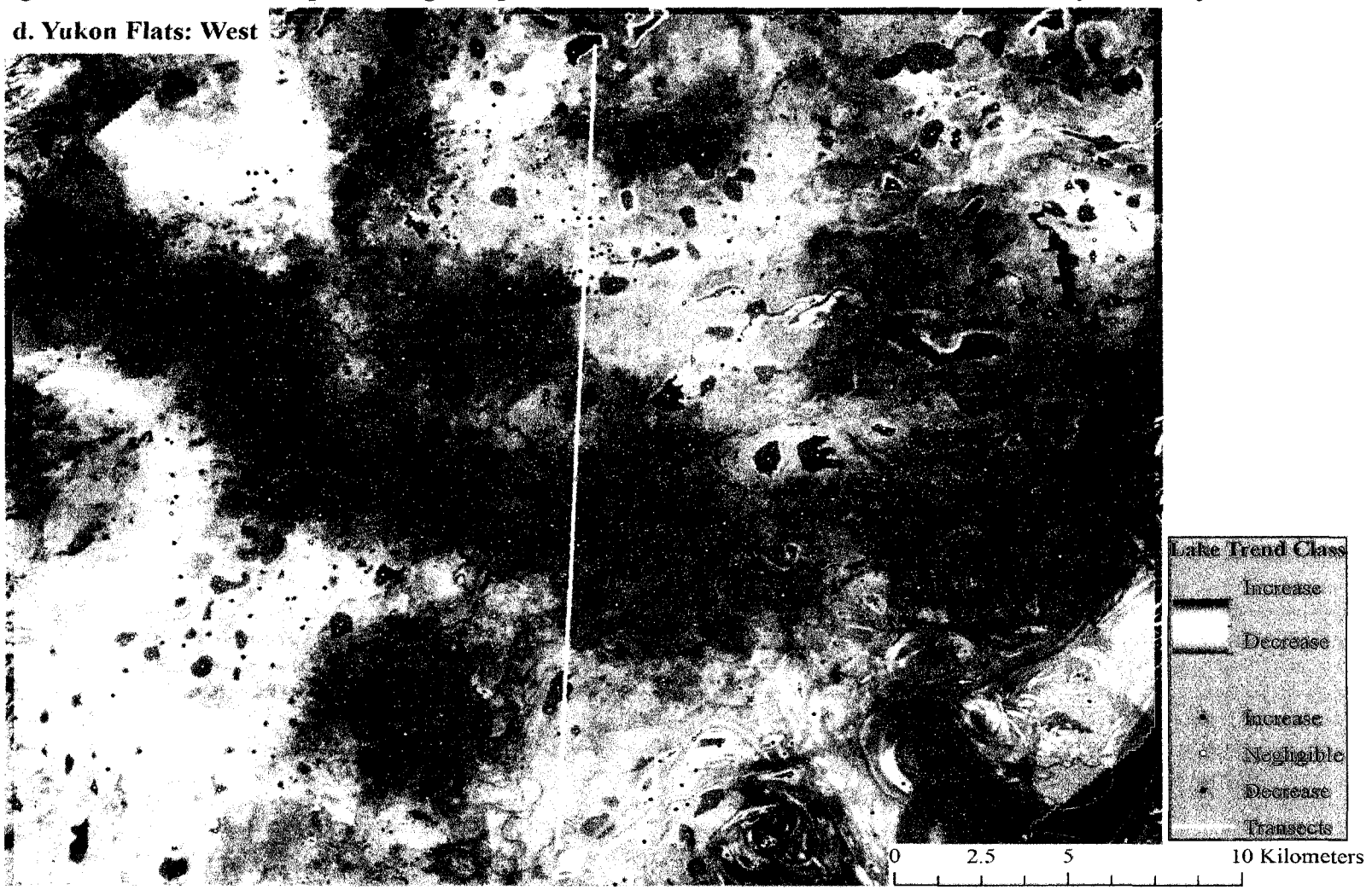

Figure 4.8 (Continued) Maps showing the spatial distribution of lake trend classes in ten study areas (a-j).

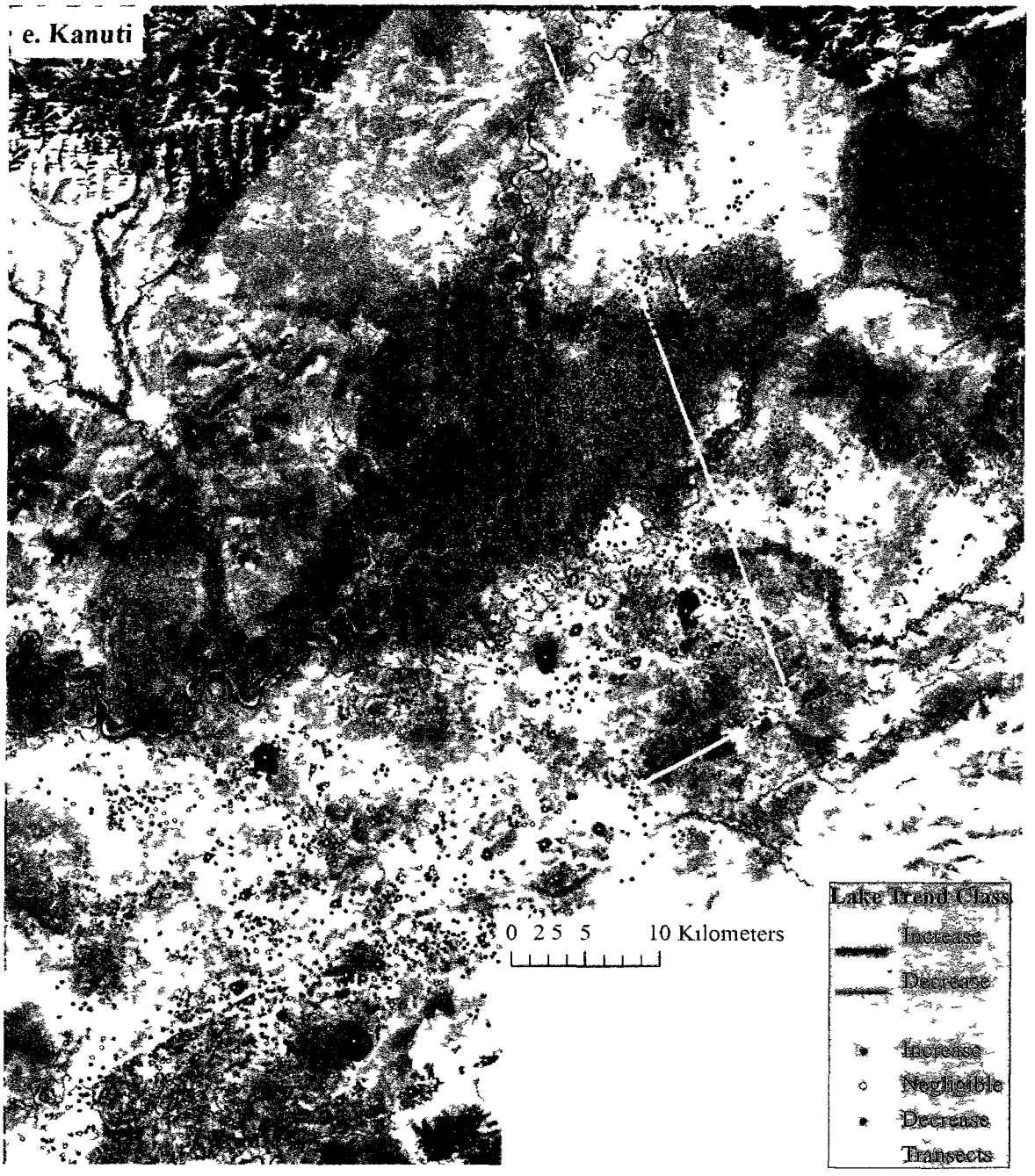

Figure 4.8 (Continued) Maps showing the spatial distribution of lake trend classes in ten study areas (a-j).

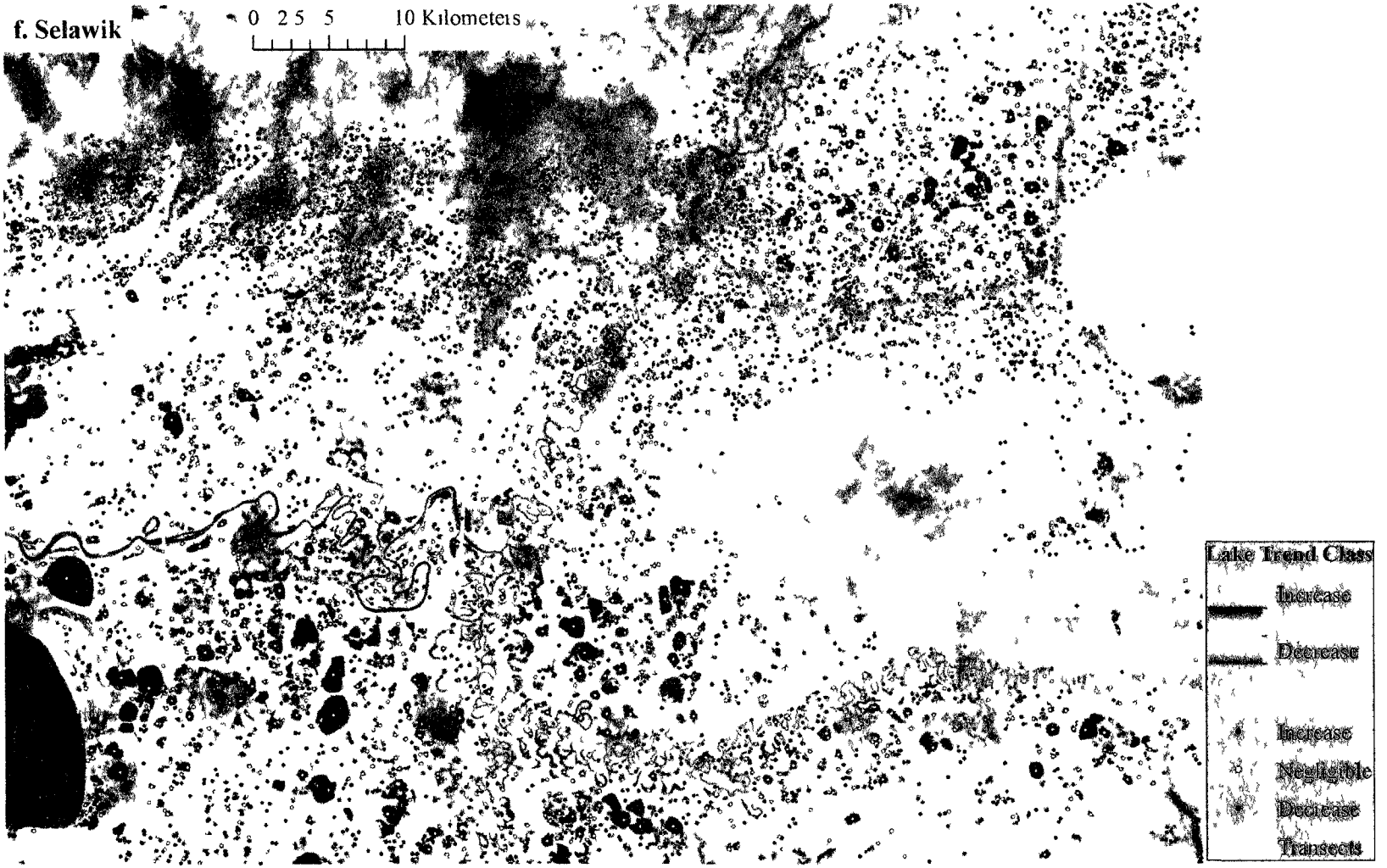

Figure 4.8 (Continued) Maps showing the spatial distribution of lake trend classes in ten study areas (a-j).

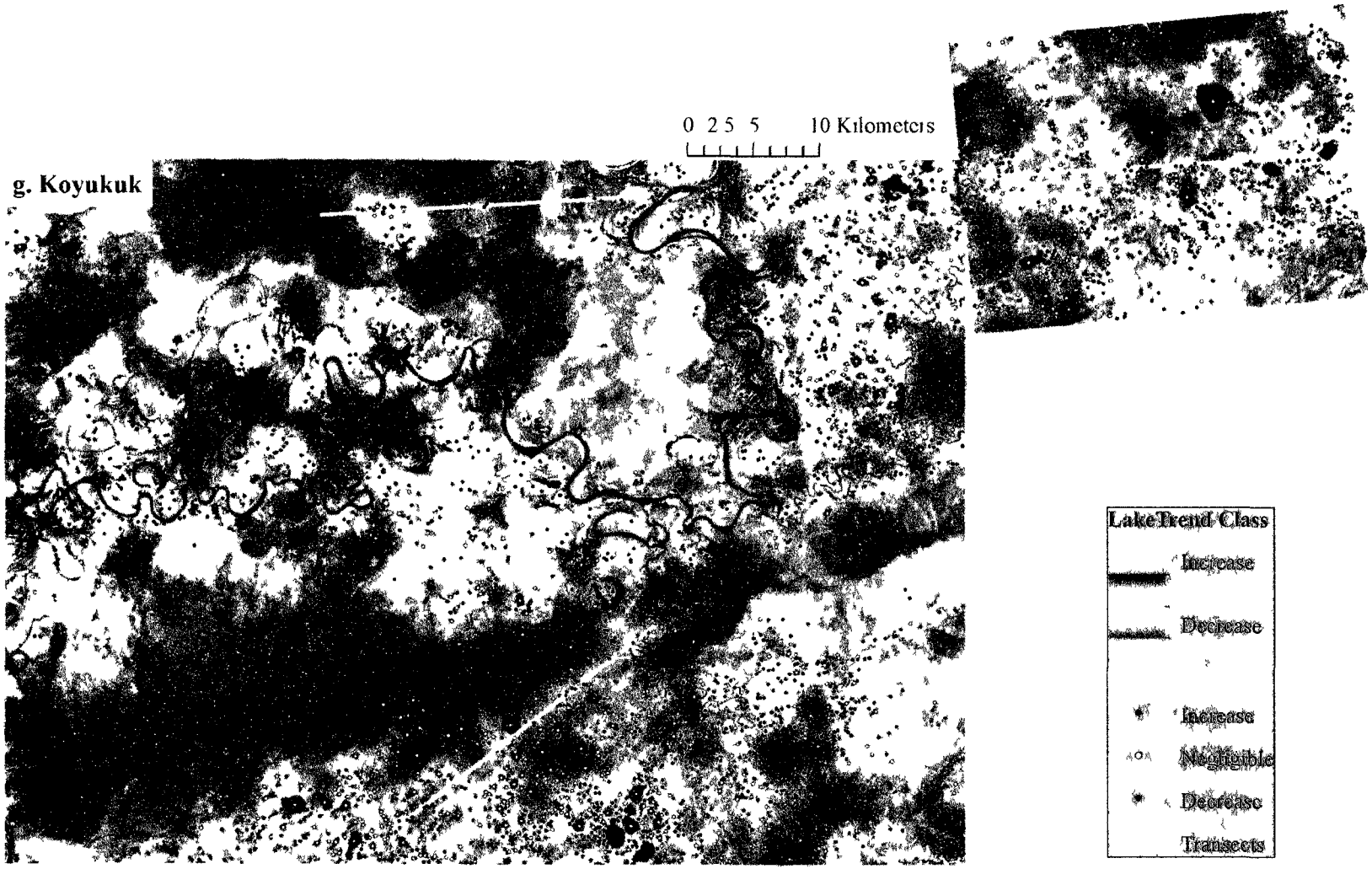

Figure 4.8 (Continued) Maps showing the spatial distribution of lake trend classes in ten study areas (a-j).

h. Innoko

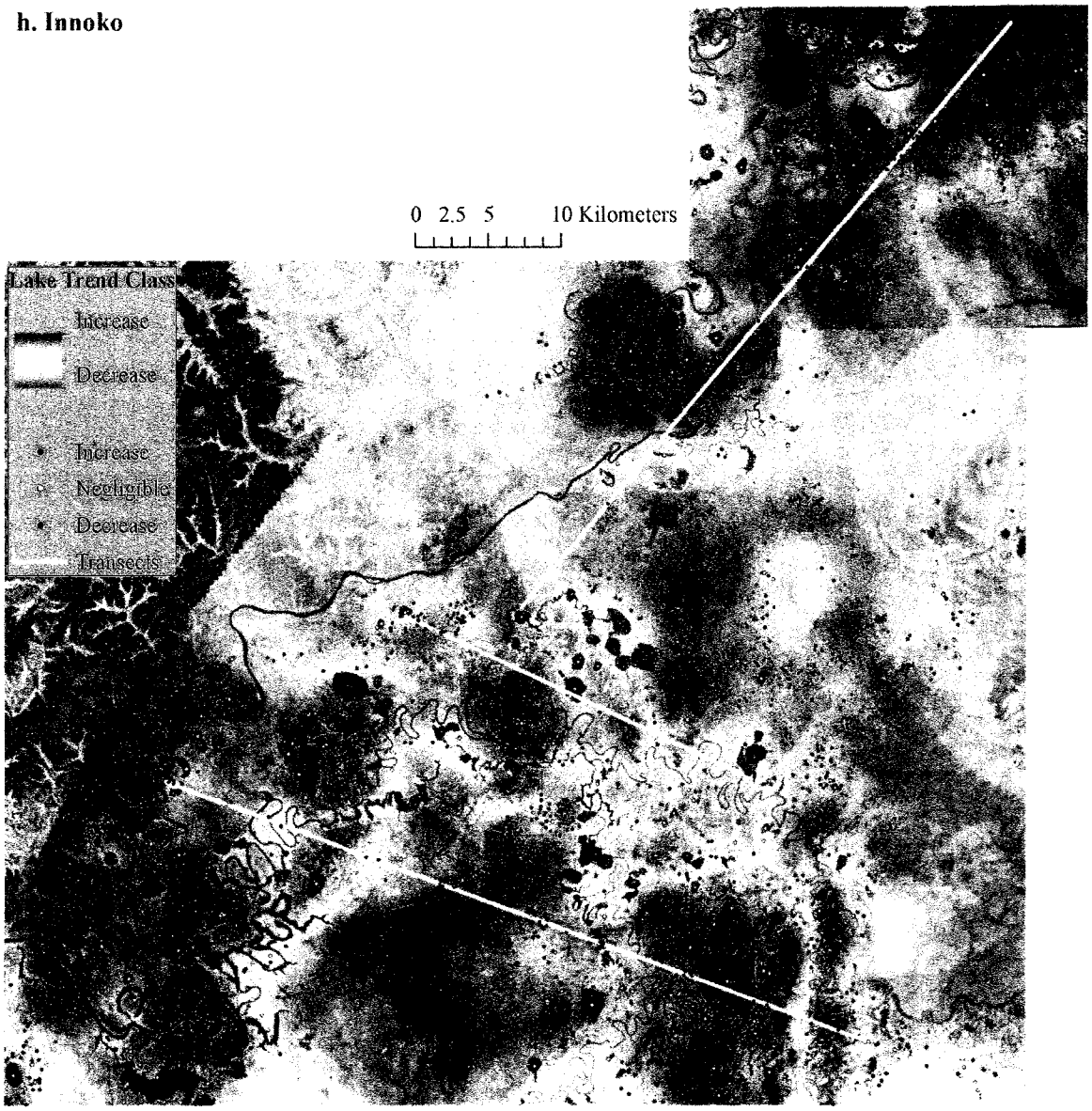

Figure 4.8 (Continued) Maps showing the spatial distribution of lake trend classes in ten study areas (a-j).

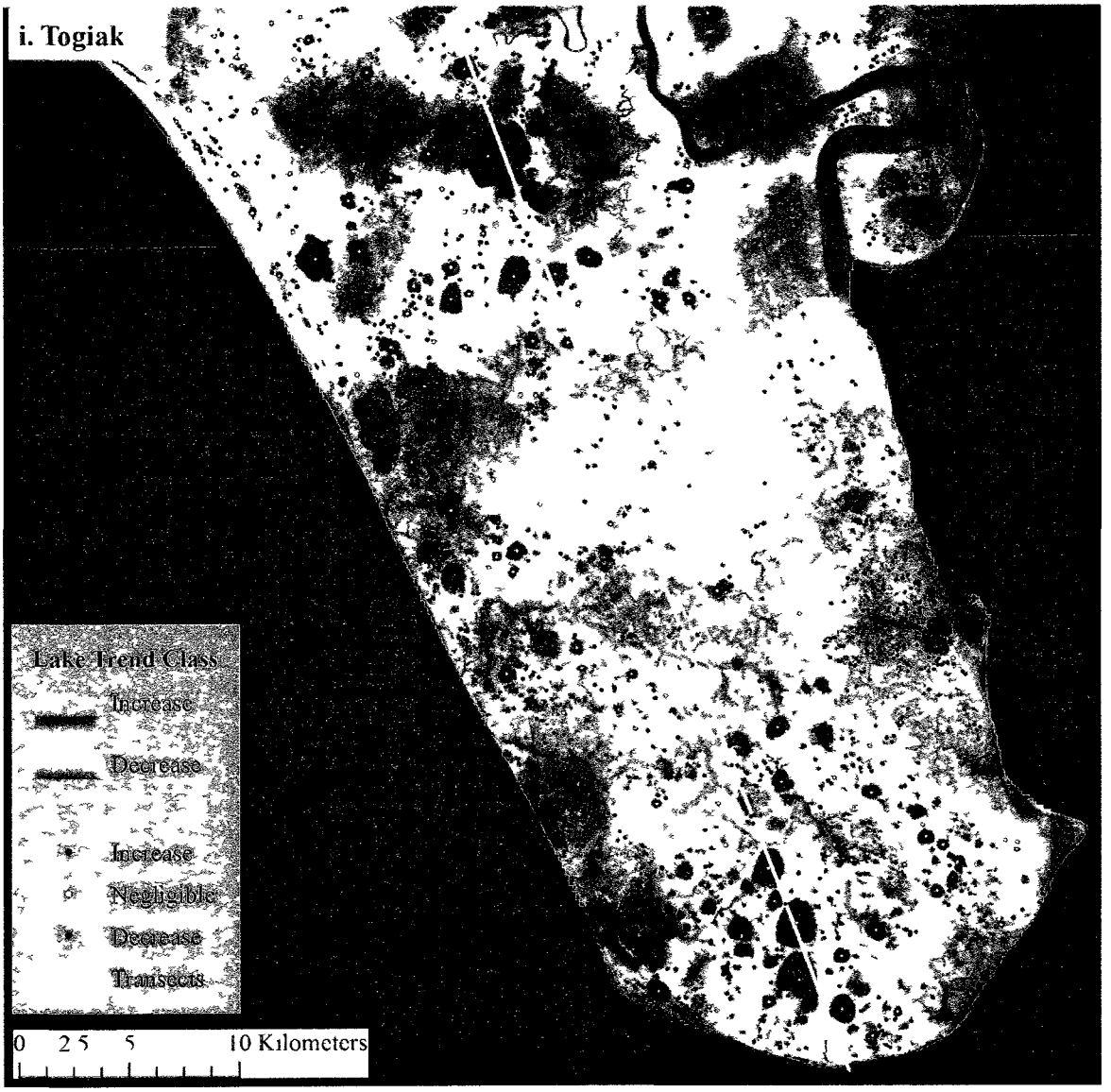

Figure 4.8 (Continued) Maps showing the spatial distribution of lake trend classes in ten study areas (a-j).

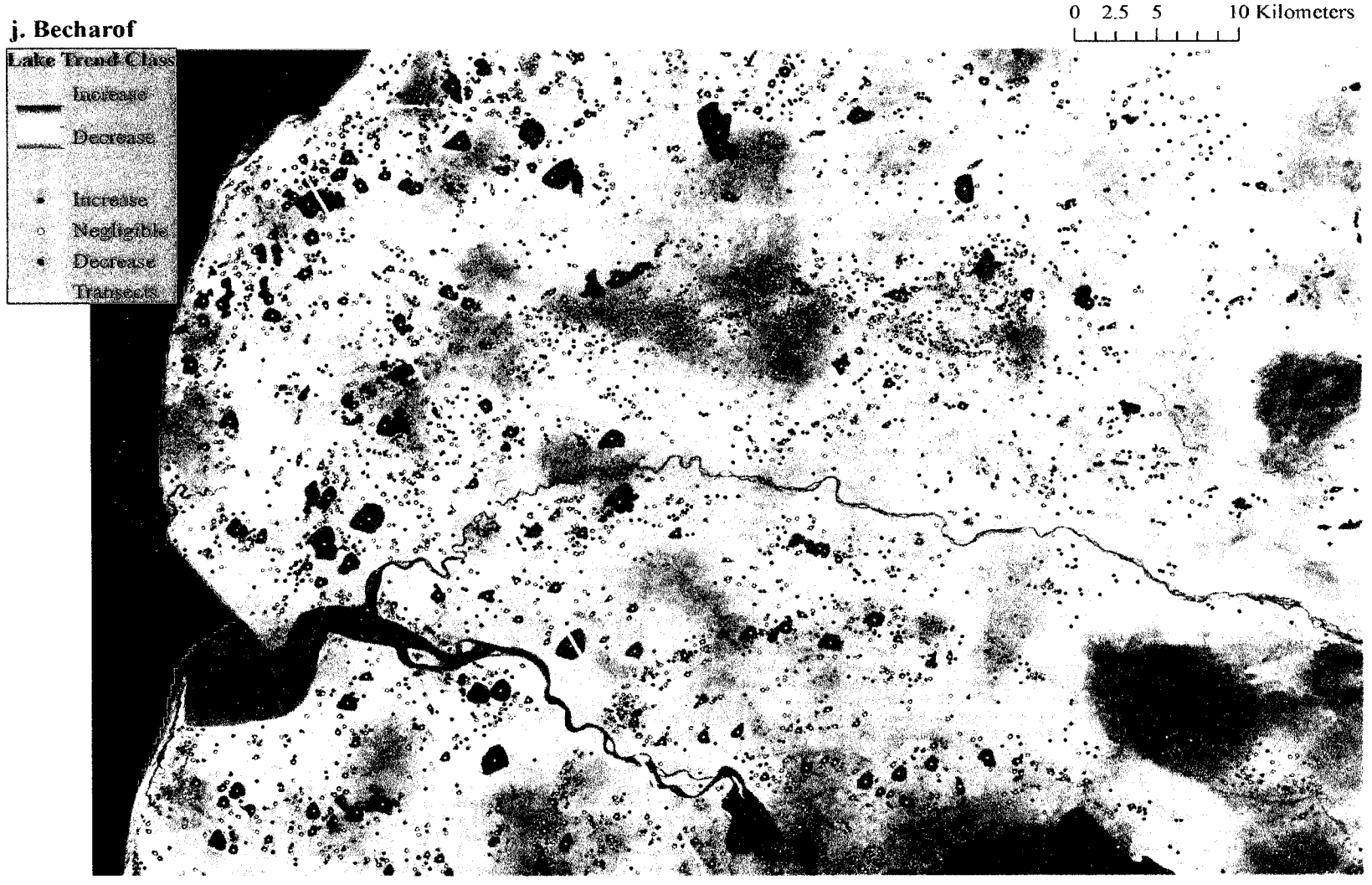

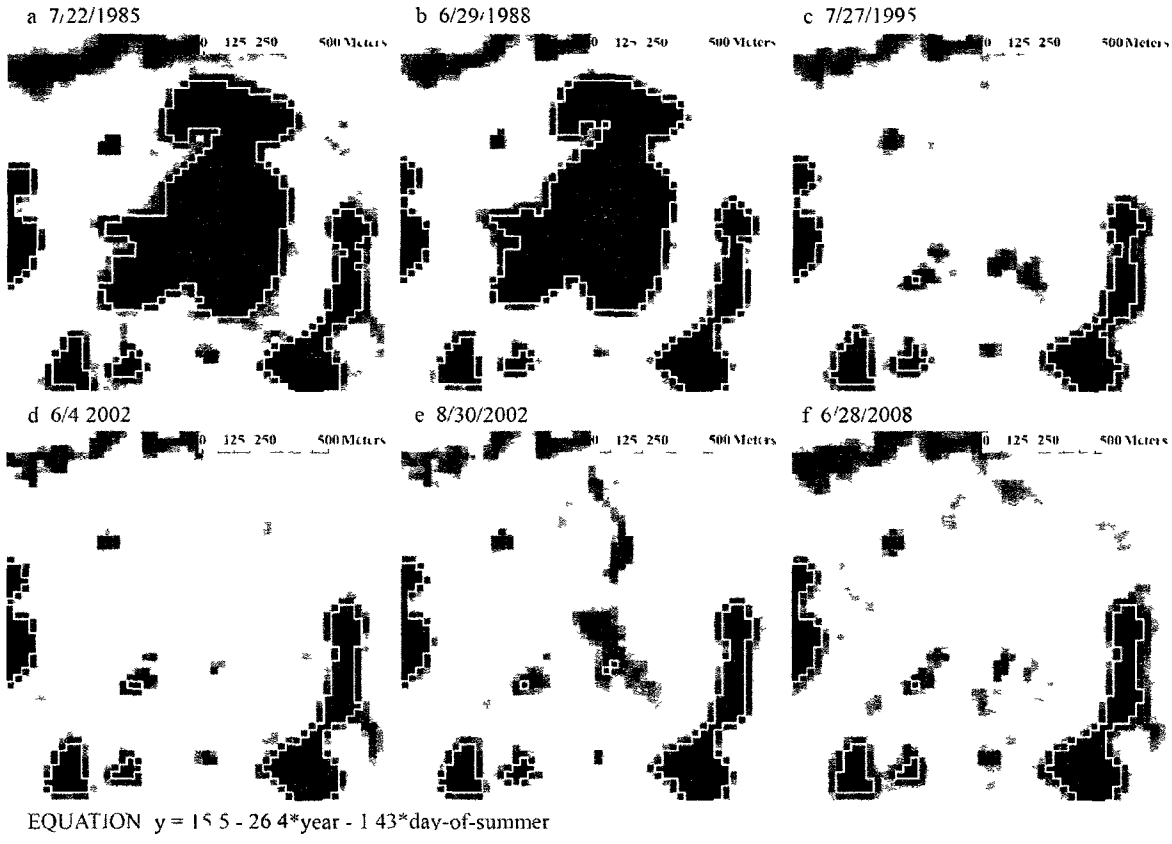

Figure 4.9 Time series of images showing a lake in the Selawik study area with a significant decreasing trend. Individual lake equation was obtained from the Selawik pooled variance regression model in which natural log-transformed lake area (m^2) was the dependent variable and year and day-of-summer were the independent variables. Year and day-of-summer variables were coded as years or days since the earliest year or day of image acquisition for each time series and then divided by 100. Variances for all lakes in the Selawik study area were pooled into a single regression model by including indicator variables for each lake and all interactions between the indicator variables and the main effects (i.e., year and day-of-summer).

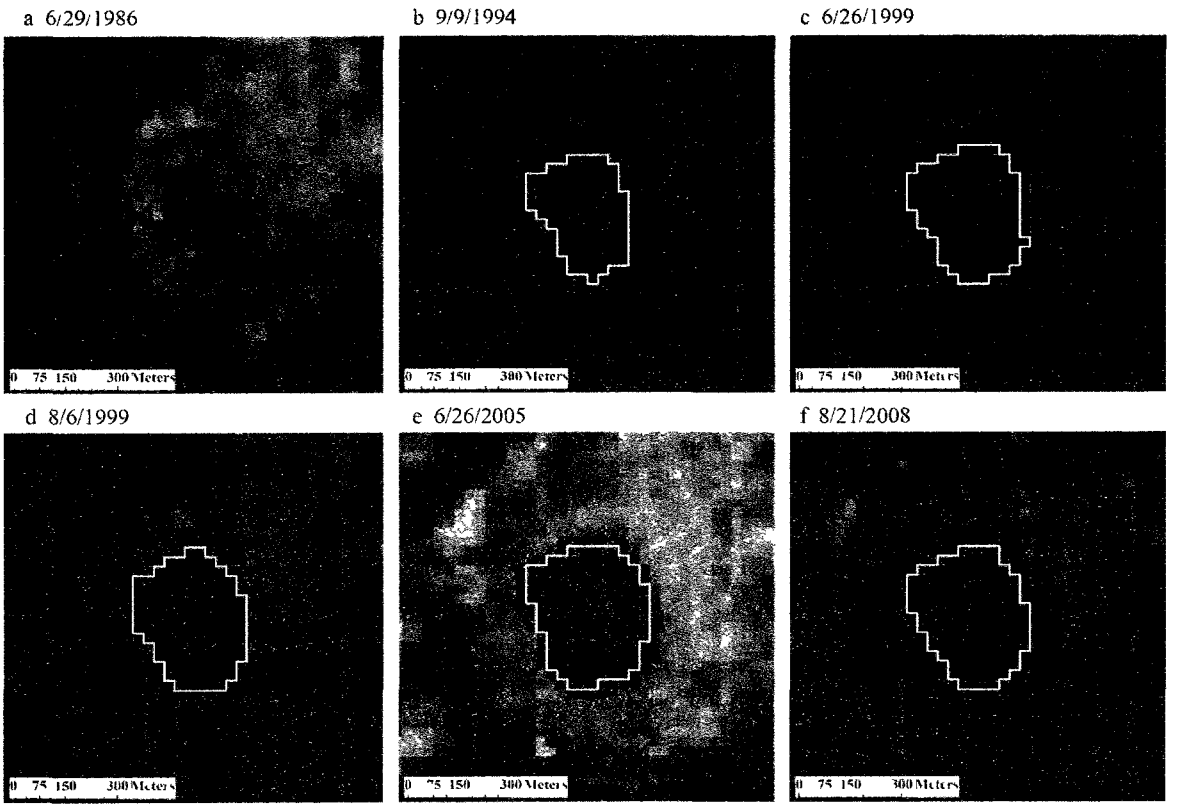

Figure 4.10 Time series of images showing a lake in the Yukon Flats West study area with a significant increasing trend. Individual lake equation was obtained from the Yukon Flats West pooled variance regression model in which natural log-transformed lake area (m^2) was the dependent variable and year and day-of-summer were the independent variables. Year and day-of-summer variables were coded as years or days since the earliest year or day of image acquisition for each time series and then divided by 100. Variances for all lakes in the Yukon Flats West study area were pooled into a single regression model by including indicator variables for each lake and all interactions between the indicator variables and the main effects (i.e., year and day-of-summer).

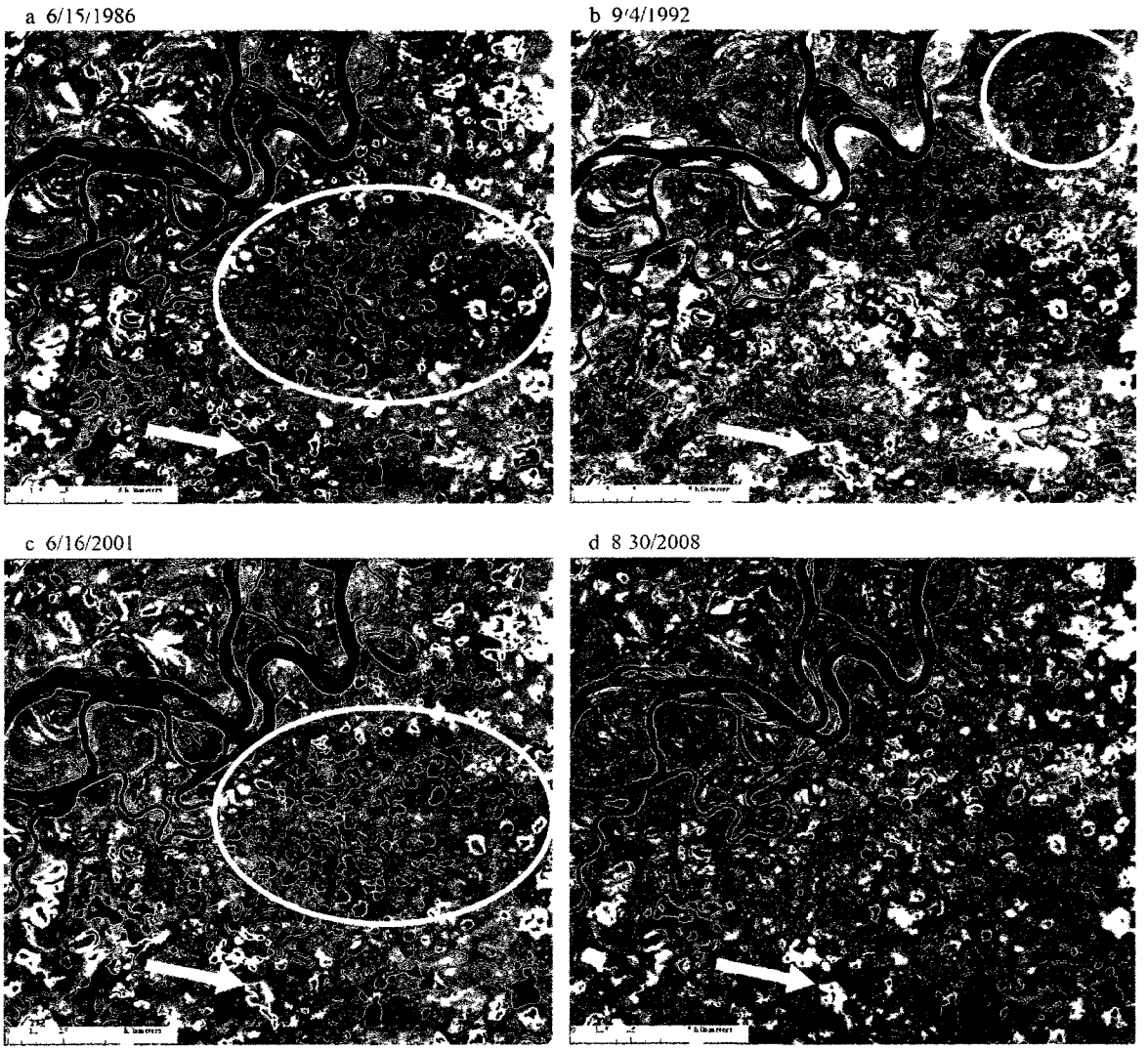

Figure 4.11 Time series of images demonstrating examples of intra-annual and inter-annual variability and annual trends in lake area in the Yukon Flats Central study area. White circles in (a) and (c) show examples of intra-annual variability in lake area with markedly larger lake areas in mid-June. The white circle in (b) shows examples of inter-annual variability in lake area. These lakes were much larger in 1992 and this change does not appear to have been associated with seasonal variability. The white arrows point to a lake that had a decreasing annual trend in lake area.

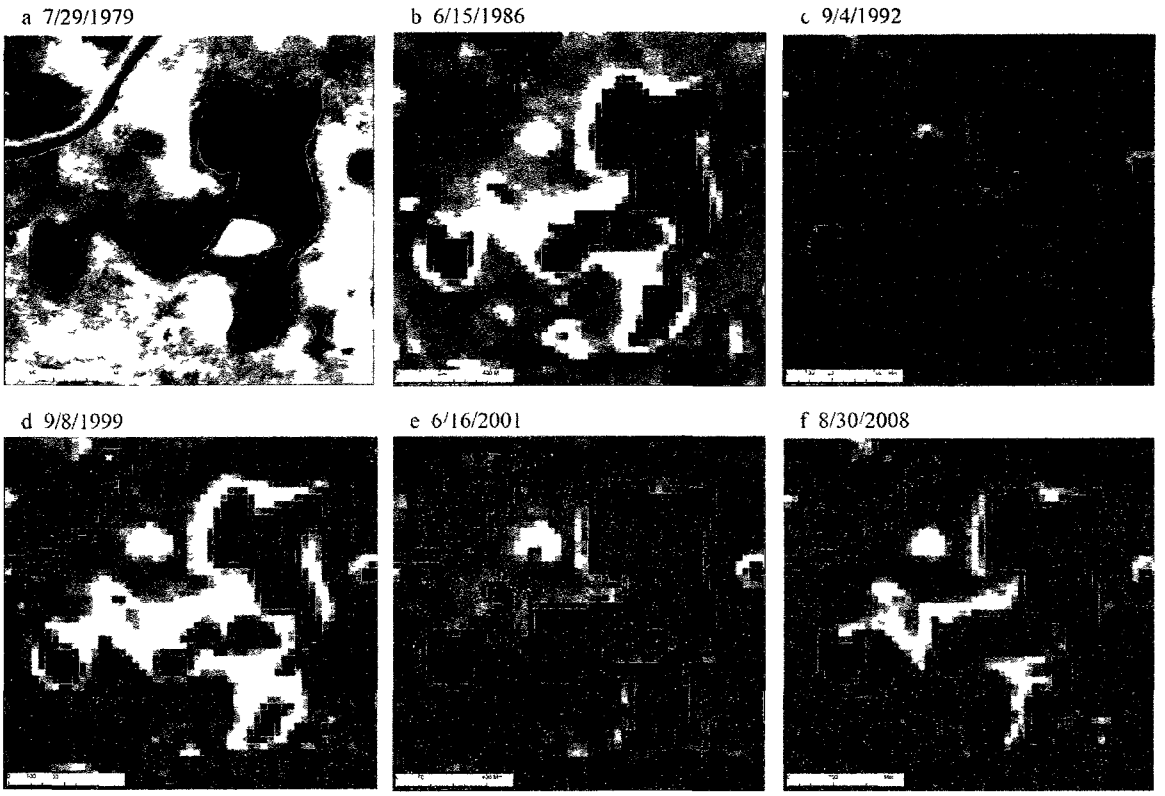

Figure 4.12 Example of a fluctuating lake in the Yukon Flats Central study area. The individual lake equation and coefficient of variation are shown. Individual lake equation was obtained from the Yukon Flats Central pooled variance regression model in which natural log-transformed lake area (m^2) was the dependent variable and year and day-of-summer were the independent variables. Year and day-of-summer variables were coded as years or days since the earliest year or day of image acquisition for each time series and then divided by 100. Variances for all lakes in the Yukon Flats Central study area were pooled into a single regression model by including indicator variables for each lake and all interactions between the indicator variables and the main effects (i.e., year and day-of-summer).

Figure 4.13 Maps showing the spatial distribution of fluctuating lakes in ten study areas (a-j). Ordinary kriging was used to provide a visual representation of the spatial distribution and degree of clustering of individual lake temporal variability (i.e., fluctuating and non-fluctuating lakes). Fluctuating lakes were lakes that had coefficients of variations within the upper 25^{th} percentile of the combined distribution of lake coefficients of variation from the negligible, small increase, and small decrease trend classes for all ten study areas (i.e., greater than 0.21). Ordinary kriging was applied to an indicator variable (0 or 1) for fluctuating or non-fluctuating lakes. White lines are North American Waterfowl Breeding Pair Survey (BPS) transects.

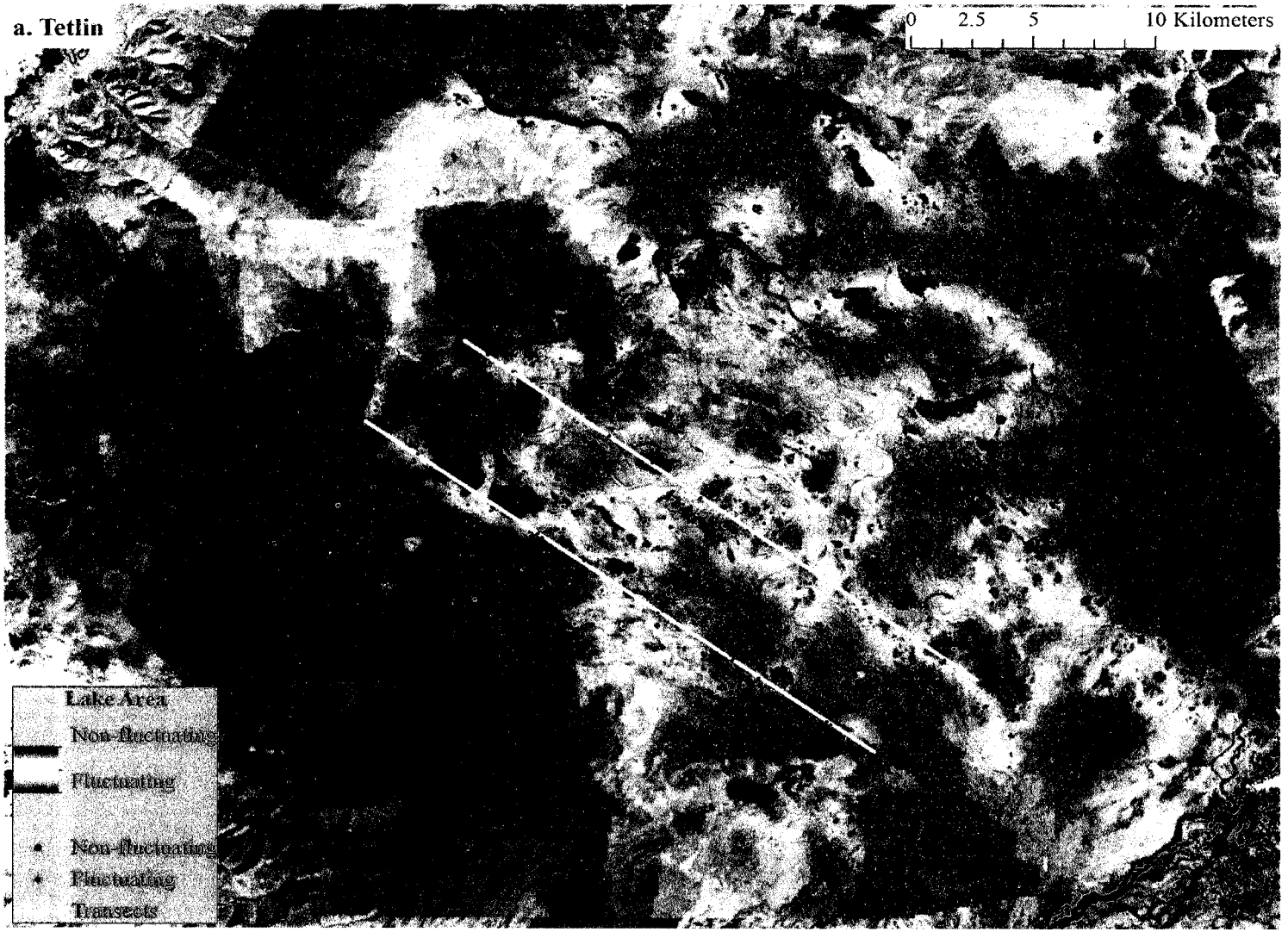
a. Tetlin
0 2.5 5 10 Kilometers
Lake Area
Non-fluctuating
Fluctuating
Non-fluctuating
Fluctuating
Transects

Figure 4.13 (Continued) Maps showing the spatial distribution of fluctuating lakes in ten study areas (a-j).

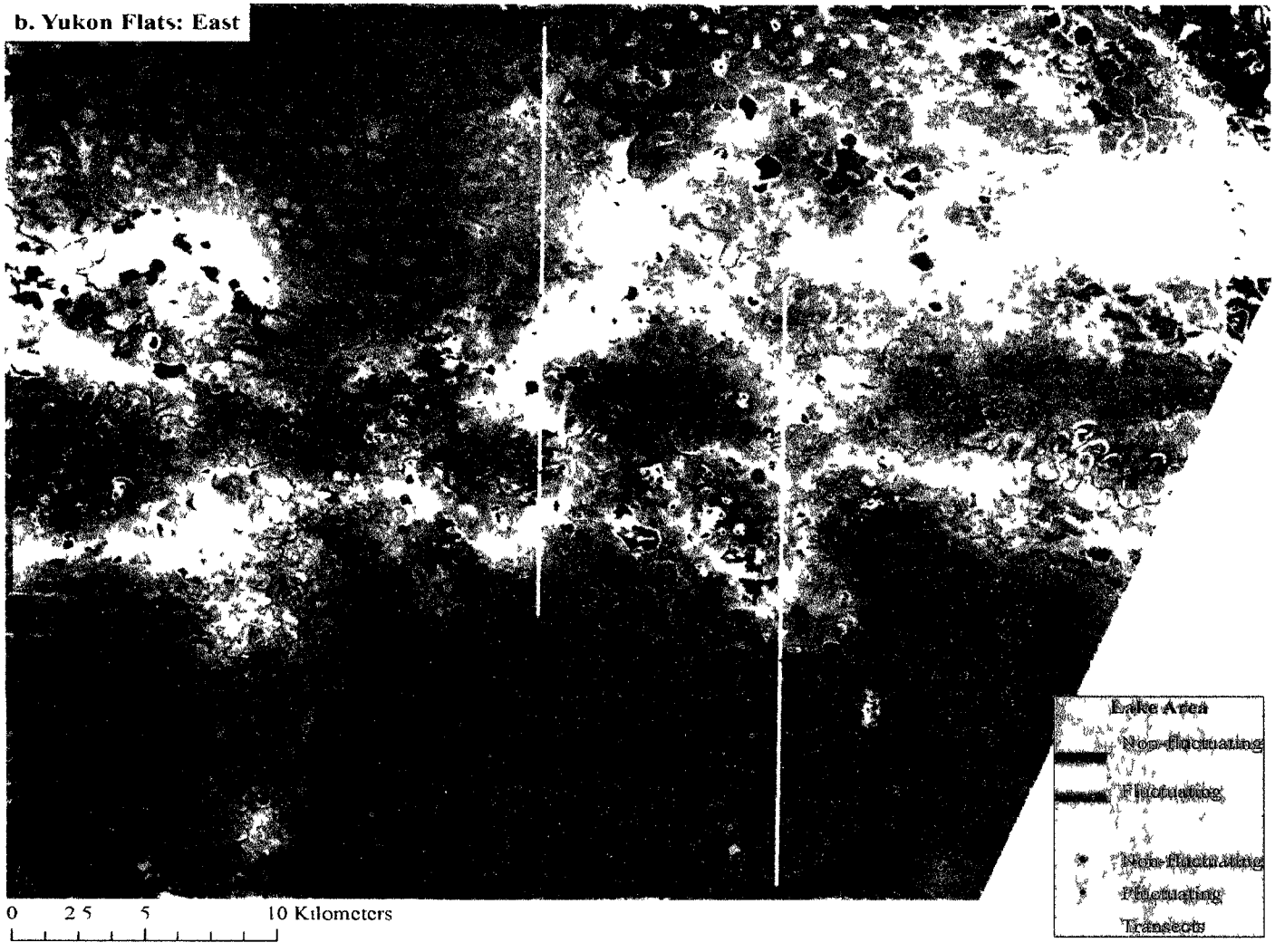

Figure 4.13 (Continued) Maps showing the spatial distribution of fluctuating lakes in ten study areas (a-j).

c. Yukon Flats: Central

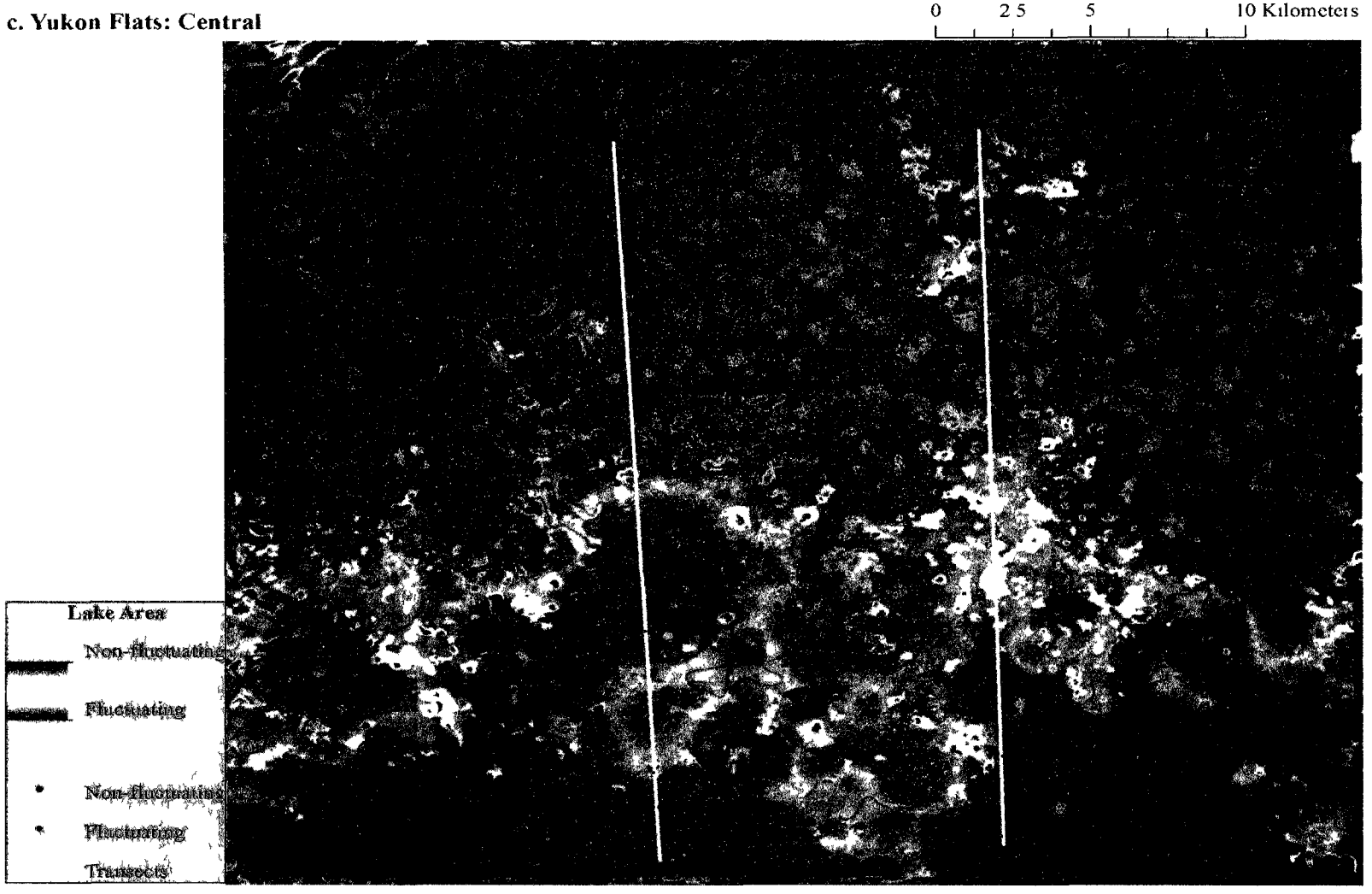

Figure 4.13 (Continued) Maps showing the spatial distribution of fluctuating lakes in ten study areas (a-j).

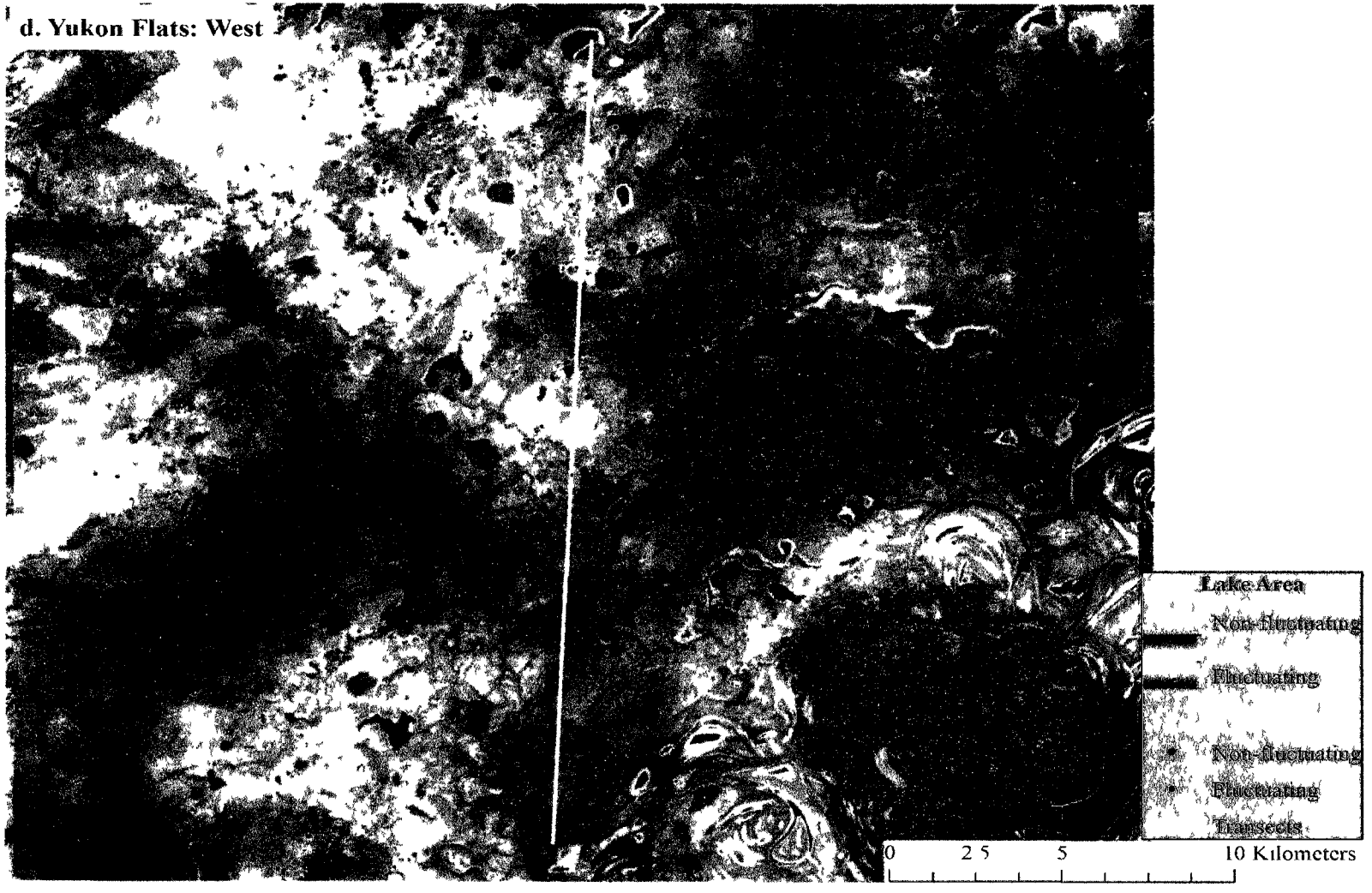

Figure 4.13 (Continued) Maps showing the spatial distribution of fluctuating lakes in ten study areas (a-j).

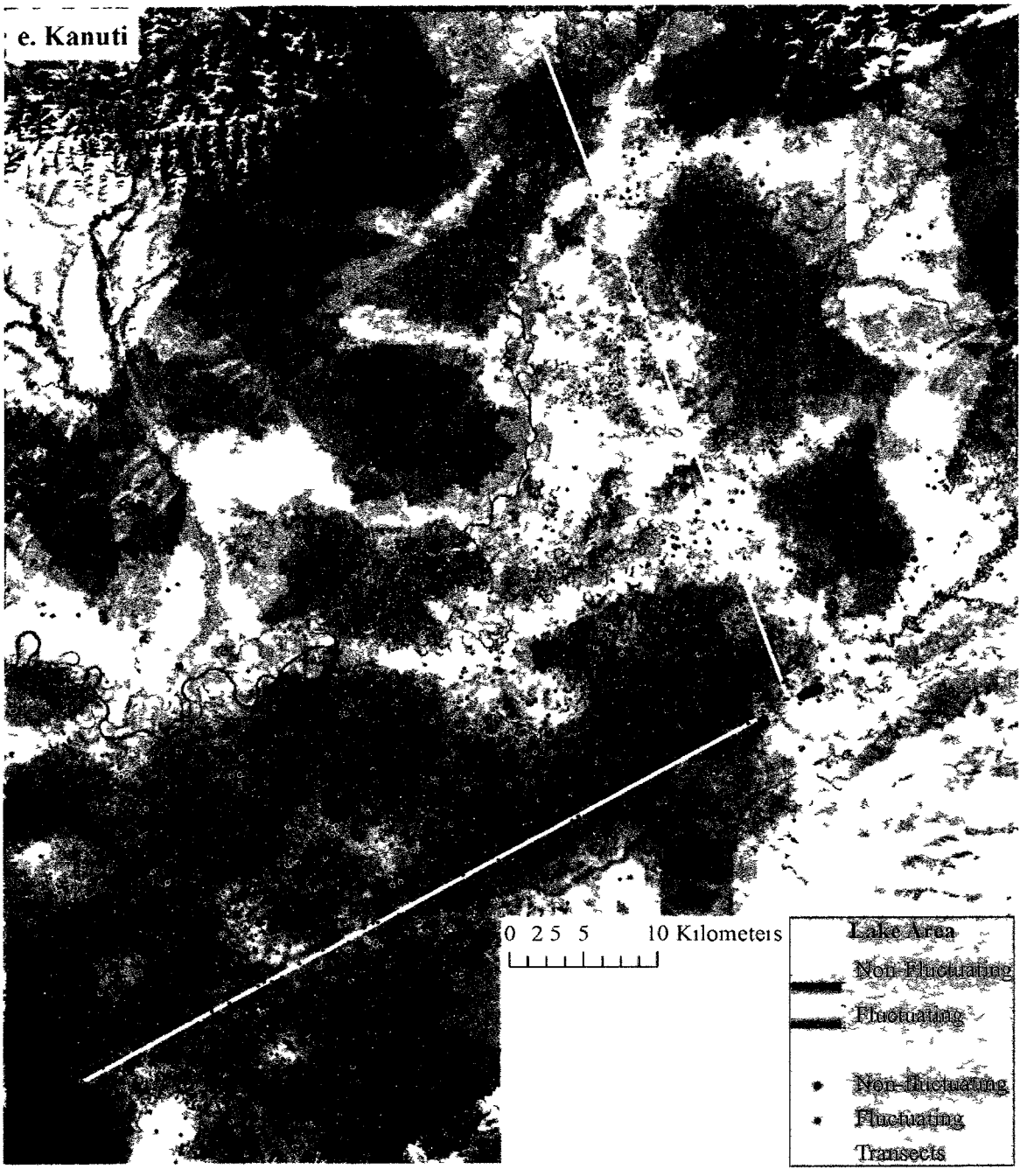

Figure 4.13 (Continued) Maps showing the spatial distribution of fluctuating lakes in ten study areas (a-j).

Figure 4.13 (Continued) Maps showing the spatial distribution of fluctuating lakes in ten study areas (a-j).

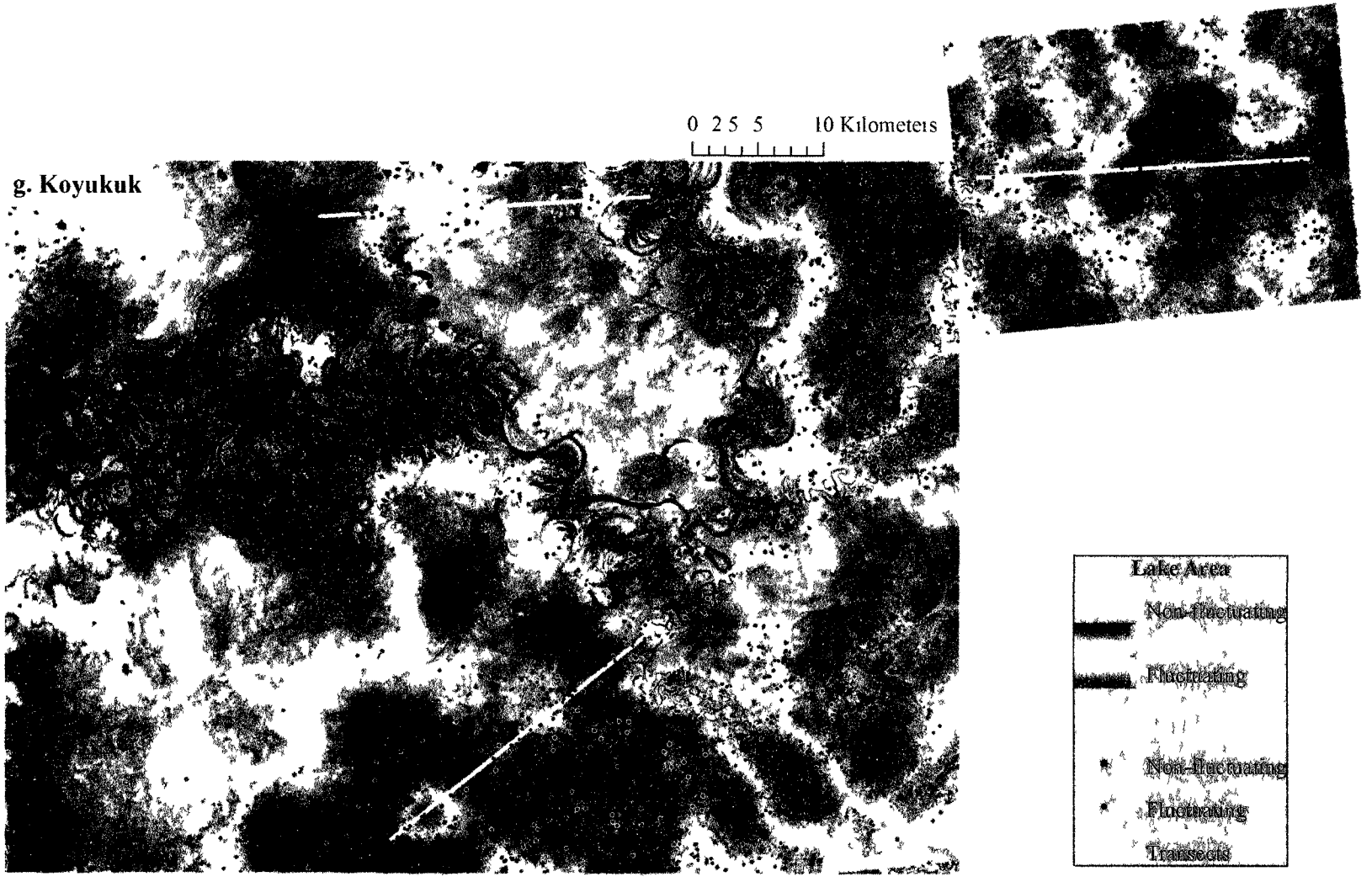

Figure 4.13 (Continued) Maps showing the spatial distribution of fluctuating lakes in ten study areas (a-j).

h. Innoko

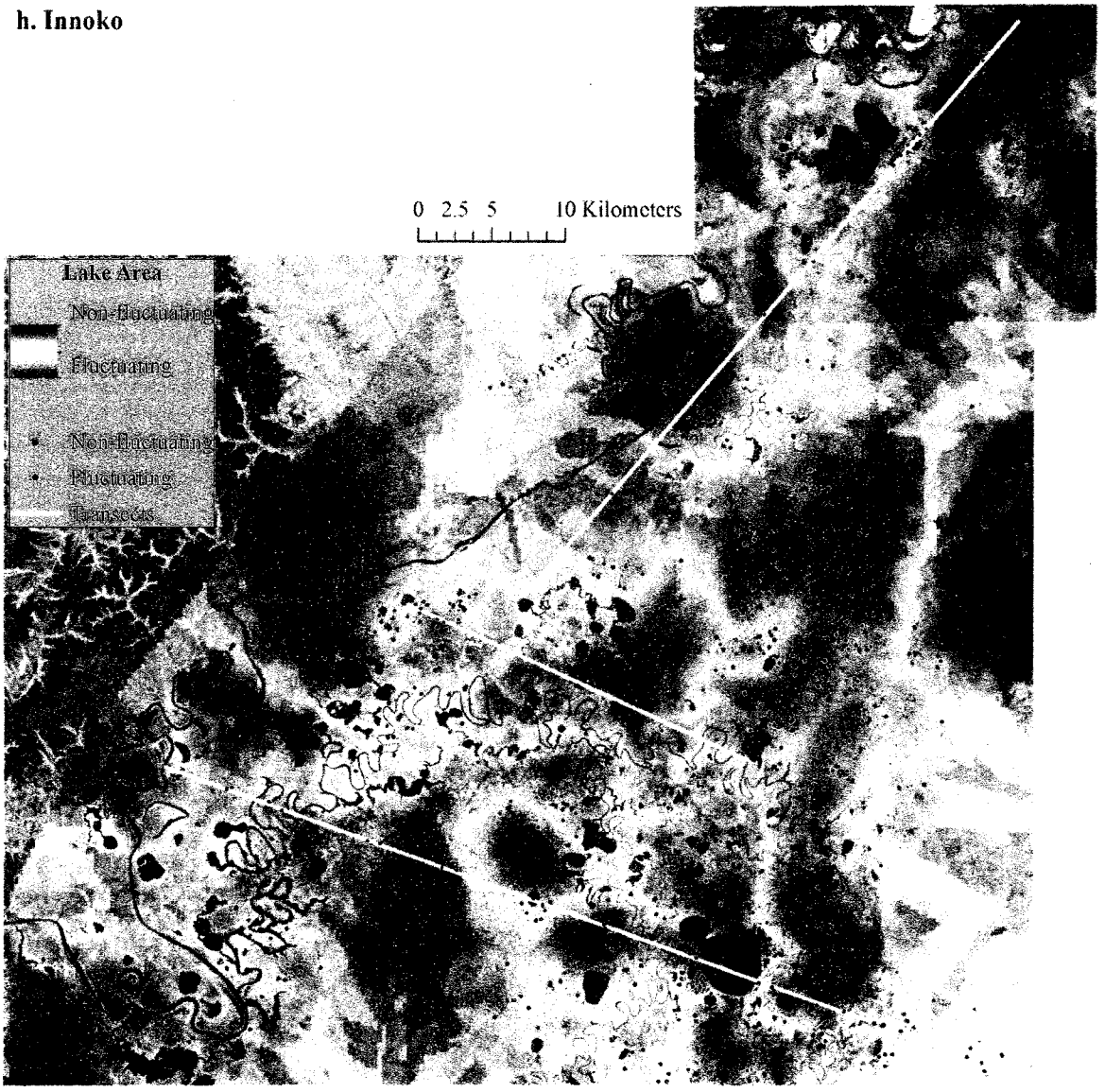

Figure 4.13 (Continued) Maps showing the spatial distribution of fluctuating lakes in ten study areas (a-j).

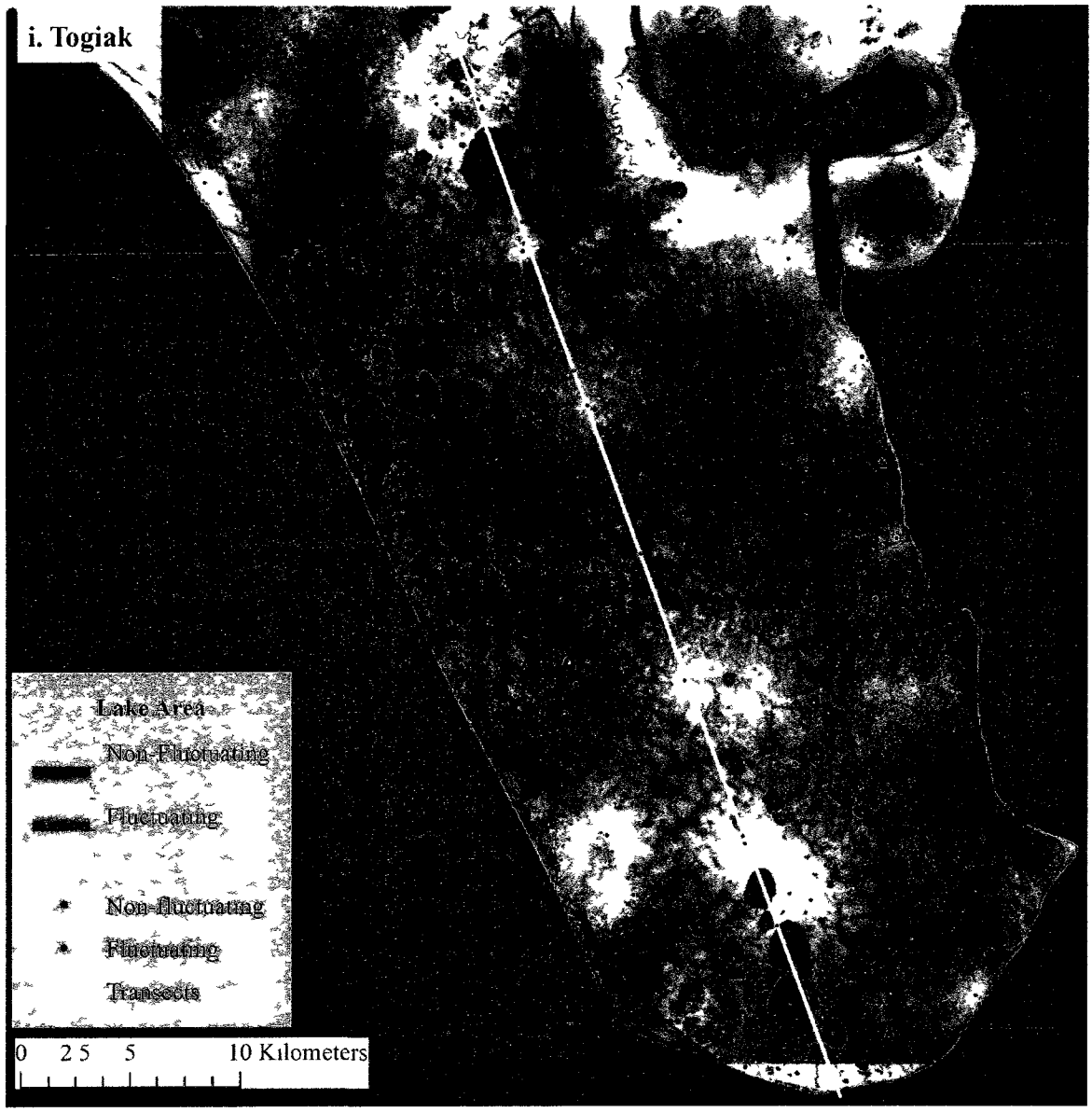

Figure 4.13 (Continued) Maps showing the spatial distribution of fluctuating lakes in ten study areas (a-j).

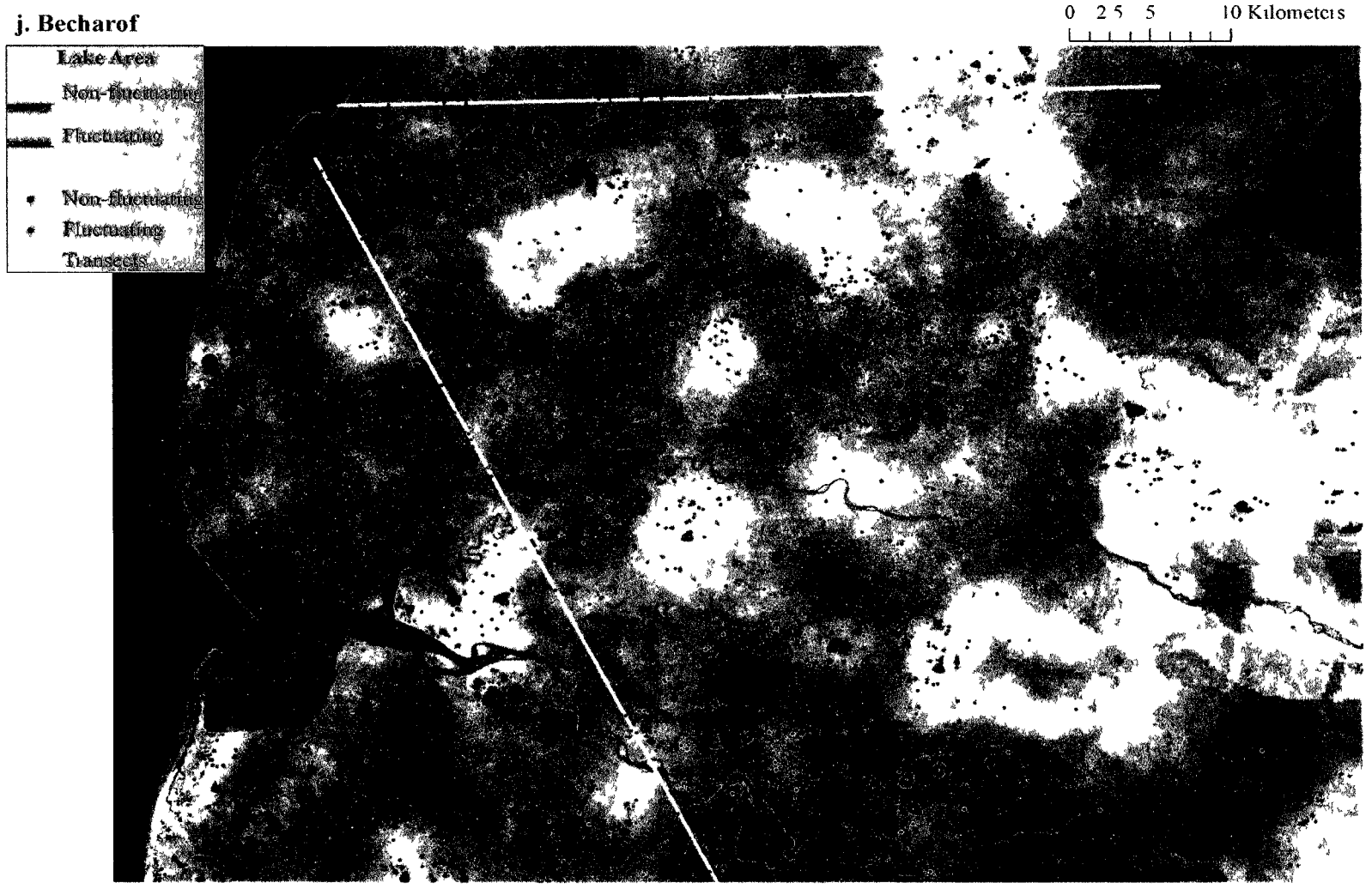

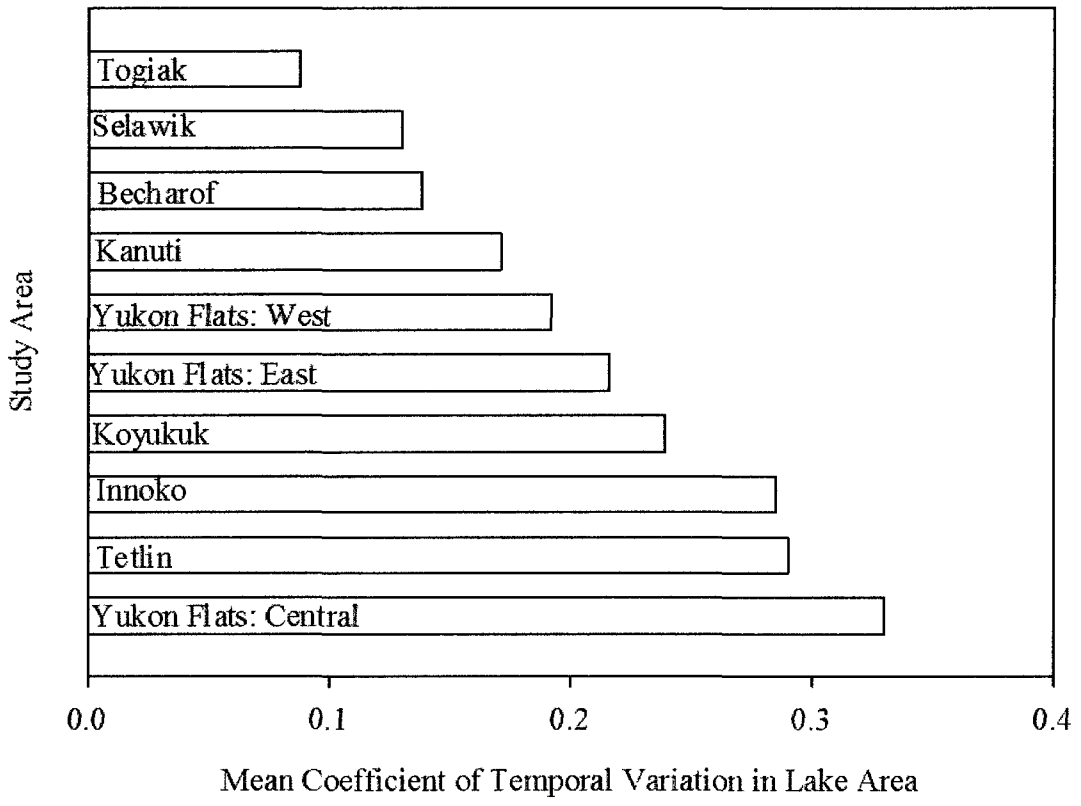

Figure 4.14 Mean coefficient of temporal variation in lake area for lakes within the small decrease, small increase, and negligible trend classes for ten study areas.

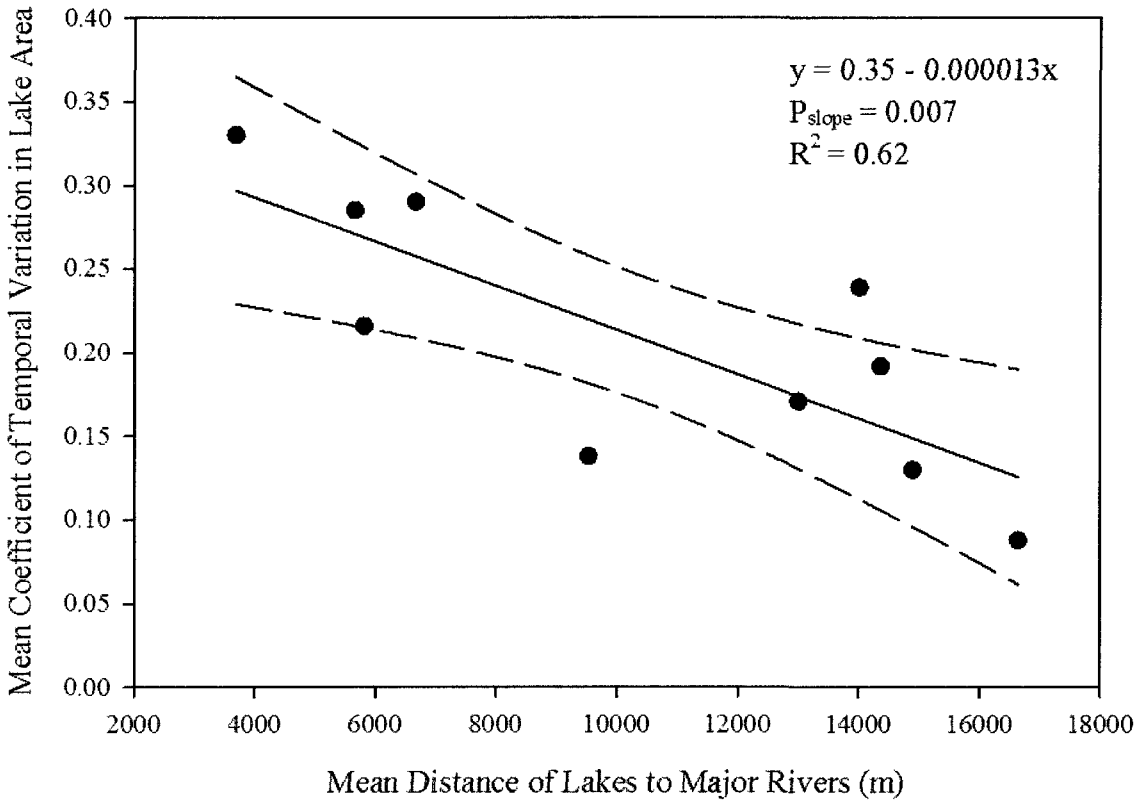

Figure 4.15 Linear regression of study area mean coefficients of temporal variation in lake area against mean distance of lakes to major rivers. The shortest straight line distance from lake centroids to the nearest stream or river was estimated using a subset of major rivers from the United States Geological Society 1:2,000,000 Digital Line Graphs dataset compiled by Alaska Department of Natural Resources. Dotted lines show 95% confidence intervals.

Table 4.1 Dates of aerial photography (1948 – 1984) and Landsat TM/ETM+ imagery (1985 – 2009) used to estimate annual and within-summer trends in lake area for ten study areas located within eight Alaskan National Wildlife Refuges. National Wildlife Refuges were Tetlin, Yukon Flats, Kanuti, Selawik, Koyukuk, Innoko, Togiak, and Becharof. Use of aerial photography was restricted to lakes intersecting 400 m wide North American Waterfowl Breeding Pair Survey (BPS) transects. Either one or two complete series of six Landsat images were used for complete coverage of each study area.

STUDY AREA/ TRANSECT	AERIAL PHOTOGRAPHY			LANDSAT TM/ETM+ SATELLITE IMAGERY					
Tetlin									
Transect 1	9/14/1948	7/9/1978	n/a	6/14/1995	9/18/1995	8/4/1999	5/24/2002	7/3/2008	7/13/2009
Transect 2	9/14/1948	7/9/1978							
Yukon Flats East									
Transect 3	8/28/1952	7/1/1977	7/12/1978	6/15/1986	7/14/1993	7/5/1999	6/16/2001	8/6/2002	8/30/2008
Transect 4	8/31/1952	8/23/1981	n/a						
Yukon Flats Central									
Transect 5	8/5/1952	n/a	7/29/1979	6/15/1986	9/4/1992	7/5/1999	9/8/1999	6/16/2001	8/30/2008
Transect 6	8/28/1952	7/1/1977	7/29/1979						
Yukon Flats West									
Transect 7	7/14/1951	7/12/1978	n/a	6/29/1986	9/9/1994	6/26/1999	8/6/1999	6/26/2005	8/21/2008
Kanuti									
Transect 8	6/3/1970 6/6/1970	7/14/1979	8/2/1981	7/19/1985	9/15/1989	7/2/1999	8/26/1999	6/24/2002	8/17/2007
Transect 9	6/3/1970	7/14/1979 8/1/1979	8/2/1981	7/19/1985	9/15/1989	7/2/1999	8/26/1999	6/24/2002	8/26/2007
Transect 10	6/6/1970	8/1/1979	n/a						
Transect 11	6/6/1970	8/1/1979	n/a						
Selawik									
Transect 12	6/25/1978	n/a	n/a	7/22/1985	6/29/1988	7/27/1995	6/4/2002	8/30/2002	6/28/2008
Transect 13	6/25/1978	7/12/1979	n/a						
Transect 14	6/25/1978	7/25/1981	n/a						
Transect 15	n/a	7/25/1981	n/a						

Table 4.1 (Continued) Dates of aerial photography (1948 – 1984) and Landsat TM/ETM+ imagery (1985 – 2009) used to estimate annual and within-summer trends in lake area for ten study areas located within eight Alaskan National Wildlife Refuges.

Koyukuk									
Transect 16	6/23/1952	6/27/1978	n/a	7/4/1986	8/26/1991	9/15/1995	6/23/2000	9/27/2000	6/14/2008
Transect 17	6/15/1952 6/23/1952 6/24/1952	6/27/1978	n/a	7/4/1986	8/26/1991	6/23/2000	9/27/2000	9/4/2006	6/14/2008
Transect 18	6/14/1952 6/24/1952 7/5/1952	8/5/1981	n/a						
Innoko									
Transect 19	6/2/1953	7/24/1981 8/28/1981	n/a	7/26/1985	8/26/1991	6/30/1999	6/22/2002	7/31/2002	7/7/2008
Transect 20	6/2/1953 6/20/1953	7/23/1980	n/a	8/26/1991	6/30/1999	6/22/2002	7/31/2002	9/13/2006	7/3/2009
Transect 21	6/2/1953 6/20/1953	8/28/1981							
Transect 22	6/2/1953 6/26/1953 6/27/1953	7/17/1980							
Transect 23	6/20/1953 6/27/1953	7/17/1980							
Togiak									
Transect 24	7/20/1952	7/16/1980	n/a	8/14/1989	9/24/1995	6/15/2002	8/2/2002	7/4/2006	6/7/2008
Transect 25	7/20/1952	7/16/1980							
Becharof									
Transect 26	8/24/1951 8/27/1951 9/24/1951	6/13/1973	8/15/1984	5/28/1986	8/30/1991	9/15/2000	6/17/2002	6/4/2006	8/12/2008
Transect 27	6/11/1951	n/a	8/15/1984						
Transect 28	7/10/1951 9/25/1951	n/a	8/15/1984						

Table 4.2 Summary statistics for the distributions of individual lake long-term and recent (i.e., since ~1985) annual and within-summer rates of change for lakes in ten study areas. Individual lake equations were obtained from the pooled variance regression models for each study area in which natural log-transformed lake area (m^2) was the dependent variable. Nine of the ten study area regression models included year and day-of-summer as independent variables. The Innoko regression model did not include a day-of-summer independent variable because it did not enter into the repeated measures regression model. Year and day-of-summer variables were coded as years or days since the earliest year or day of image acquisition for each time series and then divided by 100. For each study area, variances for all lakes were pooled into a single regression model by including indicator variables for each lake and all interactions between the indicator variables and the main effects that were entered into each model (i.e., year and day-of-summer). Distributions were summarized separately for lakes with long-term and recent temporal records (i.e., On-/Off-Transect).

Study Area	On/Off Transect	Years of Record	# of Lakes	Year Slopes					Day-of-Summer Slopes				
				Mean	Std. Error	Min	Max	Skew	Mean	Std. Error	Min	Max	Skew
Tetlin	ON	1948-2009	96	-0.93	0.13	-6.3	2.4	-1.14	-0.295	0.042	-2.09	0.84	-1.48
	OFF	1995-2009	1385	0.07	0.10	-32.0	19.0	-0.52	-0.403	0.015	-3.90	1.53	-1.14
Yukon Flats: East	ON	1952-2008	24	-1.07	0.27	-3.4	0.7	-0.45	-0.402	0.104	-1.25	0.79	0.09
	OFF	1986-2008	830	0.22	0.17	-26.2	23.1	0.13	-0.561	0.038	-7.15	3.08	-1.19
Yukon Flats: Central	ON	1951-2008	50	-2.41	0.30	-7.2	0.9	-0.41	-0.416	0.109	-3.45	0.80	-2.36
	OFF	1986-2008	1079	-3.05	0.13	-20.1	7.9	-0.67	-0.215	0.027	-4.65	3.59	-0.22
Yukon Flats: West	ON	1951-2008	22	-0.61	0.27	-3.2	2.7	0.05	-0.109	0.110	-1.75	0.61	-1.87
	OFF	1986-2008	677	0.31	0.10	-11.9	14.9	-0.07	0.190	0.031	-2.97	4.57	1.31
Kanuti	ON	1970-2007	68	-1.23	0.21	-7.4	1.7	-1.43	0.015	0.048	-1.25	1.12	0.07
	OFF	1985-2007	2366	-1.53	0.06	-18.0	7.3	-1.28	-0.091	0.012	-4.34	3.49	-0.55

Table 4.2 (Continued) Summary statistics for the distributions of individual lake long-term and recent (i.e., since ~1985) annual and within-summer rates of change for lakes in ten study areas.

Selawik	ON	1978-2008	92	-1.05	0.28	-11.9	5.9	-1.65	-0.187	0.049	-1.77	0.75	-1.10
	OFF	1985-2008	5769	-0.77	0.03	-26.4	14.4	-1.42	-0.034	0.006	-3.30	2.01	-1.09
Koyukuk	ON	1952-2008	86	-0.95	0.20	-7.0	6.9	-0.07	-0.077	0.040	-1.43	0.97	-0.64
	OFF	1986-2008	3774	-0.07	0.04	-16.2	13.9	-0.38	-0.152	0.009	-3.58	3.33	-0.24
Innoko	ON	1953-2009	74	-0.87	0.11	-2.8	2.1	0.36	-	-	-	-	-
	OFF	1985-2009	1992	-1.49	0.07	-22.5	26.2	0.35	-	-	-	-	-
Togiak	ON	1952-2008	35	-0.87	0.15	-3.1	0.1	-0.94	-0.052	0.044	-0.83	0.85	0.77
	OFF	1989-2008	1391	-1.61	0.11	-34.2	20.8	-0.23	-0.208	0.013	-2.78	1.94	-0.29
Becharof	ON	1951-2008	75	-0.83	0.23	-13.2	7.4	-2.62	0.021	0.024	-1.27	0.40	-3.43
	OFF	1986-2008	3697	-0.05	0.03	-12.7	10.2	-0.50	0.078	0.005	-3.35	1.73	-0.83
ALL AREAS	ON	1948-2009	622	-1.07	0.07	-13.2	7.4	-1.54	-0.154	0.019	-3.45	1.12	-1.96
	OFF	1985-2009	22960	-0.72	0.02	-34.2	26.2	-0.67	-0.101	0.004	-7.15	4.57	-0.99

Table 4.3 Percentages of lakes with either long-term or recent (i.e., since 1985) temporal records assigned to five trend classes based on individual lake annual rates of change from ten study areas. Individual lake equations were obtained from the pooled variance regression models for each study area in which natural log-transformed lake area (m^2) was the dependent variable. Year and day-of-summer were the independent variables for all models except for the Innoko regression model that did not include a day-of-summer variable because it did not enter into the repeated measures regression model. Year and day-of-summer variables were coded as years or days since the earliest year or day of image acquisition for each time series and then divided by 100. For each study area, variances for all lakes were pooled into a single regression model by including indicator variables for each lake and all interactions between the indicator variables and the main effects that were entered into each model (i.e., year and day-of-summer). The negligible trend class contained lakes that had annual rates of change within the 20^{th} percentile centered on zero of the combined distribution of all individual lake annual rates of change from the ten study areas. The small and large change classes were the upper and lower halves of the remaining lakes on either end of the distribution. The threshold values for annual rates of change used to assign lakes to the five trend classes were: less than -1.6486 for large decreases, less than -0.2534 for small decreases, less than 0.2551 for negligible change, less than 1.099 for small increases, and greater than 1.099 for large increases. Lakes were assigned ordinal values of 1 through 5 based on their trend class (1 = large decrease, 2 = small decrease, 3 = negligible change, 4 = small increase, 5 = large increase) and the Moran's I statistic was used to evaluate whether high or low values were clustered, dispersed, or randomly distributed across each study area. The corresponding scale was the distance band that resulted in the maximum degree of clustering.

Study Area	On/Off Transect	Years of Record	# of Lakes	% Lakes in Trend Classes					Moran's I	
				Large Decrease	Small Decrease	Negligible	Small Increase	Large Increase	Value[a]	Scale (km)
Tetlin	ON	1948-2009	96	22	48	20	7	3	0.081	10
	OFF	1995-2009	1385	19	29	12	12	28		
Yukon Flats: East	ON	1952-2008	24	37	21	29	13	0	0.078	6
	OFF	1986-2008	830	26	16	13	14	31		
Yukon Flats: Central	ON	1951-2008	50	56	28	10	6	0	0.047	6
	OFF	1986-2008	1079	62	12	6	5	15		

Table 4.3 (Continued) Percentages of lakes with either long-term or recent (i.e., since 1985) temporal records assigned to five trend classes based on individual lake annual rates of change from ten study areas.

Yukon Flats: West	ON	1951-2008	22	18	36	36	5	5	0.064	3
	OFF	1986-2008	677	15	16	17	23	29		
Kanuti	ON	1970-2007	68	29	37	24	9	1	0.063	10
	OFF	1985-2007	2366	35	32	13	12	8		
Selawik	ON	1978-2008	92	24	30	28	7	11	0.030	22
	OFF	1985-2008	5769	23	31	25	12	9		
Koyukuk	ON	1952-2008	86	23	47	22	3	5	0.078	6
	OFF	1986-2008	3774	17	22	19	21	21		
Innoko	ON	1953-2009	74	22	50	20	5	3	0.105	8
	OFF	1985-2009	1992	42	26	10	10	12		
Togiak	ON	1952-2008	35	17	54	29	0	0	0.082	22
	OFF	1989-2008	1391	39	32	11	5	13		
Becharof	ON	1951-2008	75	17	49	29	3	2	0.038	5
	OFF	1986-2008	3697	12	18	34	24	12		
ALL AREAS	ON	1948-2009	622	25	42	24	6	3	-	-
	OFF	1985-2009	22960	25	25	20	15	15	-	-

[a] All Moran's I values were statistically significant at alpha = 0.05 rejecting the null hypothesis that high and low trend class values were randomly distributed across the study areas.

Table 4.4 Results from repeated measures regression models to estimate long-term and recent (i.e., since ~1985) annual and within-summer trends in ten study areas. Natural log-transformed lake area (m^2) was the dependent variable. All models included year as an independent variable while inclusion of the day-of-summer variable was assessed using backwards model selection with alpha to remove of 0.05. The Innoko study area was the only study area that did not have a day-of-summer term enter into its regression model. Year and day-of-summer variables were coded as years or days since the earliest year or day of image acquisition for each time series and then divided by 100. To obtain separate equations for long-term and recent (i.e., since ~1985) trends, variances from on- and off-transect lake populations were pooled by including an indicator variable for lakes on- or off-transects (i.e., long-term vs. recent temporal trends) along with all interactions between the transect variable and the main effects that entered into each model (i.e., year and day-of-summer). Regression slopes were compared between long-term and recent temporal records for each study area to identify whether long-term rates of change increased and decreased since ~1985.

Study Area	On/Off Transect	Years of Record	Summer Record Length	# of Lakes	Intercept[a]	Year Slope[b]	Day-of-summer Slope[c]	Cumulative Annual % Change[d]	Cumulative Summer % Change[e]
Tetlin[A]	ON	1948-2009	5/24-9/18	96	10.67	-0.93*	-0.295**	-43.3	-29.2
	OFF	1995-2009	5/24-9/18	1385	9.67	0.07	-0.403**	1.0	-37.6
Yukon Flats: East	ON	1952-2008	6/15-8/31	24	11.03	-1.06	-0.397	-44.8	-26.3
	OFF	1986-2008	6/15-8/30	830	10.05	0.19	-0.562**	4.3	-34.8
Yukon Flats: Central	ON	1951-2008	6/15-9/8	50	11.16	-2.27**	-0.293**	-72.6	-22.1
	OFF	1986-2008	6/15-9/8	1079	10.85	-2.96**	-0.178**	-47.9	-14.0
Yukon Flats: West	ON	1951-2008	6/26-9/9	22	10.65	-0.59	-0.128	-28.6	-9.2
	OFF	1986-2008	6/26-9/9	677	9.70	0.34**	0.142**	7.8	11.2
Kanuti	ON	1970-2007	6/3-9/15	68	10.63	-1.25**	0.018	-37.0	1.9
	OFF	1985-2007	6/24-9/15	2366	10.11	-1.50**	-0.072**	-28.1	-5.8
Selawik[B]	ON	1978-2008	6/4-8/30	92	10.55	-1.08**	-0.230**	-27.7	-18.1
	OFF	1985-2008	6/4-8/30	5769	10.12	-0.81**	-0.054**	-17.0	-4.6

Table 4.4 (Continued) Results from repeated measures regression models to estimate long-term and recent (i.e., since ~1985) annual and within-summer trends in ten study areas.

Koyukuk[A]	ON	1952-2008	6/14-9/27	86	10.32	-1.00**	-0.072	-42.9	-7.3
	OFF	1986-2008	6/14-9/27	3774	9.68	-0.08	-0.153**	-1.8	-14.8
Innoko	ON	1953-2009	6/2-9/13	74	10.40	-0.87**	-	-38.6	-
	OFF	1985-2009	6/22-9/13	1992	10.10	-1.54**	-	-30.9	-
Togiak	ON	1952-2008	5/24-9/24	35	11.11	-0.86	-0.059	-38.2	-6.2
	OFF	1989-2008	5/24-9/24	1391	10.54	-1.63**	-0.217**	-26.6	-21.1
Becharof[A]	ON	1951-2008	5/28-9/25	75	10.63	-0.82**	0.021	-37.3	2.3
	OFF	1986-2008	5/28-9/25	3697	9.76	-0.05	0.078**	-1.1	9.0
AVERAGE	ON	-	-	-	-	-1.07	-0.159	-41.4	-12.7
	OFF	-	-	-	-	-0.80	-0.158	-14.0	-12.5

[a] All intercept terms were significantly different from zero at alpha = 0.05
[b] Geometric percent change in average lake area (m^2) per year
[c] Geometric percent change in average lake area (m^2) per day-of-summer
[d] Cumulative percent change in average lake area (m^2) for the years of record
[e] Cumulative percent change in average lake area (m^2) for the length of the summer records
[A] Year slope significantly different between long-term and recent temporal records at alpha = 0.05
[B] Day-of-summer slope significantly different between long-term and recent temporal records at alpha = 0.05
** Significantly different from zero at alpha = 0.05
* Significantly different from zero at alpha = 0.10

Table 4.5 Results from repeated measures regression models to estimate annual and within-summer trends in lake area on the same temporal scale (i.e., since ~1985) for on- and off-transect lake populations in ten study areas. Natural log-transformed lake area (m^2) was the dependent variable. All models included year as an independent variable while inclusion of the day-of-summer variable was assessed using backwards model selection with alpha to remove of 0.05. The Innoko study area was the only study area that did not have a day-of-summer term enter into its regression model. Year and day-of-summer variables were coded as years or days since the earliest year or day of image acquisition for each time series and then divided by 100. To obtain separate equations for on- and off- transect trends, we pooled variances from on- and off-transect lake populations by including an indicator variable for lakes on- or off- transects along with all interactions between the transect variable and the main effects that entered into each model (i.e., year and day-of-summer). Regression slopes were compared between on- and off-transect lake populations on the same temporal scale for each study area to identify if the trends of the smaller on-transect lake population were representative of the trends of the larger off-transect lake population.

Study Area	On/Off Transect	Years of Record	# of Lakes	Intercept[a]	Year Slope[b]	Day-of-summer Slope[c]
Tetlin	ON	1995-2009	96	10.04	0.20	-0.265**
	OFF	1995-2009	1385	9.66	0.08	-0.400**
Yukon Flats: East	ON	1986-2008	24	10.05	0.96	-0.574*
	OFF	1986-2008	830	10.06	0.18	-0.559**
Yukon Flats: Central	ON	1986-2008	50	10.99	-2.03**	-0.274*
	OFF	1986-2008	1079	10.85	-2.96**	-0.178**
Yukon Flats: West	ON	1986-2008	22	10.19	0.30	-0.118
	OFF	1986-2008	677	9.70	0.34**	0.141**
Kanuti	ON	1985-2007	68	10.69	-1.40**	-0.008
	OFF	1985-2007	2366	10.11	-1.50**	-0.072**
Selawik[B]	ON	1985-2008	92	10.46	-0.67**	-0.244**
	OFF	1985-2008	5769	10.12	-0.81**	-0.055**
Koyukuk	ON	1986-2008	86	9.71	0.22	-0.033
	OFF	1986-2008	3774	9.68	-0.08	-0.154**

Table 4.5 (Continued) Results from repeated measures regression models to estimate annual and within-summer trends in lake area on the same temporal scale (i.e., since ~1985) for on- and off-transect lake populations in ten study areas.

Innoko[A]	ON	1985-2009	74	10.03	-0.17	-
	OFF	1985-2009	1992	10.10	-1.54**	-
Togiak	ON	1989-2008	35	11.41	-1.44*	-0.119
	OFF	1989-2008	1391	10.54	-1.63**	-0.217**
Becharof	ON	1986-2008	75	10.30	-0.20	0.023
	OFF	1986-2008	3697	9.76	-0.05	0.078**

[a] All intercept terms were significantly different from zero at alpha = 0.05
[b] Geometric percent change in average lake area (m^2) per year
[c] Geometric percent change in average lake area (m^2) per day-of-summer
[A] Year slope significantly different between on- and off-transect populations at alpha = 0.05
[B] Day-of-summer slope significantly different between on- and off-transect populations at alpha = 0.05
** Significantly different from zero at alpha = 0.05
* Significantly different from zero at alpha = 0.10

Table 4.6 Results of one-tailed t-tests used to test the hypothesis that on-transect lakes were larger on average compared to the off-transect lake population. On-transect lakes may be larger because transects preferentially sample larger objects.

STUDY AREA	ON TRANSECT			OFF TRANSECT			P
	# Lakes	Mean Lake Area (m^2)	Standard Error	# Lakes	Mean Lake Area (m^2)	Standard Error	
Tetlin	96	184,214	74,826	1,385	101,623	49,265	0.33
Yukon Flats: East	24	342,529	147,973	830	94,238	10,672	0.0001
Yukon Flats: Central	50	106,627	23,809	1,079	53,100	5,651	0.02
Yukon Flats: West	22	170,251	66,607	677	80,241	8,074	0.03
Kanuti	68	97,621	22,769	2,366	45,143	3,664	0.01
Selawik	92	113,720	30,034	5,769	63,977	2,775	0.01
Koyukuk	86	89,178	28,104	3,774	50,751	3,275	0.04
Innoko	74	292,567	185,002	1,992	62,222	6,329	<0.0001
Togiak	35	638,259	285,533	1,391	52,445	4,843	<0.0001
Becharof	75	192,363	65,590	3,697	61,736	3,800	<0.0001

Table 4.7 Geophysical characteristics of ten study areas and relationships with recent (i.e., since ~1985) annual trends in lake area. One-tailed t-tests were conducted to test *a priori* hypotheses for the expected direction of the difference in mean values of geophysical and land cover characteristics between study areas with negligible or increasing recent annual trends in lake area (x_1: N = 5) and study areas with decreasing recent trends in lake area (x_2: N = 5).

Study Area	Soil and Permafrost Characteristics (Jorgenson *et al.* 2008)									Landform Type (Johnson *et al.*, unpublished data)			
	Surficial Geology		Soil Texture		Extent[a]		Ice Content		% Thermo-karst Features[g]	Type[b]	% Sandy	% Herb.[h] Wetlands	% Woody Wetlands
	Type[b]	% Fluvial	Type[b]	% Sandy	Type[b]	% Un-stable[e]	Type[b]	% High/ Mod.[f]					
Tetlin (x_1 Negligible)	Fluvial	94	Silty	21	Disc[c]	100	Mod[f]	77	77	Silty Lowland	12	0	36
Yukon Flats East (x_1 Negligible)	Fluvial	47	Sandy	67	Disc[c]	88	Low	34	34	Sandy Lowland	59	5	8
Yukon Flats Central (x_2 Decrease)	Fluvial	52	Sandy	87	Disc[c]	97	Low	13	16	Sandy Lowland	68	7	9
Yukon Flats West (x_1 Increase)	Fluvial	89	Silty	32	Cont[d]	0	Mod[f]	68	100	Woody Wetlands	16	2	51
Kanuti (x_2 Decrease)	Undifferentiated Alluvium & Colluvium	30	Silty	31	Cont[d]	20	High	44	80	Silty Lowland	27	1	8
Selawik (x_2 Decrease)	Coastal Old Marine & Alluvium	15	Sandy	85	Disc[c]	87	Mod[f]	81	17	Sandy Lowland	63	3	22
Koyukuk (x_1 Negligible)	Fluvial	70	Silty	27	Disc[c]	100	Mod[f]	72	73	Woody Wetlands	15	5	47

Table 4.7 (Continued) Geophysical characteristics of ten study areas and relationships with recent (i.e., since ~1985) annual trends in lake area.

Innoko (x_2 Decrease)	Undifferentiated Alluvium & Colluvium	42	Silty	41	Isolated	100	Low	59	59	Herb Wetlands[h]	15	50	19
Togiak (x_2 Decrease)	Coastal Old Marine & Alluvium	0	Sandy	67	Unfrozen	10	Unfrozen	0	10	Herb Wetlands[h]	37	36	5
Bechaiof (x_1 Negligible)	Glacial Moraines & Drift	7	Rocky	9	Isolated	64	Low	0	62	Rocky Upland	8	6	0
T-test Hypotheses and Results	H_0 $\bar{x}_1 - \bar{x}_2 > 0$ $\bar{x}_1 = 61\ 4$ $\bar{x}_2 = 27\ 8$ $P = 0\ 05$		H_a $\bar{x}_1 - \bar{x}_2 < 0$ $\bar{x}_1 = 31\ 2$ $\bar{x}_2 = 62\ 2$ $P = 0\ 04$		H_0 $\bar{x}_1 - \bar{x}_2 < 0$ $\bar{x}_1 = 70\ 4$ $\bar{x}_2 = 62\ 8$ $P = 0\ 61$		H_a $\bar{x}_1 - \bar{x}_2 > 0$ $\bar{x}_1 = 50\ 2$ $\bar{x}_2 = 39\ 4$ $P = 0\ 31$		H_a $\bar{x}_1 - \bar{x}_2 > 0$ $\bar{x}_1 = 69\ 2$ $\bar{x}_2 = 36\ 4$ $P = 0\ 05$	H_0 $\bar{x}_1 - \bar{x}_2 < 0$ $\bar{x}_1 = 22$ $\bar{x}_2 = 42$ $P = 0\ 09$		H_0 $\bar{x}_1 - \bar{x}_2 < 0$ $\bar{x}_1 = 3\ 6$ $\bar{x}_2 = 19\ 4$ $P = 0\ 08$	H_a $\bar{x}_1 - \bar{x}_2 > 0$ $\bar{x}_1 = 28\ 4$ $\bar{x}_2 = 12\ 6$ $P = 0\ 09$

[a] Categories for permafrost extent were continuous (90-100%), discontinuous (50-90%), sporadic (10-50%), and isolated (>0-10%)

[b] Type that contained the largest number of lake centroids

[c] Discontinuous Permafrost Extent

[d] Continuous Permafrost Extent

[e] Unstable permafrost types include discontinuous, sporadic, and isolated permafrost extents.

[f] Moderate Permafrost Ice Content

[g] Thermokarst features include troughs, pits, slumps, gullies, water tracks, and sinks.

[h] Herbaceous Wetlands

Table 4.8 Topographical characteristics of ten study areas and relationships with recent (i.e., since ~1985) annual trends in lake area. One-tailed t-tests were conducted to test *a priori* hypotheses for the expected direction of the difference in mean values of topographical characteristics between study areas with negligible or increasing recent annual trends in lake area (x_1: N = 5) and study areas with decreasing recent trends in lake area (x_2: N = 5).

Study Area	Total Area (km^2)	Ecoregion[a] (Nowacki *et al.* 2001)	Mean Elevation[b] (m)	Elevation-Relief Ratio[b,c]	Mean Distance from Lakes to Rivers and Streams[d] (m)	Mean Distance from Lakes to Major Rivers[e] (m)
Tetlin (x_1: Negligible)	2,283	Boreal	625 (SE = 1.00)	0.13	1,389 (SE = 26)	6,672 (SE = 120)
Yukon Flats East (x_1: Negligible)	1,845	Boreal	146 (SE = 0.23)	0.17	1,803 (SE = 57)	5,816 (SE = 148)
Yukon Flats Central (x_2: Decrease)	1,133	Boreal	112 (SE = 0.05)	0.22	2,904 (SE = 75)	3,692 (SE = 83)
Yukon Flats West (x_1: Increase)	927	Boreal	104 (SE = 0.27)	0.04	1,595 (SE = 44)	14,362 (SE = 256)
Kanuti (x_2: Decrease)	4,565	Boreal	238 (SE = 0.47)	0.15	1,760 (SE = 28)	13,002 (SE = 169)
Selawik (x_2: Decrease)	4,497	Boreal	40 (SE = 0.17)	0.08	2,023 (SE = 31)	14,892 (SE = 102)
Koyukuk (x_1: Negligible)	4,537	Polar: Bering Tundra	68 (SE = 0.12)	0.12	2,393 (SE = 31)	14,012 (SE = 147)
Innoko (x_2: Decrease)	4,342	Boreal	46 (SE = 0.14)	0.11	3,337 (SE = 58)	5,663 (SE = 89)

Table 4.8 (Continued) Topographical characteristics of ten study areas and relationships with recent (i.e., since ~1985) annual trends in lake area.

Togiak (x_2: Decrease)	1,272	Polar: Bering Taiga	13 (SE = 0.12)	0.04	3,870 (SE = 26)	16,642 (SE = 279)
Becharof (x_1: Negligible)	3,932	Polar: Bering Taiga	55 (SE = 0.24)	0.15	1,871 (SE = 21)	9,533 (SE = 96)
T-test Hypotheses and Results	-	-	H_a: $\bar{x}_1 - \bar{x}_2 > 0$ $\bar{x}_1 = 199.6$ $\bar{x}_2 = 89.8$ P = 0.18	H_a: $\bar{x}_1 - \bar{x}_2 < 0$ $\bar{x}_1 = 0.122$ $\bar{x}_2 = 0.12$ P = 0.52	H_a: $\bar{x}_1 - \bar{x}_2 < 0$ $\bar{x}_1 = 1810.2$ $\bar{x}_2 = 2778.8$ P = 0.03	H_a: $\bar{x}_1 - \bar{x}_2 < 0$ $\bar{x}_1 = 10079$ $\bar{x}_2 = 10778$ P = 0.42

[a] Ecoregion that contained the largest number of lake centroids
[b] Derived from 300m Alaska Digital Elevation Model
[c] Approximation of hypsometric integral used to describe the topographical distribution of a land area using the following equation: (Mean Elevation – Minimum Elevation) / (Maximum Elevation – Minimum Elevation) (Pike & Wilson 1971). Low values occur in terrains characterized by isolated relief features standing above extensive level surfaces typical of runoff dominated drainages. High values describe broad, somewhat level surfaces broken by occasional depressions typical of groundwater influenced terrain (Pike & Wilson 1971; Luo 2002).
[d] Rivers and streams from the USGS 1:2,000,000 DLG dataset
[e] Subset of major rivers from the United States Geological Society (USGS) 1:2,000,000 Digital Line Graghs (DLG) dataset compiled by Alaska Department of Natural Resources

Table 4.9 Lake size and density characteristics of ten study areas and relationships with recent (i.e., since ~1985) annual trends in lake area. Estimates were based on the average size of lakes across all images included in each study area analysis. Large lakes were > 10 ha. Small lakes were < 1 ha. One-tailed t-tests were conducted to test *a priori* hypotheses for the expected direction of the difference in mean values of lake size and density characteristics between study areas with negligible or increasing recent annual trends in lake area (x_1: N = 5) and study areas with decreasing recent trends in lake area (x_2: N = 5).

Study Area	Total Area (km^2)	Limnetic ratio[a] (%)	Mean Lake Area (ha)	# Lakes	% Small Lakes	% Large Lakes	Lake Density (# lakes/ km^2)	Small Lake Density (# lakes/ km^2)	Large Lake Density (# lakes/ km^2)
Tetlin (x_1: Negligible)	2,283	6.9	10.7 (SE = 4.63)	1,481	45	9	0.65	0.29	0.06
Yukon Flats East (x_1: Negligible)	1,845	4.7	10.1 (SE = 1.12)	854	35	20	0.46	0.16	0.09
Yukon Flats Central (x_2: Decrease)	1,133	5.5	5.6 (SE = 0.55)	1,129	46	11	1.00	0.46	0.11
Yukon Flats West (x_1: Increase)	927	6.3	8.3 (SE = 0.81)	699	39	18	0.75	0.29	0.14
Kanuti (x_2: Decrease)	4,565	2.5	4.7 (SE = 0.36)	2,434	40	9	0.53	0.21	0.05
Selawik (x_2: Decrease)	4,497	8.4	6.5 (SE = 0.28)	5,861	31	13	1.30	0.40	0.17
Koyukuk (x_1: Negligible)	4,537	4.4	5.2 (SE = 0.33)	3,860	43	10	0.85	0.37	0.08
Innoko (x_2: Decrease)	4,342	3.4	7.0 (SE = 0.90)	2,066	56	9	0.48	0.27	0.05

Table 4.9 (Continued) Lake size and density characteristics of ten study areas and relationships with recent (i.e., since ~1985) annual trends in lake area.

Togiak (x_2: Decrease)	1,272	7.5	6.7 (SE = 0.87)	1,426	41	10	1.12	0.46	0.11
Becharof (x_1: Negligible)	3,932	6.2	6.4 (SE = 0.40)	3,772	37	11	0.96	0.36	0.10
T-test Hypotheses and Results	-	-	H_a: $\bar{x}_1 - \bar{x}_2 > 0$ $\bar{x}_1 = 8.14$ $\bar{x}_2 = 6.10$ P = 0.05	-	H_a: $\bar{x}_1 - \bar{x}_2 < 0$ $\bar{x}_1 = 39.8$ $\bar{x}_2 = 42.8$ P = 0.26	H_a: $\bar{x}_1 - \bar{x}_2 > 0$ $\bar{x}_1 = 13.6$ $\bar{x}_2 = 10.4$ P = 0.11	-	-	-

[a] (Total lake area / Total area) x 100%

Table 4.10 Climatic conditions of ten study areas based on 2-km grid Scenarios Network for Alaska Planning (SNAP) historical Climate Research Unit (CRU) data and relationships with recent (i.e., since ~1985) annual trends in lake area. Seasonal mean temperature and total precipitation data were averaged across all 2-km grids within each study area. Seasonal mean temperature was averaged from 1950-2009 and total precipitation was averaged from 1950-2006. Seasons were summer (June, July, and August), fall (September, October, and November), winter (December, January, and February), and spring (March, April, May). One-tailed t-tests were conducted to test *a priori* hypotheses for the expected direction of the difference in mean values of topographical and fire history characteristics between study areas with negligible or increasing recent annual trends in lake area (x_1: N = 5) and study areas with decreasing recent trends in lake area (x_2: N = 5).

Study Area	Mean temperature (°C)					Total Precipitation (mm)				
	Summer	Fall	Winter	Spring	Annual Mean	Summer	Fall	Winter	Spring	Annual Total
Tetlin (x_1 Negligible)	13.5	-5.6	22.2	1.7	4.00	163	65	35	38	301
Yukon Flats East (x_1 Negligible)	15.8	-7.3	-25.2	-4.4	-5.28	101	54	34	22	211
Yukon Flats Central (x_2 Decrease)	16.0	7.0	25.9	-3.7	-5.15	109	53	34	23	219
Yukon Flats West (x_1 Increase)	15.0	-6.9	25.8	4.0	-5.43	94	58	33	24	209
Kanuti (x_2 Decrease)	13.6	-7.5	-24.3	5.3	5.88	162	109	56	43	370
Selawik (x_2 Decrease)	13.3	5.8	-20.7	-6.5	-4.93	195	143	75	72	485
Koyukuk (x_1 Negligible)	14.3	-4.9	-21.5	-4.2	4.08	168	106	65	47	386

Table 4.10 (Continued) Climatic conditions of ten study areas based on 2-km grid Scenarios Network for Alaska Planning (SNAP) historical Climate Research Unit (CRU) data and relationships with recent (i.e., since ~1985) annual trends in lake area.

Innoko (x_2 Decrease)	13 9	-2 0	-18 2	-1 8	-2 03	178	114	65	51	408
Togiak (x_2 Decrease)	12 0	1 7	-9 4	-0 5	0 95	214	200	121	109	644
Becharof (x_1 Negligible)	11 9	1 8	-8 3	-0 2	1 30	193	179	89	82	543
T-test Hypotheses and Results	H_1 $\bar{x}_1 - \bar{x}_2 < 0$ $\bar{x}_1 = 14\ 1$ $\bar{x}_2 = 13\ 8$ P = 0 64	H_1 $\bar{x}_1 - \bar{x}_2 > 0$ $\bar{x}_1 = -4\ 58$ $\bar{x}_2 = -4\ 12$ P = 0 43	H_1 $\bar{x}_1 - \bar{x}_2 > 0$ $\bar{x}_1 = -20\ 6$ $\bar{x}_2 = 19\ 7$ P = 0 42	H_a $\bar{x}_1 - \bar{x}_2 > 0$ $\bar{x}_1 = -2\ 90$ $\bar{x}_2 = -3\ 56$ P = 0 68	H_1 $\bar{x}_1 - \bar{x}_2 > 0$ $\bar{x}_1 = -3\ 50$ $\bar{x}_2 = -3\ 41$ P = 0 48	H_1 $\bar{x}_1 - \bar{x}_2 > 0$ $\bar{x}_1 = 143\ 8$ $\bar{x}_2 = 171\ 6$ P = 0 84	H_1 $\bar{x}_1 - \bar{x}_2 > 0$ $\bar{x}_1 = 92\ 4$ $\bar{x}_2 = 123\ 8$ P = 0 81	H_1 $\bar{x}_1 - \bar{x}_2 > 0$ $\bar{x}_1 = 51\ 2$ $\bar{x}_2 = 70\ 2$ P = 0 84	H_1 $\bar{x}_1 \quad \bar{x}_2 > 0$ $\bar{x}_1 = 42\ 6$ $\bar{x}_2 = 59\ 6$ P = 0 81	H_1 $\bar{x}_1 - \bar{x}_2 > 0$ $\bar{x}_1 = 330$ $\bar{x}_2 = 425$ P = 0 83

Table 4.11 Summary statistics for coefficients of variation in lake area for lakes within the small decrease, small increase, and negligible trend classes for ten study areas. Fluctuating lakes were lakes that had coefficients of variation within the upper 25th percentile of the combined distribution of lake coefficients of variation from these three trend classes for all ten study areas (i.e., greater than 0.21). Moran's I values were used to evaluate whether fluctuating lakes were clustered, dispersed, or randomly distributed across each study area. The corresponding scale was the distance band that maximized the degree of clustering.

Study Area	# of Negligible and Small Change Lakes	Mean Coefficient of Variation	Coefficient of Variation Std. Error	% of Fluctuating Lakes in Negligible and Small Change Classes	Moran's I	
					Value[a]	Scale (km)
Tetlin	815	0.290	0.0095	45	0.032	21
Yukon Flats: East	369	0.216	0.0117	35	0.079	21
Yukon Flats: Central	280	0.330	0.0181	49	0.121	17
Yukon Flats: West	394	0.192	0.0105	28	0.064	4
Kanuti	1390	0.171	0.0045	23	0.024	37
Selawik	3984	0.130	0.0021	15	0.003	26
Koyukuk	2387	0.239	0.0052	35	0.059	16
Innoko	976	0.285	0.0067	52	0.044	6
Togiak	693	0.088	0.0036	7	0.006	23
Becharof	2861	0.138	0.0030	16	0.003	29
ALL AREAS	14150	0.180	0.0017	25	-	-

[a] All Moran's I values were statistically significant at alpha = 0.05 rejecting the null hypothesis that fluctuating lakes were randomly distributed across the study area.

Chapter 5: General Conclusion

This dissertation provides the most spatially extensive and contemporary assessment of the magnitude and mechanisms of historical lake area change for Alaskan National Wildlife Refuges and is an important source of information for the prioritization and planning of future research and management at multiple scales. By comparing characteristics of spatially and temporally paired decreasing and non-decreasing closed-basin lakes, I found that the expansion of floating mat vegetation into open water with a potential trajectory towards peatland development (i.e., terrestrialization) was the primary mechanism for lake area reduction and that thermokarst (i.e., ice-rich permafrost degradation) was the primary mechanism for non-decreasing lake area. Terrestrialization and thermokarst may have been enhanced by recent warming, which has both accelerated permafrost thawing and lengthened the growing season, thereby increasing plant growth, floating mat encroachment, transpiration rates, and the accumulation of organic matter in lake basins. In the third chapter, I identified density slicing as the least biased of three supervised classification methods for the estimation and monitoring of historical and future trends in lake area. In the fourth chapter, I used this method to estimate trends in lake area at multiple spatial and temporal scales in Alaskan National Wildlife Refuges. Trends were estimated at two temporal scales, a long-term scale (since ~1948) and a shorter recent scale (since ~1985), and at two spatial scales: broad-scale estimates were obtained for ten study areas and finer-scale estimates were obtained for ~23,000 individual lakes within these study areas. Across the ten study areas, lakes overall were

decreasing in size. Seven of the ten study areas had significant long-term declines in lake area and five study areas had significant recent declines. The average rate of change across study areas was -1.07 % per year for the long-term records and -0.80 % per year for the recent records. The presence of net declines in lake area statewide and for several study areas suggests that, while there was substantial among-lake heterogeneity in trends at scales as small as 3 km, a dynamic equilibrium in lake area may not be present.

An understanding of the mechanisms underlying both among-study area and among-lake heterogeneity may help to identify the relative susceptibility of broad-scale regions and individual lakes to changes in lake area and will improve spatial and temporal projections of future change. Study areas with decreasing trends tended to have non-fluvial, sandy soils and fewer thermokarst features. Coarse-grain sandy soils may facilitate decreasing lake area due to their better drainage properties while finer-grained fluvial soils may be more susceptible to large subsidence events due to their higher ice content (i.e., thermokarst) which may promote lake expansion. Study areas with decreasing trends also tended to have a smaller mean lake area which may be indicative of shallower subsidence events and enhanced susceptibility to terrestrialization (i.e., expansion of floating mat vegetation into open water with a potential trajectory towards peatland development). Field-based studies should be conducted to test and verify these potential sources of broad-scale spatial heterogeneity in lake area trends.

Fine-scale studies may also be able to identify whether potential sources of among-study area heterogeneity also apply to among-lake heterogeneity in lake area trends. For example, soil type and texture may vary at a similar scale as among-lake

heterogeneity in trends and may be correlated with lake bathymetry and relative susceptibility to terrestrialization or thermokarst. Alternatively, relative lake bathymetry alone may be the source of among-lake heterogeneity within a single regional soil type/texture.

In order to project future landscape conditions, there is a need for better estimates of the rate of terrestrialization. While losses in lake surface area due to encroaching floating mat vegetation from shallow lake perimeters can occur at rapid rates, this process may slow as it reaches the deeper portions of lakes. Losses in water volume due to transpiration and lake basin infilling with organic matter may also proceed at slower rates relative to losses in lake surface area. Analysis of peat stratigraphies at terrestrializing lakes may clarify the rate at which peat accumulates in relation to rates of lake area decline.

Paleoecological analyses of peat stratigraphies may also clarify whether decreasing and non-decreasing lakes are distinct lake types following different trajectories or whether they may be at different phases of the same cyclical process. Several studies have described the formation of thermokarst lakes and fen-bog succession via terrestrialization as distinct stages of a cyclical process involving alternating phases of permafrost degradation and regeneration as peat accumulates and insulates the ground surface (Drury 1956; Luken & Billings 1983; Zoltai 1993; Payette *et al.* 2004). If increasing, stable, and decreasing trends of individual lakes are different phases of a natural cyclical process, then there would be a net balance in lake area change (i.e., negligible trend) at the study area- or regional-scale. However, I found net declines in

lake area in several study areas suggesting that, at the study area-scale, a dynamic equilibrium in lake area may not be present. A warming climate may have accelerated terrestrialization while slowing or preventing the regeneration of permafrost required to complete the cycle, and tipped the balance toward a net loss in lake area and a net gain in terrestrial peatland or forested ecosystems. An improved understanding of the rate and trajectory of terrestrialization will help to identify both the nature and timing of short-term and long-term effects of terrestrialization on fish and wildlife habitats.

In the short-term, terrestrialization may have the most positive implications for waterfowl habitat compared to other decreasing mechanisms such as evaporation or drainage because it may be characterized by a slower transition to a shrub and tree dominated ecosystem and may lead to an increase in high quality floating mat nesting habitat (Arnold *et al.* 1993). However, increased aquatic productivity may also lead to a re-organization of freshwater food webs which could negatively affect waterfowl food sources (Corcoran *et al.* 2009). In the long-term, if declining trends continue, losses in individual lake surface area may eventually reach a threshold at which aquatic species can no longer be supported. Future studies should focus on clarifying the short- and long-term effects of terrestrialization on individual lake aquatic food webs and waterfowl habitat.

The broad-scale (e.g. study area or refuge) implications of lake area change on waterfowl habitats may depend on the scale of spatial heterogeneity in individual lake area trends. Because clustering of individual lake trends tended to occur at fairly small scales (3-22 km), clusters of stable or increasing lakes may provide suitable habitat

alternatives for aquatic species that may be displaced from clusters of shrinking lakes that become unsuitable. The suitability of these alternative habitats will depend on the similarity of stable and increasing lake characteristics (e.g., water chemistry, invertebrates) to shallow, shrinking lake characteristics and whether stable and increasing lake habitats are already fully saturated. By identifying the processes (i.e., terrestrialization/thermokarst) and lake characteristics (i.e., bathymetry) underlying the fine-scale among-lake heterogeneity in trends, this work provides a starting point to begin characterizing the relative habitat qualities of decreasing, increasing, and stable lakes for fish, waterfowl, and mammal populations and the potential resiliency of large-scale lake systems. For example, stable and increasing lakes tended to be deeper, which can affect lake stratification and the vertical mixing and recycling of nutrients in the water column (Fee *et al.* 1994). Stable and increasing lakes also tended to be more susceptible to thermokarst which may lead to sediment and nutrient loading to aquatic systems (Bowden *et al.* 2008). Water chemistries of stable and increasing lakes may not support the same species (Guildford *et al.* 1994) that are supported by the chemistries of shallower lakes susceptible to terrestrialization.

The identification of the magnitude and mechanisms of lake area change at multiple scales provides insight into the potential implications for the global carbon balance which is closely linked to the hydrological cycle and to permafrost dynamics in northern regions. Broad-scale net declines in lake area due to terrestrialization may lead to an initial increase in carbon storage in former lake basins (Payette *et al.* 2004) enhancing the role of northern peatlands as major stores of global carbon. However, the

overall effect on global radiative forcing is likely to be complex because both peatland development and lake expansion due to thermokarst may lead to an increase in the release of methane (Roulet *et al.* 1992; Walter *et al.* 2006) which is a more powerful greenhouse gas than carbon dioxide (Laine *et al.* 1996). Future research should focus on identifying the net effect of terrestrialization in Alaskan boreal forest on global radiative forcing including both gas emissions and albedo responses.

References

Arnold TW, Sorenson MD, Rotella JJ (1993) Relative success of overwater and upland mallard nests in southwestern Manitoba. *Journal of Wildlife Management*, **57**, 578-581.

Bowden WB, Gooseff MN, Balser A, Green A, Peterson BJ, Bradford J (2008) Sediment and nutrient delivery from thermokarst features in the foothills of the North Slope, Alaska: Potential impacts on headwater stream ecosystems. *Journal of Geophysical Research,* **113**, G02026.

Corcoran RM, Lovvorn JR, & Heglund PJ (2009). Long-term change in limnology and invertebrates in Alaskan boreal wetlands. *Hydrobiologia*, **620**, 77-89.

Drury WH (1956) *Bog Flats and Physiographic Processes in the Upper Kuskokwim River Region, Alaska* eds (Rollins RC, Foster RC), pp 130, The Gray Herbarium of Harvard University, Cambridge.

Fee EJ, Hecky RE, Regehr GW, Hendzel LL, Wilkinson P (1994) Effects of lake size on nutrient availability in the mixed layer during summer stratification. *Canadian Journal of Fisheries and Aquatic Sciences*, **51**, 2756-2768.

Guildford SJ, Hendzel, Kling HJ, Fee EJ, Robinson GGC, Hecky RE, Kasian SEM (1994) Effect of lake size on phytoplankton nutrient status. *Canadian Journal of Fisheries and Aquatic Sciences*, **51**, 2769-2783.

Laine J, Silvola J, Tolonen K, *et al.* (1996) Effect of water-level drawdown on global climatic warming: Northern peatlands. *Ambio*, **25**, 179-184.

Luken JO, Billings WD (1983) Changes in bryophyte production associated with a thermokarst erosion cycle in a subarctic bog. *Lindbergia*, **9**, 163-168.

Payette S, Delwaide A, Caccianiga M, Beauchemin M (2004) Accelerated thawing of subarctic peatland permafrost over the last 50 years. *Geophysical Research Letters*, **31**, L18208.

Roulet N, Moore T, Bubier J, Lafleur P (1992) Northern fens: methane flux and climatic change. *Tellus*, **44B**, 100-105.

Walter KM, Zimov SA, Chanton JP, Verbyla D, Chapin III FS (2006) Methane bubbling from Siberian thaw lakes as a positive feedback to climate warming. *Nature*, **443**, 71-75.

Zoltai SC (1993) Cyclic development of permafrost in the peatlands of Northwestern Alberta, Canada. *Arctic and Alpine Research*, **25**, 240-246.